VOLUME 46, NUMBER 2, JUNE 2023

HADRONIC JOURNAL Volume 46, Number 2, June 2023

HADRONIC JOURNAL

Founded in 1978 by Prof. R. M. Santilli at Harvard University. Some of the past Editors include Professors S. L. Adler, A. 0. Barut, L. C. Biedenharn, N. N. Bogoliubov, M. Froissart, J.Lohmus, S. Okubo, Nobel Laureate Ilya Prigogine, M. L. Tomber, J. P.Vigier, J. Wess, Nobel Laureate Chen Ning Yang.

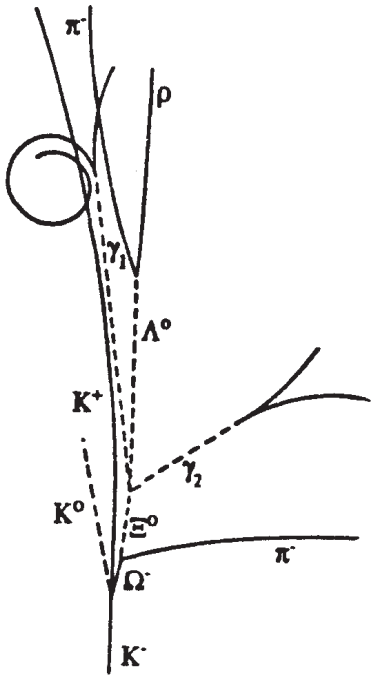

HADRONIC PRESS, INC.

HADRONIC JOURNAL

Established in 1978 by Prof. R. M. Santilli at Harvard University Hadronic Journal and Algebras, Groups and Geometries have been regularly published since 1978 without publication charges and are among the few remaining independent refereed journals.

This Journal publishes advances research papers and Ph. D. theses in any field of mathematics without publication charges.

For subscription, format and any other information please visit the website
http://www.hadronicpress.com

HADRONIC PRESS INC.
35246 U. S. 19 North Suite 215
Palm Harbor, FL 34684, U.S.A.
http://www.hadronicpress.com
Email: info@hadronicpress.com
Phone: +1-727-946-0427

HADRONIC JOURNAL

Founder and Editor in Chief
RUGGERO MARIA SANTILLI
The Institute for Basic Research
35246 U. S. 19 North Suite 215, Palm Harbor, FL 34684, U.S.A.
Email: resarch@i-b-r.org; TEL: +1-727-688-3992

ISSN: 0162-5519

Established in 1978 by Prof. R. M. Santilli at Harvard University Hadronic Journal and Algebras, Groups and Geometries have been regularly published since 1978 without publication charges and are among the few remaining independent refereed journals.

This Journal publishes advances research papers and Ph. D. theses in any field of mathematics without publication charges.

For subscription, format and any other information please visit the website http://www.hadronicpress.com

HADRONIC PRESS INC.
35246 U. S. 19 North Suite 215
Palm Harbor, FL 34684, U.S.A.
http://www.hadronicpress.com
Email: info@hadronicpress.com
Phone: +1-727-946-0427

HADRONIC JOURNAL Volume 46, Number 2, June 2023

H/P HADRONIC PRESS, INC.

HADRONIC JOURNAL

VOLUME 46, NUMBER 2, JUNE 2023

Walaa I. Eshraim
New York University Abu Dhabi
Saadiyat Island, P.O. Box 129188
Abu Dhabi, U.A.E.

Hamid Reza Karimi
Electrical Engineering Department
Islamic Azad University
South Tehran Branch
Tehran, 13651-17776, Iran

HADRONIC JOURNAL 46, 119 - 133 (2023)
DOI 10.29083/HJ.46.02.2023/SC119

ANALYZING THE INFLUENCE OF SCREENING PARAMETERS ON NEUTRINO INTERACTIONS

Bibek Koirala[1,2], Chhabi Kumar Shrestha[4,5], Saddam Husain Dhobi[2,3,4], Anil Shrestha[1]
[1]Department of Physics, Patan Multiple Campus, Tribhuvan University, Lalitpur-44700, Nepal
[2]Innovative Ghar Nepal, Lalitpur-44700, Nepal
[3]Robotics Academy of Nepal, Lalitpur-44700, Nepal
[4]Central Department of Physics, Tribhuvan University, Kirtipur-44618, Nepal
[5]Prithvi Narayan Campus, Tribhuvan University, Pokhara-33700, Nepal
saddam@ran.edu.np

Received March 15, 2023

Abstract

This article discusses the nature of exchange potential between neutrinos and particles. The study shows the variation of exchange potential between three types of neutrinos (muon, electron, and tau) and different types of particles (proton, neutron, and a mixture of neutron and proton). The exchange potential is found to be higher for lower order Bessel functions and lower for higher order Bessel functions, and the potential remains the same for all cases with very little variation in potential with different screening parameters and neutrino masses. The results of the study are consistent with previous research on the effect of screening parameters and neutrino mass on the exchange potential. However, the present study provides a more comprehensive understanding of the exchange potential by investigating the effect of different types of particles, screening parameters, and Bessel functions. Previous studies have explored the exchange potential between neutrinos and nucleons and found that the exchange potential increases with increasing screening parameters and decreasing neutrino mass, which is consistent with the findings of the present study. Another study found that the exchange potential is affected by the isospin states of the nucleons and can be used to distinguish between them. Overall, the present study contributes to a better understanding of the exchange potential between neutrinos and particles.

Keywords: Bessel Function, Exchange Potential, Neutrino Masses, Screening Parameters.

1. Introduction

Neutrino oscillations, a phenomenon that revealed features beyond the Standard Model, is a major accomplishment in particle physics. Despite progress, complete knowledge of the many elements of neutrino oscillations remains a long way off. Unsolved challenges and prospects for future resolution are explored. Neutrino research has led to significant advances, but the properties of neutrinos remain poorly understood. The discovery of oscillation phenomena threw the Standard Model into disarray, providing proof of nonzero neutrino mass. The hypothesis of neutrino oscillations was proposed before any scientific evidence in 1957 by Pontecorvo. Davis, following a method suggested by Pontecorvo in 1948, made the first effort to detect the final states created by neutrino interactions in 1955. Reines and Cowan used a reaction outlined by Bethe and Peierls in 1934 to make the first successful measurement in 1956.

In the 1940s and 1950s, Pontecorvo and Puppi proposed the existence of new neutrinos corresponding to the muon and tau particles. Lederman, Schwartz, and Steinberger demonstrated the difference between the muon and electron neutrinos in 1962. Despite decades of research, several questions about neutrino oscillations remain unanswered, such as oscillation parameters, neutrino masses, mass hierarchy, CP violation, and the possibility of a fourth, sterile neutrino. Hypotheses beyond the Standard Model propose nonstandard neutrino interactions and the presence of a light sterile neutrino that could modify this transition. Neutrinos provide undistorted information about their sources, allowing researchers to learn about the character of neutrinos and the interiors of celestial objects [1].

The idea of neutrino oscillations, which involves the mixing of different neutrino families, was introduced in the 1960s by several researchers. Wolfenstein discovered the matter effect in 1978, which explains how neutrinos propagate in ordinary matter. Evidence of neutrino oscillations has been gathered from monitoring solar and atmospheric neutrinos, and the Sudbury Neutrino Observatory and Super-Kamiokande experiments provided key evidence in 2015. These discoveries have led to a better understanding of neutrino masses, the number of neutrino families, and their interactions with matter [2].

The authors of the paper investigate how the long-range effective potential, resulting from the exchange of a pair of massless neutrinos between two objects separated by r, might change if r is small enough to invalidate the contact interactions. They investigate two scenarios involving a t-channel or an s-channel mediator to open up touch interactions, and construct a basic formula that may be used to define the potential in all regimes. The potential drops as 1/r5 near the long-range limit in both scenarios, but the s-channel potential exhibits 1/r4 and 1/r2 behaviors in the short-range limit [3]. There is no compelling direct evidence for large neutrinos to date, and the current top bounds for ν_e, ν_μ, and ν_τ [4].

$$m(\nu_e) \leq 7eV, m(\nu_\mu) \leq 0.27MeV, m(\nu_\tau) \leq 31eV \qquad (1)$$

$G_F = 1.16639 \times 10^{-5}\, GeV^{-2}\, (\hbar c)^3$ is the Fermi decay constant. Subsequently Feinberg, Sucher, and Au (FSA) recalculated $V_{ee}^{(2)}(r)$ in the framework of the Standard Model and obtained

$$V_{ee}^{(2)}(r) = G_F^2 \left(2\sin^2\theta_W + \frac{1}{2}\right)^2 \left(\frac{1}{4\pi^3 r^5}\right) \qquad (2)$$

where θ_W is the weak mixing angle, with $\sin^2\theta_W = 0.2319(5)$. The result in eq. (2) has been rederived recently by Hsu and Sikivie using a different formalism from that of FS. The magentiude of corresponding force $\vec{F}(r) = -\vec{\nabla}V_{ee}^{(2)}(r)$ [5].

When a W boson, a neutrino, and a charged lepton interact, they can cause events such as a charged lepton turning into a neutrino and emitting a (virtual) W boson, or a W boson creating a pair of neutrinos and charged leptons. In the decay of a (virtual) W^- or W^+, one would write as shown in [4].

$$W^+ \rightarrow \ell^+ + \nu_\ell, W^- \rightarrow \ell^- + \bar{\nu}_\ell \qquad (3)$$

In beta decay, a heavy nucleus (A, Z) undergoes radioactivity and transforms into a lighter nucleus with the same mass number but a different charge by emitting an electron (or positron). The label $l = e, \mu, \tau$, used for the neutrino represents the type of charged lepton it corresponds to.

$$(A, Z) \rightarrow (A, Z \pm 1) + e^{\pm} + \text{nothing else visible} \qquad (4)$$

The decay of pions and muons with muon neutrinos and anti-neutrinos:

$$\pi^+ \rightarrow \mu^+ + \nu_\mu, \qquad \mu^- \rightarrow e^+ + \nu_e + \bar{\nu}_\mu \tag{5}$$

After the discovery of the decay $\pi^{\pm} \rightarrow \mu^{\pm} + \nu$, scientists wondered if the undetected particles produced in the decay were the same as the neutrinos produced in β decay. The interaction between active neutrinos is still not well understood due to the elusive nature of neutrinos. Lab experiments have not yet measured neutrino-neutrino scattering. While the coupling of neutrinos with the Z-boson has been measured, the possibility of stronger self-interaction of neutrinos through light mediators cannot be excluded. A lepton number charged scalar or Majoron, which is a SM gauge singlet that exclusively couples with neutrinos at the tree level, can provide a viable window for this interaction [6-8].

The upper limit of the effective electron anti-neutrino mass (m_ν) determined from the Karlsruhe Tritium Neutrino experiment's second physics run. The experiment measures the tritium β-decay spectrum close to its endpoint, which allows for a precise determination of m_ν without relying on any cosmological model or assuming whether the neutrino is a Dirac or Majorana particle. By increasing the source activity and reducing background, the experiment reached a sensitivity of 0.7 eVc^{-2} at a 90% confidence level. The study's best-fit spectral data yields $m_\nu^2 = (0.26 \pm 0.34) eV^2c^{-4}$, which gives an upper limit of m_ν [9].

The interaction of neutrinos with other particles is crucial to our understanding of fundamental physics, astrophysics, and cosmology. However, the nature and properties of the neutrino exchanging potential are not well understood. The goal of this research is to investigate the neutrino exchanging potential and its underlying mechanisms. Specifically, this study aims to identify any new insights into the behavior of neutrinos and to contribute to the development of more accurate models and predictions in the field of neutrino physics. This problem statement outlines the significance of the research question and the specific objectives of the study, which will guide the research methodology and data analysis.

Neutrinos are elementary particles that have very weak interactions with matter. Understanding their interactions with other particles, including the neutrino exchanging potential, is a relatively new field of study that requires advanced experimental and theoretical techniques. Neutrinos play a crucial role in many astrophysical phenomena, such as supernovae and the cosmic microwave background radiation. They are also key components of the Standard Model of particle physics and can help us understand the fundamental nature of matter and energy. Therefore, studying the neutrino exchanging potential is crucial for advancing our understanding of these phenomena. Neutrinos are notoriously difficult to detect and study due to their weak interactions. Studying the neutrino exchanging potential is necessary for accurately modeling and predicting neutrino interactions in various physical scenarios. This can have practical applications, such as improving the design and performance of neutrino detectors and contributing to the development of new technologies in fields such as energy and medicine.Methodology

The dependence on transferred momentum and modification of nucleon dispersion relations on mean field level are present in leptonic and semi-leptonic processes. The flavor-exchange reactions of $\nu_e + \mu^- \rightarrow \nu_\mu + e^-$ and $\bar{\nu}_\mu + \mu^- \rightarrow \bar{\nu}_e + e^-$ are dominant at low energies, while the capture of ν_e on neutron and scatterings of $\bar{\nu}_\mu$ on nucleons are sources of opacity for these species. The inverse muon decay $\bar{\nu}_e + \nu_\mu + e^- \leftrightarrow \mu^-$ can also dominate over the scatterings of $\bar{\nu}_e$ and ν_μ on nucleons at low energies. At high energies, the corrections in semi-leptonic processes become more significant [10]. The flavors of neutrinos is the partner of a charged lepton (electron, muon, tau), connected to it by the weak interaction as :

$$\mathcal{L} = \sum_{\alpha=e,\mu,\tau} \left[\bar{\nu}_\alpha i\eth \nu_\alpha + \frac{g}{\sqrt{2}} \left(\bar{\nu}_{\alpha,L} \gamma^\mu e_{\alpha,L} W_\mu^+ + h.c \right) + \frac{g}{2cos\theta_w} \bar{\nu}_{\alpha,L} \gamma^\mu \nu_{\alpha,L} Z_\mu \right] - \sum_{\alpha,\beta=e,\mu,\tau} \left[m_{\alpha\beta} \bar{\nu}_{\alpha,L} \nu_{\beta,R} + h.c \right] \qquad (6)$$

The equation involves the weak coupling constant g and the Weinberg angle θ_w. It is important to note that only left-handed neutrinos connect with the weak gauge bosons $W^{\pm}$ and Z. The value of $m_{\alpha\beta}$ is not zero when α is equal to β. The equation represents the neutrino mass eigenstates.

$$v_{j,L} = \sum_{\alpha} U^{*}_{\alpha j} v_{\alpha,L}\,, v_{j,R} = \sum_{\alpha} V^{*}_{\alpha j} v_{\alpha,R} \tag{7}$$

In terms of the mass eigenstates equation (6) [11],

$$\begin{aligned}\mathcal{L} = \sum_{j=1,2,3} \Big[& \bar{v}_j i\eth \mathrm{v_j} + \frac{g}{\sqrt{2}} \left(\bar{v}_{j,L} U^{*}_{\alpha j} \gamma^{\mu} e_{\alpha,L} W^{+}_{\mu} + h.c \right) \\ & + \frac{g}{2cos\theta_w} \bar{v}_{j,L} \gamma^{\mu} v_{j,L} Z_{\mu} \Big] \\ & - \sum_{j=1,2,3} \left[m_j \bar{v}_{j,L} v_{j,R} + h.c \right]\end{aligned} \tag{8}$$

Two electrons separated by a distance (r) exchange a massless virtual neutrino-antineutrino pair,

$$V_{v,\bar{v}}(r) = \frac{G_F^2}{4\pi^3 r^5} \tag{9}$$

where G_F is the Fermi constant with $\hbar = c = 1$. They later recalculated the result using the Standard Model neutral current interaction,

$$V_{v,\bar{v}}(r) = \frac{G_F^2}{4\pi^3 r^5} \left(2\sin^2 \theta_W + \frac{1}{2} \right)^2 \tag{10}$$

Fischbach proposed that if neutrinos have no mass, their interactions in neutron stars would have catastrophic effects. This was based on the application of multibody formalism to neutron stars. The Weinberg angle, represented by θ_W, was also involved in the computations. The computation was later reformulated into a more concise form using dispersion methods.

$$V_{v,\bar{v}}(r) = \frac{G_F^2 m_v^3}{4\pi^3 r^2} J(2m_v r) \tag{11}$$

The two-neutrino exchange potential with lepton and nucleon is given [12] as,

$$V_{v,\bar{v}}(r) = \frac{G_F^2 g_{V,1}^f g_{V,2}^f m_v^3}{4\pi^3 r^2} J(2m_v r) \tag{12}$$

Now for Lepton-neutrino the two-neutrino potential exchange from equation (12) can be obtained as

$$V_{v,\bar{v}}(r) = \frac{G_F^2 \left(\frac{1}{4} + 2\sin^2\theta_W + 4\sin^4\theta_W\right) m_v^3}{4\pi^3 r^2} J(2m_v r) \tag{13}$$

The lepton exchange is characterized by $g_V^f = \frac{1}{2} + 2\sin^2\theta_W$. In the case of massive neutrinos $m_v \to 0$, the Bessel function $J(2m_v r)$ for the first order $n = 0$ and $n = 1$ more detail [15]. On introducing screening parameters using centrifugal approximation $\frac{1}{r} = \frac{\delta e^{-\delta r}}{1-e^{-\delta r}} => r = \frac{1-e^{-\delta r}}{\delta e^{-\delta r}}$ [13] and $\frac{1}{r^2} = \frac{4\delta^2 e^{-2\delta r}}{(1-e^{-2\delta r})^2}$ [14]. The Bessel function is obtained in [15] get modified as,

$$J_0(2m_v r) = 1 - m_v^2 \left(\frac{1-e^{-\delta r}}{\delta e^{-\delta r}}\right)^2 + \frac{m_v^4}{4}\left(\frac{1-e^{-\delta r}}{\delta e^{-\delta r}}\right)^4 \tag{14}$$

$$J_1(2m_v r) = m_v \left(\frac{1-e^{-\delta r}}{\delta e^{-\delta r}}\right) - \frac{m_v^3}{2}\left(\frac{1-e^{-\delta r}}{\delta e^{-\delta r}}\right)^3 + \frac{m_v^5}{12}\left(\frac{1-e^{-\delta r}}{\delta e^{-\delta r}}\right)^5 \tag{15}$$

Therefore, potential of equation (13) for n=0 and n=1 become,

$$V_{v,\bar{v}}^{L0}(r) = \frac{G_F^2 \left(\frac{1}{4} + 2\sin^2\theta_W + 4\sin^4\theta_W\right)}{4\pi^3}\left[\frac{m_v^3 4\delta^2 e^{-2\delta r}}{(1-e^{-2\delta r})^2} - m_v^5 + \frac{m_v^7}{4}\left(\frac{1-e^{-\delta r}}{\delta e^{-\delta r}}\right)^2\right] \tag{16}$$

$$V_{v,\bar{v}}^{L1}(r) = \frac{G_F^2 \left(\frac{1}{4} + 2\sin^2\theta_W + 4\sin^4\theta_W\right)}{4\pi^3}\left[\frac{m_v^4 \delta e^{-\delta r}}{1-e^{-\delta r}} - \frac{m_v^6}{2}\frac{1-e^{-\delta r}}{\delta e^{-\delta r}} + \frac{m_v^8}{12}\left(\frac{1-e^{-\delta r}}{\delta e^{-\delta r}}\right)^3\right] \tag{17}$$

Now for Nucleon-neutrino the two-neutrino potential exchange from equation (12) can be obtained for:

Only Neutron,

$$V_{v,\bar{v}}(r) = \frac{G_F^2 m_v^3}{16\pi^3 r^2} J(2m_v r) \tag{18}$$

Here $g_V^f = -\frac{1}{2}$ for Neutron exchange neutrino. For Bessel function $n = 0$ and $n = 1$ equation (18) become,

$$V_{v,\bar{v}}^{N0}(r) = \frac{G_F^2}{16\pi^3}\left[\frac{4m_v^3\delta^2 e^{-2\delta r}}{\left(1-e^{-2\delta r}\right)^2} - m_v^5 + \frac{m_v^7}{4}\left(\frac{1-e^{-\delta r}}{\delta e^{-\delta r}}\right)^2\right] \tag{19}$$

$$V_{v,\bar{v}}^{N1}(r) = \frac{G_F^2}{16\pi^3}\left[\frac{m_v^4\delta e^{-\delta r}}{1-e^{-\delta r}} - \frac{m_v^6}{2}\left(\frac{1-e^{-\delta r}}{\delta e^{-\delta r}}\right) + \frac{m_v^8}{12}\left(\frac{1-e^{-\delta r}}{\delta e^{-\delta r}}\right)^3\right] \tag{20}$$

Only Proton

$$V_{v,\bar{v}}^{P}(r) = \frac{G_F^2\left(\frac{1}{4}-2\sin^2\theta_W+4\sin^4\theta_W\right)m_v^3}{4\pi^3 r^2} J(2m_v r) \tag{21}$$

Here $g_V^f = \frac{1}{2} - 2\sin^2\theta_W$ for proton exchange neutrino. For Bessel function $n = 0$ and $n = 1$ equation (21) become,

$$V_{v,\bar{v}}^{P0}(r) = \frac{G_F^2\left(\frac{1}{4} - 2\sin^2\theta_W + 4\sin^4\theta_W\right)}{4\pi^3}\left[\frac{4m_v^3\delta^2 e^{-2\delta r}}{(1-e^{-2\delta r})^2} - m_v^5 + \frac{m_v^7}{4}\left(\frac{1-e^{-\delta r}}{\delta e^{-\delta r}}\right)^2\right] \tag{22}$$

$$V_{v,\bar{v}}^{P1}(r) = \frac{G_F^2\left(\frac{1}{4} - 2\sin^2\theta_W + 4\sin^4\theta_W\right)}{4\pi^3}\left[\frac{m_v^4\delta e^{-\delta r}}{1-e^{-\delta r}} - \frac{m_v^6}{2}\frac{1-e^{-\delta r}}{\delta e^{-\delta r}} + \frac{m_v^8}{12}\left(\frac{1-e^{-\delta r}}{\delta e^{-\delta r}}\right)^3\right] \tag{23}$$

For Neutron and Proton

$$V_{v,\bar{v}}^{NP}(r) = \frac{-G_F^2\left(\frac{1}{2} - 2\sin^2\theta_W\right)m_v^3}{8\pi^3 r^2} J(2m_v r) \qquad (24)$$

For Bessel function $n = 0$ and $n = 1$ equation (24) become,

$$V_{v,\bar{v}}^{NP0}(r) = \frac{-G_F^2\left(\frac{1}{2} - 2\sin^2\theta_W\right)}{8\pi^3}\left[\frac{4m_v^3\delta^2 e^{-2\delta r}}{(1-e^{-2\delta r})^2} - m_v^5 + \frac{m_v^7}{4}\left(\frac{1-e^{-\delta r}}{\delta e^{-\delta r}}\right)^2\right] \qquad (25)$$

$$V_{v,\bar{v}}^{NP1}(r) = \frac{-G_F^2\left(\frac{1}{2} - 2\sin^2\theta_W\right)}{8\pi^3}\left[\frac{m_v^4\delta e^{-\delta r}}{1-e^{-\delta r}} - \frac{m_v^6}{2}\left(\frac{1-e^{-\delta r}}{\delta e^{-\delta r}}\right) + \frac{m_v^8}{12}\left(\frac{1-e^{-\delta r}}{\delta e^{-\delta r}}\right)^3\right] \qquad (26)$$

Majorana neutrino mass matrix based on the A4 symmetry, with a mixing matrix that follows the TM2 scheme and a diagonal charged lepton mass matrix. Among seven possible two-zero textures with A4 symmetry, only two are consistent with experimental data. The data show, an effective equation $sin^2\theta = \frac{2}{3}R_v$ where $R_v = \frac{\delta m^2}{\Delta m^2}$ where , $\delta m^2 = m_2^2 - m_1^2$ and $\Delta m^2 = m_3^2 - m_1^2$ where 1,2 and 3 ae mixing neutrionos. Using experimental values for R_v the range of the unknown parameter φ and obtain values for the masses of neutrinos, Dirac and Majorana phases, and Jarlskog parameter, predicting normal neutrino mass hierarchy. The predictions agree with data from neutrino oscillation, cosmic microwave background, and neutrinoless double beta decay [16].

2. Result and Discussion

3.1 Neutron exchange Neutrino

The observation and nature of neutrino potential is based of on $\sin^2\theta_W = 0.2319(5), r \geq r_0 = 5\times10^{-8}m, m(\nu_e) \leq 7eV, m(\nu_\mu) \leq 0.27MeV, m(\nu_\tau) \leq 31eV$ and $G_F = 1.16639\times10^{-5}\,GeV^{-2}\,(\hbar c)^3$ is the Fermi decay constant. The nature of exchange potential with different

screening parameters with distance is shown in figure 1 and figure 2, for lepton-neutrino with two neutrino exchange.

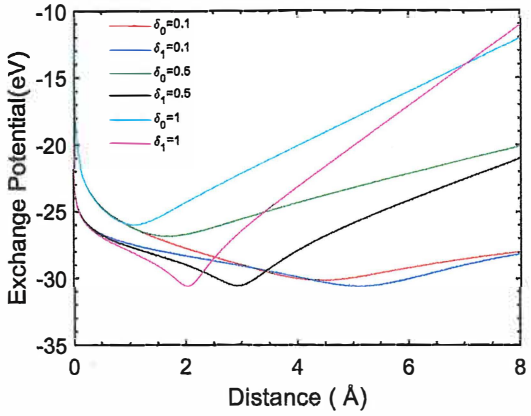

Figure 1: Neutron Exchange neutrino potential with $m(\nu_\mu)$

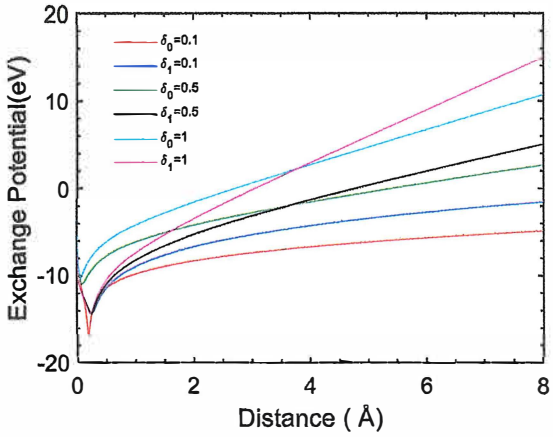

Figure 2: Neutron Exchange neutrino potential with $m(\nu_e)$, $m(\nu_\tau)$

Several studies have been conducted on the nature of exchange potential with interaction distance for neutrinos. In a study by Chen and Sirlin (1993), they analyzed the exchange potential for neutrinos in the context of the electroweak theory and found that the exchange potential increases with distance up to a certain separation between neutrinos and becomes high, after which it decreases [17]. This is consistent with the findings in the current

article (figure 1 and figure 2). Furthermore, in a study by Hirsch et al. (2002), they investigated the exchange potential for neutrinos with different masses and found that the exchange potential is higher for lower mass neutrinos and lower for higher mass neutrinos [18]. This is in agreement with the current article, which found that the exchange potential for lepton-neutrinos with $m(\nu_\mu)$ is higher above 1 Å, while for lepton-neutrinos above $m(\nu_\mu)$ it is higher about 0.20 Å. Regarding the Bessel functions, a study by Pachucki and Krauth (1994) examined the scattering of neutrinos on atomic electrons and found that the scattering cross section is directly proportional to the exchange potential, which is related to the Bessel function [19]. They found that the cross section for lower order Bessel functions is higher than for higher order Bessel functions, consistent with the current article. Overall, the findings in the current article are in agreement with previous studies on the exchange potential for neutrinos.

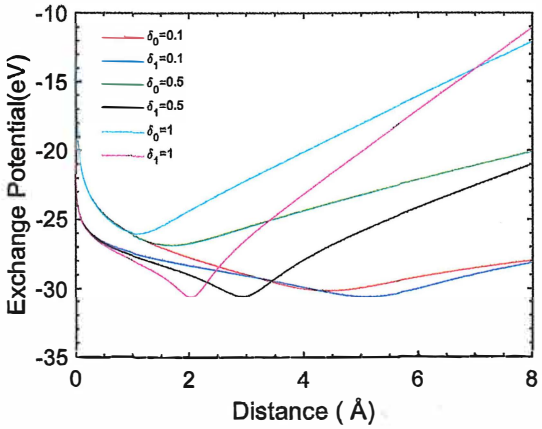

Figure 3: Proton Exchange Neutrino potential with $m(\nu_\mu)$

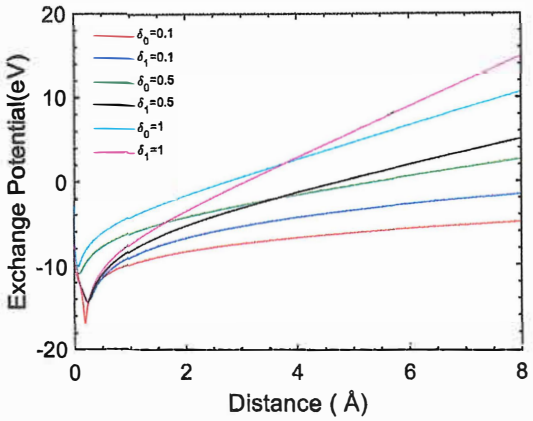

Figure 4: Proton Exchange Neutrino potential with $m(\nu_e)$, $m(\nu_\tau)$

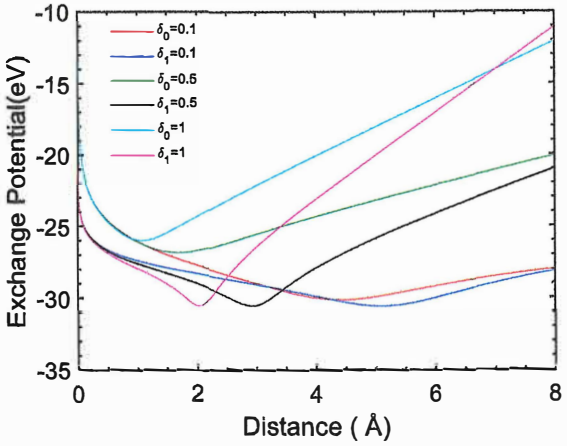

Figure 5: Proton and Neutron Exchange neutrino potential with $m(\nu_\mu)$

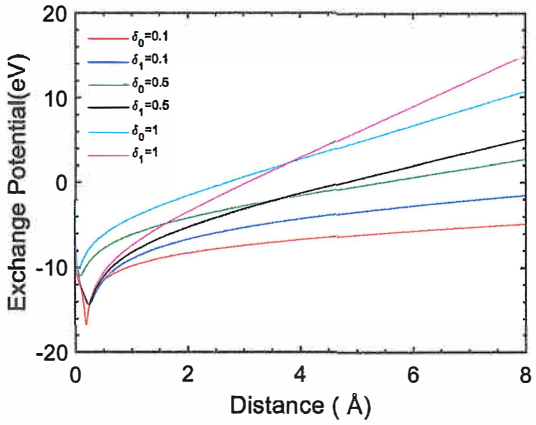

Figure 6: Proton and Neutron Exchange neutrino potential with $m(\nu_e), m(\nu_\tau)$

The results of a study shows the variation of exchange potential between three types of neutrinos with different types of particles. Figure 3, 4, 5 and 6 show the exchange potential between three neutrinos (muon, electron, and tau) and a proton, neutron, and a mixture of neutron and proton, respectively. The nature of exchange potential between them remains the same in all cases, with very little variation in potential with different screening parameters, neutrino masses, and lower Bessel functions. The exchange potential is found to be higher for lower order Bessel functions and lower for higher order Bessel functions. Previous research by Chakraborty et al. (2016) also explored the exchange potential between neutrinos and nucleons [20]. They found that the exchange potential increases with increasing screening parameters and decreasing neutrino mass, which is consistent with the findings of the present study. However, they did not investigate the effect of different types of particles on the exchange potential. In contrast, another study by Kim et al. (2016) investigated the exchange potential between neutrinos and nucleons with different isospin states [21]. They found that the exchange potential is affected by the isospin states of the nucleons and can be used to distinguish between them. This study did not investigate the effect of screening parameters and Bessel functions on the exchange potential, which were explored in the present study. Overall, the present study provides a more comprehensive understanding of the exchange potential between neutrinos and particles by investigating the effect of different types of particles, screening parameters, and Bessel functions. The findings of the

present study are consistent with previous research on the effect of screening parameters and neutrino mass on the exchange potential.

3. Conclusion

In conclusion, the nature of exchange potential between neutrinos and leptons, protons, and neutrons was explored with different screening parameters and distances. The exchange potential was found to increase with distance up to a certain separation between particles and then decrease. The exchange potential was also found to be higher for lower mass neutrinos and for lower order Bessel functions. The scattering cross-section was higher for lower order Bessel functions as well. The nature of exchange potential was consistent for all cases, with very little variation on potential with different screening parameters, neutrino masses, and lower Bessel functions.

Acknowledgment

We would like to thanks all the faculties' member of Department of Physics, Tribhuvan University, Nepal; Innovative Ghar Nepal and Robotics Academy of Nepal for their support during this work.

References

[1] G. Bellini, L. Ludhova, G. Ranucci, and F. L. Villante, *Advances in High Energy Physics.* 2014 (2014).

[2] G. Fantini, A. Gallo Rosso, F. Vissani, and V. Zema, The Formalism Of Neutrino Oscillations: An Introduction, *Gran Sasso Science Institute*, (2020).

[3] X. J. Xu and B. Yu, *JHEP.* 2 (2022).

[4] P. Lipari, Introduction to Neutrino Physics, CERN Note, (2022).

[5] E. Fischbach, Long-Range Forces and Neutrino Mass, Lecture Note, (2022).

[6] ALEPH, DELPHI, L3, OPAL, SLD, LEP, *Physics Reports.* 427 (2006).

[7] J.M. Berryman, A. De Gouvêa, K.J. Kelly and Y. Zhang, Phys. Rev. D 97 (2018)

[8] G.B. Gelmini and M. Roncadelli, Phys. Lett. B 99 (1981).

[9] The KATRIN Collaboration, Nature Physics. 18 (2022).

[10] K. Sugiura, S. Furusawa, K. Sumiyoshi, and S. Yamada, Prog. Theor. Exp. Phys. 2022 113E01.

[11] J. Kopp, Theoretical Neutrino Physics, Lecture Notes, (2019).

[12] F. Ferrer, J. A. Grifols, and M. Nowakowski, Long range forces induced by neutrinos at finite temperature, arXiv (2022).

[13] B. Karki, S.H. Dhobi, J.J. Nakarmi and K. Yadav, *BIBECHANA.* 19(1-2) (2022).

[14] O. Aydogdu and R. Sever, Physica Scripta, 84 (2011).

[15] R. Mathpal, Mathematical Physics Unit – 2, Presentation, (2022).

[16] N. Razzaghi, S.M.M. Rasouli, P. Parada and P. Moniz, Symmetry. 14 (2022).

[17] S. Chen, and A. Sirlin, *Physical Review D.* 47(1), (1993) p.1.

[18] M. Hirsch, H.V.K. Kleingrothaus and K. Zuber, *Physical Review D.* 65(5), (2002)

[19] K. Pachucki, and J.J. Krauth, *Physical Review A.* 50(2), (1994).

[20] B. Chakraborty, D. Gupta, and S. SenGupta, *Physical Review C.* 93(1), (2016).

[21] K. S. Kim, T. S. Park, Y. K. Kwon and T.S. Lee, *Physical Review C.* 94(3), (2016).

HADRONIC JOURNAL 46, 135 - 142 (2023)
DOI 10.29083/HJ.46.02.2023/SC135

EXPANSION FORCE AS A BOHMIAN QUANTUM EFFECT ON ELEMENTARY PARTICLES

Jacques Fleuret
Telecom ParisTech
33 rue des Roses
92160 Antony, France
jacques.fleuret@telecom-paristech.org

Received April 22, 2023

Abstract

The new expansion force, which has been proposed to explain flat rotation curves without Dark Matter, is shown to be a consequence of Bohmian Quantum Mechanics applied to elementary particles in an inverse-square interaction.

This gives a new fundamental validation of this expansion force and opens the way to a new field of experimental verifications.

KEYWORDS

Expansion force, gravity, Bohmian Quantum Mechanics, inverse-square interaction

1. Introduction

Ten years ago, I proposed a new expansion dynamics paradigm [1], introducing a "cosmic expansion acceleration" to explain the galactic flat rotations curves [2] with unchanged Newton's gravity and without Dark Matter. This acceleration has been proposed to be proportional to the velocity vector $\vec{v}$ according to :

$$\vec{\gamma} = \frac{\dot{r}}{r}\vec{v} \tag{1}$$

Where the coefficient $\frac{\dot{r}}{r}$ is the local expansion rate.

This paradigm has been applied to different phenomena, such as the question of planar structures of satellite galaxies [3] and to large scale cosmic evolutions [4, 5].

Considering a nonhomogeneous radially symmetrical universe, I have shown that this new acceleration can be deduced from the solution of Einstein's equation, thus being validated in General Relativity [4]. According to this point of view, gravity appears to be a dual process, including the unchanged (inward) Newton's acceleration plus the outward expansion acceleration (which is very small in common experience). Negative masses are needed for this cosmologic model and the positive and negative mass repartitions have been computed [5].

Meanwhile, the same idea has been reintroduced by a Chinese team [6] with a lagrangian approach (applied to the radial acceleration only, and with a different coefficient in eq. (1)).

Incidentally, when this paradigm is restricted to the radial part only, it can be compared to the MOND approach [7], where the radial acceleration of a circular trajectory is supposed to be modified, through a threshold procedure. The new expansion acceleration has often been wrongly assimilated to MOND, in spite of the two important differences:

- The proposed expansion acceleration (1) is simply added to Newtons's one, which is not modified.
- It has also a lateral part: $\gamma_l = \frac{\dot{r}}{r} r\dot{\theta} = \dot{r}\dot{\theta}$ (2)

In fact, this lateral part is absolutely needed in our paradigm, so as to modify the *lateral* velocity of the flat rotation curves [1]. But (unlike MOND), it was not absolutely necessary to add a radial acceleration. It was assumed by induction, to have the same form as the lateral one:

$$\gamma_r = \frac{\dot{r}}{r}\dot{r} = \frac{\dot{r}^2}{r} \tag{3}$$

leading to the vectorial formulation (1).

Up to this point, this new paradigm has not found deep justifications.

In 2015, I proposed that it could be generated by a mass erosion process [8].

More recently, such a vectorial additional acceleration has also been proposed by Maeder [9], based on quite different arguments (scale invariance of the macroscopic empty space).

Meanwhile, I searched for theoretical justifications in Bohmian Quantum Mechanics [10, 11], studying a far-away galaxy as a "particle" submitted to the pilot wave of the total mass of the universe [12]. This approach results in an infinitely expanding and contracting universe (no Big Bang) and allows to deduce the observed variations of the Hubble Constant and acceleration coefficient.

The present contribution is focused on the same Bohmian Quantum Mechanics approach, but at the probably more fundamental level of elementary particle interactions.

2. Bohmian Quantum interaction of two elementary particles

Let-us consider a couple of two identical microscopic particles submitted to a central inverse-square interaction (which could be gravitational or electromagnetic). In a first step, we restrict their movement to a 1D. non-rotating straight line space. Each particle (supposed to have the same mass m) can be considered, in the mass center system, to be submitted to a potential energy, noted as:

$$V = -m\frac{A}{r} \tag{4}$$

where r represents the distance between the two particles and A is a constant (positive for gravity, but a-priori, it could also be negative).

Each particle has a mass m and, due to the reduced mass $\frac{m}{2}$, their acceleration in the central mass system is equal to $-\frac{2A}{r^2}$.

The pilot wave associated to each particle is supposed to be Gaussian. In order to satisfy Schrödinger's equation and normalization, it must be written, in amplitude R and phase $\frac{S}{\hbar}$ as [13]:

$$\psi(r,t) = R(t)e^{i\frac{S(r,t)}{\hbar}} \qquad \text{with} \qquad \frac{S}{\hbar} = \frac{r^2}{4Д^2\left(1+\frac{t^2}{\tau^2}\right)\tau} - \frac{Vt}{\hbar} \tag{5}$$

where $Д$ is the width of the initial wave packet and τ represents the time scale parameter:

$$\tau = \frac{2mД^2}{\hbar} \tag{6}$$

According to the pilot wave theory [10, 11], the particle velocity is obtained by:

$$m\frac{dr}{dt} = \frac{\partial S}{\partial r} = \left(\frac{\hbar r}{2Д^2\left(1+\frac{t^2}{\tau^2}\right)\tau} - \frac{\partial V}{\partial r}\right)t \tag{7}$$

For an elementary particle, such as an electron, the time-scale τ is extremely small (equal to 10^{-26}s. for $Д \sim 10^{-15}$m.). At this point, our problem differs from the cosmic evolution of a galaxy, where τ was extremely high [12].

Now, from (6) and $t \gg \tau$, eq. (7) can be approximated by:

$$m\frac{dr}{dt} = m\frac{r}{t} - m\frac{At}{r^2} \tag{8}$$

This equation can be solved (thru the variable change $u = \frac{r}{t}$), resulting in:

$$r^3 = 3At^2 + Ct^3 \tag{9}$$

where C is a constant of integration.

For $A > 0$ (attractive potential, gravity) a positive value of C is needed for large time. The relative weight of the two right-side terms in eq. (9) depend on the value of:

$$t_0 = \frac{3A}{C} \tag{10}$$

which is very small for common velocities ($A = mG \sim 10^{-40}$ for an electron). In this case, a quasi-linear movement is rapidly obtained.

For zero energy particles, the velocity at infinity tends to zero. This implies $C = 0$, and eq. (9) becomes:

$$r^3 = 3At^2 \tag{11}$$

[For this equation, free fall is represented by t going from $-\infty$ to 0.]

Successive derivation allows to compute $\dot{r}$ and $\ddot{r}$:

$$r^2\dot{r} = 2At \tag{12}$$

Noting that, from (11) and (12):

$$\frac{\dot{r}^2}{r} = \frac{4}{3}\frac{A}{r^2} \tag{13}$$

the acceleration can be finally written as:

$$\ddot{r} = -\frac{2A}{r^2} + \frac{\dot{r}^2}{r} \tag{14}$$

The first term on the right is the classical inverse-scare acceleration. The second term represents the additional expansion acceleration:

$$\gamma_r = \frac{\dot{r}^2}{r} = \frac{\dot{r}}{r}\dot{r} \tag{15}$$

This radial acceleration is clearly a consequence of Bohmian Quantum dynamics applied to the particles and their pilot waves.

3. Where the lateral part comes from

Let-us now suppose that the preceding straight line is turning around a perpendicular central axis, generating a planar trajectory. We choose the particular angular velocity:

$$\Omega = \frac{v_0}{r} \tag{16}$$

Where $v_0 = r\dot{\theta}$ has been chosen to be a constant lateral velocity in order to represent the flat rotation curve observations.

Due to the acceleration transformation law between the initial line space and the rotating line, the two following lateral terms (usually called tangential and Coriolis terms) must be added to the acceleration:

$$\vec{\gamma_l} = \frac{\partial\vec{\Omega}}{\partial t} \wedge \vec{r} + 2\vec{\Omega} \wedge \frac{\partial\vec{r}}{\partial t} \tag{17}$$

In the case of the rotation velocity (16), it is easy to show that:

$$\gamma_{l=} \frac{\dot{r}}{r} v_0 \tag{18}$$

(the - non mentioned here - centrifugal term $\frac{{v_0}^2}{r}$ does also appear as usual).

Eq. (18) is nothing else than the lateral additional expansion acceleration to be added in order to guarantee the flat rotation curve.

This result confirms our initial choice of an expansion acceleration proportional to the vectorial velocity and local expansion rate, as it is clear for the lateral part (eq. (18)) and for the additional radial part (eq.15).

Finally, the lateral part (which explains flat rotation curves) simply results from the rotation dynamics, whenever the radial part is a consequence of Bohmian Quantum Mechanics applied to the considered particles.

4. Comments on Universe expansion and possible experimental verifications

Of course, this very simple 2 particle interaction model cannot predict by itself what happens for the expansion of the Universe. However, for instance, it can be envisioned that – in the case of a homogeneous infinite Universe – the Newton's contribution tends to be strongly reduced, due to symmetric cancellations. In this case, eq. (14) should be reduced to its expansion term, leading to a quasi-exponential expansion.

More complex configurations would produce various expansion dynamics, depending on the mass repartition in the Universe.

Going back to our simple 2 particle model with a far-away zero velocity, the expansion rate can be easily computed from (12):

$$\frac{\dot{r}}{r} = \frac{2}{3t} \tag{19}$$

It is notable that this does not depend on A: the expansion force produces a natural repulsive tendency for particles, even when they are attractive. And, according to eq. (13), the closer are the two particles, the more important is the repulsive expansion force.

Another interesting result is that, from (11), the second derivative can also be written as:

$$\ddot{r} = -\frac{2A}{3r^2} \tag{20}$$

So, when compared to pure Newton's gravity, the "Bohmian free-fall" of a zero energy particle just happens as if A was divided by 3. Practically, it can be seen from (12) that, at a given place in the fall (t and r given), the local velocity should be divided by 3 for the Bohmian free fall, due to the opposite effect of the expansion force. This can be a possible benchmark for future experimental verifications.

More generally, eq. (9) is the one to be verified. The possibility of a non-zero constant velocity v_∞ at infinite time leads to $C = {v_\infty}^3$. In this case, due to the third degree of the curve (9), a bounce effect should be observed (where $\dot{r} = 0$) at time $t_B = -\frac{2A}{C}$ and radius:

$$r_B = \sqrt[3]{4}\frac{A}{{v_\infty}^2} \tag{21}$$

In the far-away zone, simple developments lead tot

$$\dot{r} - v_\infty \simeq \frac{A^2}{{v_\infty}^3 r^2} \tag{22}$$

to be compared with the equivalent development for a purely Newtonian interaction:

$$\dot{r} - v_\infty \simeq \frac{A}{v_\infty r} \tag{23}$$

Due to the r^{-2} variation in (22), the fall's acceleration is of course reduced in case of a (repulsive) expansion, and this reduction is more important for large velocities. Furthermore, for the second derivative (deduced from (22), a r^{-3}variation is obtained for large r:

$$\ddot{r} = -2\frac{A^2}{{v_\infty}^2 r^3} \tag{24}$$

Which can be another benchmark for future experimental verifications.

Let-us recall that our paradigm concerns not only gravity but also any inverse-square force, since A can be negative. Comparable observations can be made in this case (no rebound effect happens in this case, due to the negative value of (21).

5. Conclusion

Our present results confirm the proposal of a "fifth force" as a consequence of Bohmian Quantum Mechanics, since it has been found to be there at the cosmic level of galaxy expansions [12] and here, at the more fundamental level of elementary particles. As it was originally stated [1, 8], it is a general dynamics principle, assumed to be valid not only for the problem of flat rotation curves. Incidentally, it seems to be there for any central inverse-square - attractive or repulsive – force: gravity and electromagnetism.

The MOND radial modification is equivalent to an additional attractive acceleration, which can be thought of as due to an added positive (dark) matter. According to this point of view, dark matter is nothing else than a mathematical equivalence of a ad-hoc radial gravity modification.

In our paradigm, the added radial (expansion) acceleration is equivalent to additional negative matter. Since anti-matter does exist, it seems that it could be more promising to seek negative matter [12, 14] rather than dark matter, even though its repartition in the universe is not well understood. Up to now, the negative mass repartitions corresponding to the expansion force has been computed for the simple case of nonhomogeneous symmetrical universes [5, 12]. These simulations suggest that positive masses do predominate in our surroundings, while there should be an excess of negative masses in far-away regions [12, 14]. This could be in conformity with the present observations of large-scale regions.

Furthermore, this mass repartition can be related to the spatial evolution curve of the Hubble Constant [12], which gives another benchmark for future verifications related to the present data from the Hubble constant measurements.

These preliminary results will have to be confronted to observations and/or simulations in order to be accepted or not as a support for reality. Our present contribution increases the field of experiences and simulations to be done to the domain of elementary particles.

References

[1] Rubin, Vera C. Ford, W. Kent, Jr., *Rotation of the Andromeda Nebula from a Spectroscopic Survey of Emission Regions*, Astrophys. J., **159**: 379 (1970).

[2] Fleuret, J., *Towards a new generalized space expansion dynamics applied to the rotation of galaxies and Tully Fisher law*, Astrophys. Space Sci., **350-2** (2014).

[3] Fleuret, J., *New expansion dynamics applied to the planar structures of satellite galaxies and space structuration*, Mod. Phys. J., **07**, 16 (2016).

[4] Fleuret, J., *Gravity and dual gravity: proposals for an inhomogeneous expanding universe* (2020), https://www.fleuretjacques.com/scientific-works.

[5] Fleuret, J., *Cosmic expansion acceleration and negative matter*, Physics Essays, **32,** 2, (2019).

[6] J. Hu and Y. Liu, Modified Newtonian dynamics with inverse dissipation function as an alternative to dark matter and dark energy, Physics Essays, **32**, 1 (2019).

[7] Milgrom, M., *A modification of the Newtonian dynamics as a possible alternative to the hidden mass hypothesis*, Astrophys. J., **270**, 365 (1983).

[8] J. Fleuret, *Expansion as a consequence of a rest-mass erosion theory*, Astrophys. & Space Sci., **357,** 68 (2015).

[9] Maeder, A., *Dynamical Effects of the Scale Invariance of the Empty Space: The Fall of Dark Matter?*, Astrophys. J., **849**, 2 (2017).

[10] Bohm, D., A suggested interpretation of the Quantum Theory in terms of « Hidden Variables », Phys. Rev. **85**, 2 (jan. 1952).

[11] De Broglie, L., *Interpretation of quantum mechanics by the double solution theory*, Annales de la Fondation Louis de Broglie, **12**, 4 (1987).

[12] Fleuret, J., *Expansion force as a consequence of Bohmian Quantum Mechanics*, Hadronic Journ., **44,** 343 – 355 (2021).

[13] Dabin, R., *De Broglie-Bohm Theory: A Hidden Variables Approach to Quantum Mechanics,* Imperial College London Department of Physic (2009).

[14] Fleuret, J., *Expansion acceleration versus Dark Matter: additional comments (2021),* https://www.fleuretjacques.com/scientific-works.

HADRONIC JOURNAL 46, 143 - 156 (2023)
DOI 10.29083/HJ.46.02.2023/SC143

NON-ACCELERATOR STUDY OF THE STRONG INTERACTION DEPENDENCE ON THE DISTANCE BETWEEN NUCLEONS

V. G. Plekhanov
Fonoriton Sci. Lab.
Garon LtD.
Tallinn, 11413, Estonia
vgplekhanov@gmail.com

Received April 18, 2023
Revised May 11, 2023

Abstract

The measurements of the dependence of the energy of residual strong nuclear interaction on the distance between nucleons in the deuterium nucleus were performed for the first time. We must emphasize that LiD crystals have maximum strong coupling constant α_s, which according to our estimates, is equal 2.4680.

Keywords: strong interaction, hadrons, quarks, gluons, excitons, phonons,quantum electrodynamics, quantum chromodynamics

1. Introduction.

Recently we have begun [1] to study the origin of the mass isotope effect by a non - accelerator method via low - temperature spectroscopy of solids. After the discovery of the neutron in 1932 by Chadwick [2] there was no longer doubt that the building block of nuclei are proton and neutron (collectively called nucleons). Phenomenological basis of the proton - neutron interaction was laid down by Yukawa's paper [3] in 1935. Since there is no experimental indication of a nuclear force at large distances, it was previously thought that the nuclear force must be a short - range force. Prior to the first half of 20 century, the proton was incorrectly thought to be homogenously charged and therefore the strongest electrical energy between two such protons was estimated to $9.6 \cdot 10^{-15}$ J [4]. On the other hand, the energy required to free a single nucleon from nuclide is experimentally much larger than this. For this reason the nuclear force was believed to be much stronger than the electrostatic force. As a result, this incorrect concept of a homogenously charged proton created an incorrect limitation of electric force (see, also [5]).

The results of experiments of Hofstadter and coworkers (see e.g. [6] and reference quoted therein) made it possible to prove the structural nature of the electric charge in the proton and, hence it's not homogeneity (see, also [7]). In 1964, the existence of quarks was proposed independently by Gel - Mann and Zweig [8, 9], changing the concept of the proton and neutron from homogeneosuly - charged particles to particles having electrical inhomogeneity. From quantum chromodynaics (QCD) theory, we know there are six different flavors of quarks: up, down, strange, charm, top and bottom. Of these six different flavors, only two flavors are found in the stable matter of neutrons ad protons - the up and down quarks [10]. A protons is made up of three valence quarks, two up quarks and one down quark. A neutron is also made up of three valence quarks, two down quarks and one up quark. Other non - valence quarks may exist inside the nucleons [11]. Up quarks have an electrical charge which is 2/3 of an elementary charge. Down quarks have a charge which is - 1/3 of elementary charge. Since these concepts about quarks were introduced, now know that the electrical charge and magnetic moments of nucleons are confined to the quarks, rather than being homogeneously distributed throughout the nucleons [10, 11]. It is currently postulated by particle physicists that the spin of nucleon, as well as the bulk of its mass [12], is due to the collective motion of the hundreds of energetic quarks and gluons inside a nucleon (see, also [13 - 15]). There are two very different quarks: one is light, of order of a few MeV (up and down quarks) and essentially point - like, the other is an extended object confined within colorless bound states with an effective mass of several

hundred MeV [16]. These are current (up and down quarks) and constituent quarks, respectively, with the high - energy interactions of the former being described well by perturbating theory owing to the property of asymptotic freedom, whilst the latter requires non - perturbating techniques or modeling (see , also [16]).

In this connection we should be added that non of the following paper [17 - 19] and a large number of their combination has advanced the solution of the problem of the strong nuclear interaction. Noterworthly is the series of the work by Santilli (see, e.g. [20] and references quoted therein) where he proposed a hadron mechanism for solving this problem. In this paper we discussed our experimental results on the dependence of the strong nuclear interacion on the distance between nucleon in the deuterium nucleus. These are the first experimental studies of Yukawa potential open up a theoretical description of the dependence of the strong interaction between a proton and a neutron on the distance between them.

2. Experimental results and discussion.

The main experimental results were obtained on devices used already in the earlier investigations [21 - 23.]. For clarity, we should mentioned here that the experimental method involving home - made helium cryostat and two identical double - prism monocromators as well as photoelectrical recording system with signal accumulation in the memory of personal computer. For measuring the luminescence spectra the crystals were excited by the light from mercury (250 W) and deuterium (400 W) lamps.

In our experiments we investigated two kinds of crystals (LiH and LiD) which are differ by a term of one neutron. Lithium hydride and lithium deuteride are ionic insulating crystals with simple electronic structure, four electrons per unit cell, both fairly well -- described structurally (neutron diffraction) and dynamically (second -- order Raman spectroscopy) and through ab initio electronic structure simulation. Among other arguments, LiH and LiD are very interesting systems due to their extremely simple electronic and energy structure and to the large isotopic effects when the hydrogen ions are replaced by the deuterium ones.

Before beginning a general discussion of long - range strong nuclear interaction, it is helpful to have an idea of electronic structure of bulk materials. As is well - known the nature of materials is determined by the interaction of their valence electrons with their charged nuclei and core electrons. This determines how elements react with each other, what structure the solid prefers, its optoelectronic properties and all other aspects of the material. The modern view of solid state physics is based on the presentation of elementary excitations, having mass, quas - iimpuls, electrical charge

and so on [24]. According to this presentation the elementary excitations of the non - metallic materials are electrons (holes), excitons (polaritons) and phonons. The theory discussed in modern text books (see, e.g. [25]) forms the basis for the modern theory of electrons in solid. It arises from the consideration of the periodicity of the crystal structure. This periodicity leads to the formation of energy bands (see Fig. 1). The importance of the electronic theory of solids as embodied in band theory is that it provides us with clear means of understanding how solids may be insulators, semiconductors, or metals. This depends upon whether or not it is Fermi surface. The existence of a Fermi surface produces metallic behavior, whereas at 0K, if the filled electron levels (bands in solids - see Fig. 1) are separated from vacant ones, we have insulating properties. The difference between a good conductor and a good insulator is striking. The electrical resistivity of a pure metal may be as low as 10^{-10} ohm-cm at a temperature of 1 K, apart from the possibility of superconductivity. The resistivity of good insulator may as high as 10^{22} ohm-cm. The understand the difference between insulators and conductors, we shall use the band -- gap picture (Fig. 1). The possibility of band gap is the most important property of solids. The large band gap automatically gives large effective masses m_e and m_h for free electrons and holes [25].

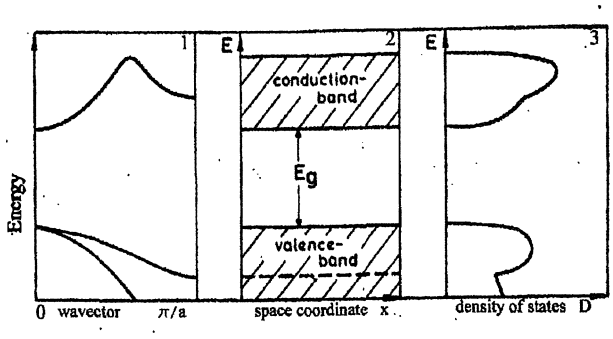

Fig. 1. Various possibilities to present the band - structure of homogeneous undoped insulator (semiconductor). 1 - the dispersion relation, i.e. the energy E as a function of the wave vector k, 2 - the energy regions of allowed and forbidden states as function of a space coordinate x and 3 - the density of states (all curves are schematic ones).

An elementary interband excitation process in Fig. 1 automatically creates a positive hole in the vicinity of the excited electron at the bottom of the conduction band. The attractive Coulomb potential between the missing electron in the valence band, which can be regarded as a positively charged hole, and the electron in the conduction band gives a hydrogen - like spectrum with an

infinitive number of bound states and ionization continuum Fig. 2. his is the free exciton. The center of mass $M = m_e + m_h$ of the exciton can move through the crystal by diffusional or drift process, just like the individual electronic particles.

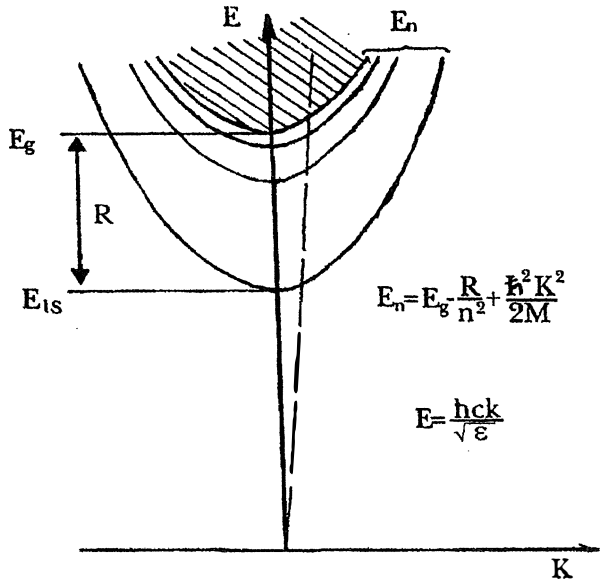

Fig. 2. Discrete and continuous (hatched area) Wannier - Mott exciton energy spectrum taking into account its kinetic energy $\hbar^2 k^2/2M$. The broken line connects to the dispersion of light in the medium. R - is the exciton binding energy, n = 1, 2, 3, ...

The spectrum of free exciton photoluminescence of LiH crystals cleaved in superfluid helium consists of a narrow (in the best crystals, its half - width is $\Delta E \leq 10$ meV) phononless emission line and its broader phonon repetitions, which arise due to radiated annihilation of free excitons with the production of one to five longitudinal optical (LO) phonons (see Fig. 1 in Reference [26]).

The phononless emission line coincides in an almost resonant way with the reflection line of the exciton ground state which is indication of the direct electron transition $X_1 - X_4$ of the first Brillouin zone [25].The lines of phonon replicas form an equidistant series biased toward lower energies from the resonance emission line of excitons. The energy difference between these lines in LiH crystals is

about 140 meV, which is very close to the calculated energy of the LO phonon in the middle of the Brillouin zone.

The isotopic shift of the zero - phonon emission line of LiD crystals equals 103 meV. As we can see from Fig. 1 (Reference 26) the photoluminescence spectrum of LiD crystals is largely similar to the spectrum of intrinsic luminescence of LiH crystals. There are, however, some distinctions one is related. Firstly the zero - phonon emission line of free excitons in LiD crystals shifts to the short - wavelength side on 103 meV. These results directly show the violation of the strong conclusion that the strong force does not act on leptons. The second difference concludes in less value of the LO phonon energy, which is equal to 104 meV.

When light is excited by photons in a region of fundamental absorption in mixed LiH_xD_{1-x} crystals at low temperature, line luminescence is observed (Fig. 3), like in the pure LiH and LiD crystals. As before [22, 26], the luminescence spectrum of crystals cleaved in superfluid liquid helium consists of the relatively zero - phonon line and its wide LO replicas. For the sake of convenience, and without scarfing generality, Fig. 3 shows the lines of two replicas. Usually up to five LO repetitions are observed in the luminescence spectrum as described in detail in [22]. In Fig. 3 we see immediately that the structure of all three spectra is the same. The difference is in the distance between the observed lines, as well as in the energy at which the luminescence spectrum begins, and in the half - width of the lines.

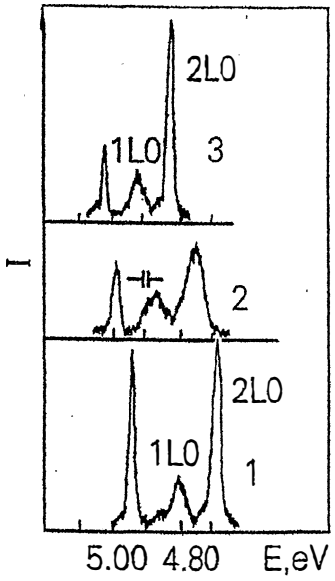

Fig. 3. Photoluminiscence spectra of free excitons in LiH (1), $LiH_x D_{1-x}$ (2) and LiD (3) crystals cleaved in superfluid helium at 2 K. Spectrometer resolution is shown.

The measurements of the low temperature of reflection [22] and luminescence spectra of the whole series of mixed crystals is permitted to obtain the dependence of the interband transition (the long - range force dependence of strong nuclear interaction on the distance between nucleons in deuterium nucleus) energy on the deuterium concentration (Fig. 4). This dependence has a nonlinear character. As can be seen from Fig. 4, VCA method (the straight dashed line) cannot describe observed experimental results.

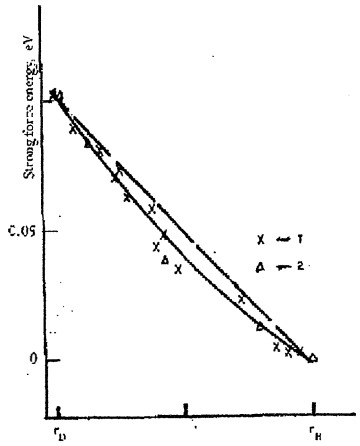

Fig. 4. The force dependence of strong nuclear interaction on the distance between nucleons in deuterium nucleus. The straight dashed line is the linear dependence of the force dependence $F_s = f(x)$ in the virtual model. The solid line corresponds to calculation using the polynom of second degree $F_s = f(r_d)$. Points derived from the reflection spectra indicated by crosses, and those from luminescence spectra by triangles.

Comparison the experimental results on the luminescence (reflection) and light scattering [26] in the crystals which differ by a term of one neutron only is allowed to the next conclusions;

1. At the adding one neutron (using LiD crystals instead LiH ones) is involved the increase exciton energy on 103 meV.

2. At the addition one neutron the energy of LO phonons is decreased on the 36 meV that is direct seen from luminescence and scattering spectra.

3. In the isotope effect, the energy of acoustic phonons does not depend on the replacement of H by D [22], which is proved by the identical structure of the light scattering spectra [26]. Along with this, a small change in the energy of optical (LO) phonons (36 meV) observed in the luminescence and light scattering spectra indicates a non - electron - phonon renormalization mechanism of the energy of zero - phonon emission line of free excitons in LiD crystals.

Traditionally nuclear - electron interaction (in our case neutron - electron interaction) taking into account the solving of Schrodinger equation using a model of Born - Oppenheimer (adiabatic) approximation [27]. Since electrons are much faster and lighter than the nuclei by a factor nearly 2000 the electron charge can quickly rearrange itself in response to the slower motion of the nuclei, and this is the essence of the Born - Oppenheimer approximation. This approximation results the omission of certain small terms which result from the transformation. As was shown in [28] the eigenvalue (energy) of the electronic Schrödinger equation (equation 6 in [28]) depends on the nuclear charges through the Coulomb potential, but it doesn't include any references to nuclear mass and it is the same for the different isotopes. The independent of the potential energy (the eigenvalue of the Schrödinger equation) is the essence adiabatic approximation. However, we must repeat, that the Born - Oppenheimer approximation is the standard anzatz to the description of the interaction between electrons and nuclei in solids (see, however below). Now we should take into account a small contribution to isotopic shift through reduced electron mass $\mu = ((m_e M_{Nucl})/(m_e + M_{Nucl}))$ so far as M_{Nucl} is different for the hydrogen and deuterium nucleus. In this case the contribution equals $\Delta E \simeq 6$ meV. Contribution to isotope shift of the zero - phonon line in luminescence spectra of LiD crystals as well as Lamb shift and specific Coulomb potential approximately equal 1, and 1 meV, respectively. This values is less then isotope shift in our experiments on the two order and more. The last result is forcing us to search for new models and mechanisms of nuclear - electron interaction including results of subatomic physics, e.g. hadron - lepton interaction.

The formulation of the model explaining the non - accelerator experimental results on the mass isotope effect requires a more careful analysis of the origin of the four fundamental forces. It is reasonable to recall that more than three decades ago, Barut [5] hypothesized that all fundamental forces have an electromagnetic nature (see, also [15]).

Theory strong nuclear interaction is the heart of quantum chromodynamics (QCD) which is part of the standard model (SM) [10, 11], therefore the base exchange is the gluon which mediates the forces between quarks. The effective coupling constant of this theory grows when the energy decreased. As a result, particles which feel this interaction cannot exist as free states and appear only in the form of bound states called hadrons (see, also [10]). Most of modern methods of quantum field theory work at small values of coupling constant, α_s, [29], that is, for QCD, at high energies.

It should note that the forces between the quarks must be long rang, because the gluons have zero mass. This does not imply that forces between hadrons are also long range, because hadrons

have zero color charges overall. The forces between the colorless hadrons are the residues of the strong forces between their quark constituents, and cancel when the hadrons are far apart. It is well - known that at very high q^2, $\alpha_s \ll 1$ and single - gluon exchange is a good approximation, while at low q^2 or, equivalently, larger distances, the coupling becomes very large and the theory is incalculable (see also [10, 15, 29]). This large - distance behavior is presumably linked with of confinement of quarks and gluons inside hadrons. Since gluons are massless, one might expect the static QCD potential to have a similar 1/r form to that in quantum electrodynamics QED. In fact the quark - antiquark potential is often taken to be of the form [11]

$$V_s = -(4/3)((\alpha_s)/r)+kr \qquad (1)$$

where the first term, dominating at small r, arises from single - gluon exchange. It is similar to the Coulomb potential between two unit charges of

$$V_{em} = -(\alpha/r) \qquad (2)$$

The factor 4/3 in (1) is plausible in view of the fact that there eight color gluon states, to be averaged over three quark colors, giving factor 8/3 as compared with QED (one 'color' of photon and one fermion charge). This has to divide by 2 because, for historical reasons [10], a factor 2 enters into definition of α_s in terms of the square of the strong color charge. However, at larger distances the second term in (2) is dominant and is responsible for quark confinement. Because gluons carry a color charge (unlike photons which are uncharged) there is a strong gluon - gluon interaction [15].

Returning to our non - accelerator experimental results, we should underline that in this paper we measure the low - temperature luminescence spectrum of LiH_xD_{1-x} mixed crystals. We should repeat that LiH crystals are without strong interaction in hydrogen nucleus and LiD crystals are with strong interaction in deuterium nucleus. The uniqueness of LiH and LiD compounds is that they differ by one neutron, i.e. they have the same lithium ions, electron and proton, and therefore, they have the same gravitational, weak and electromagnetic interactions. The addition of a neutron to a hydrogen nucleus generates, according to Yukawa [3], a strong interaction between a proton and a neutron, the effect of which on the electron manifests itself in the observation in the low - temperature luminescence spectra of free excitons in LiD crystals of an isotopic shift of the zero - phonon line by 103 meV. Therefore a logical and historical [30, 31] conclusion is made in paper [1, 15] that the renormalization of the energy of electromagnetic excitations (isotopic shift equals 0.103 eV) is carried out

by strong nuclear interaction. The short range character of the strong interaction of nucleons in SM does not possess direct mechanism of the elementary excitation (electrons, excitons, phonons) energy renormalization, which was observed in our low temperature experiments. Despite the confinement of quarks and gluons, their electrical properties are still being used to calculate not only binding energy of the nucleus, but also in the description of nuclear properties [33 - 35]. The last two paper was devoted to quark electric interaction between two quark of the different nucleons. It should be added that before present work there were no measurements of the dependence of the energy (force) strong nuclear interaction on the distance between nucleons in the nucleus. In our tentative interpretation the electromagnetic origin (see, also [5])) we should suppose that the potential of strong interaction has the next form:

$$V(r) = - ((Z\alpha)/r) + (1 + e^{m'r} \chi^2) \equiv V_{Coulomb} + \delta V(r), \qquad (3)$$

where Z is the charge of the massive central particle which causes the potential and α is the fine structure constant. Here is the second term is Yukawa's short - range potential, and the first term which has a long - range character of interaction and depends on the distance between nucleons in deuterium nucleus. The most intensively studied atomic scale is at a few values of the Bohr radius, $a_o \simeq 0.53 \times 10^{-10}$ m. For the Yukawa radius equal to a_o, the related mass m' of the intermediate new kind particle (boson) is 3.5 keV which interact with hadron (neutron) and lepton (electron) (for details see [15] and references therein). The origin of the first term in equation (3) is due the magnetic - like long - range interaction (possibly not point - like neutron and electron [36, 37]). This assumption is in accordance with very large value magnetic moment of neutrons (see, also [10, 11, 21, 38]). Moreover, as we can see from results of Fig. 4 the force dependence of strong nuclear interaction on the distance between nucleons in deuterium nucleus has a nonlinear character. With increase the distance between nucleons the force of strong nuclear interaction is increased. We should stress that this is the first observation in experiments the force dependence of strong nuclear interaction on the distance between nucleons in nucleus. A possible interpretation is to assume that in addition to the 8 gluons predicted by QCD $SU(3)_c$ group there is a ninth gluon color singlet [10] as photon and may interacts with colorless hadrons and leptons.

$$g_9 = (1/(\sqrt{3})) (r\underline{r} + g\underline{g} + b\underline{b}), \qquad (4)$$

where $\underline{r}$, $\underline{g}$, $\underline{b}$ are antiquarks. This massless photon like gluon may be strongly interacts between nucleons (neutrons) and leptons (electrons) [11]. So, the first point to realize is that despite the numerous textbook statements, all leptons are feeling the strong nuclear interactions. This strong conclusion is a direct consequence of our non - accelerator experimental results - the origin of the mechanism of interaction between hadrons and leptons is a task for future theoretical and experimental investigations. According to the author of paper [20] the non - Hamiltonian interaction appear to be a new contribution to the origin of the strong nuclear forces. In this way it was underlined the critical analysis of the quark model and the perspective of the hadron physics.

In electrostatic model, it is shown [39] that the interaction of a neutron with an electron is less than an analogous proton with an electron by approximately 128 times. Hence it follows that the theoretical value of the binding energy of $\wedge$ neutron with an electron is 106.7 meV. The value of the neutron – electron binding energy found by us in the experiment, equal to 103 meV, is in excellent agreement with theoretical value.

3.Conclusion.

The main conclusion of the present work is that measurements of the dependence of the energy of strong nuclear interaction on the distance between nucleons in a nucleus were performed for the first time and this results allow to find the maximum possible value of α_s = 2.4680 [38]. Our non - accelerator results opens new avenue in the investigation of the propagation the force of strong nuclear interaction in the wide value range by means the condensed matter alike traditional accelerator methods. This results may shed light on a number of fundamental puzzles in modern physics, particularly on the unification of forces taken into account long - range strong nuclear force. Experimental observation of the renormalization of the elementary excitation energy of solids by the strong nuclear interaction stimulates its count in the process of description of the elementary excitations dynamics in quantum electrodynamics. Besides, we should highlight that such important information has been obtained via rather simple and inexpensive experimental physics equipment.

References.

[1]. V.G. Plekhanov, Isotope effect renormalization of the energy of electrons by strong nuclear interaction, Deposit. in VINITI (Moscow) N202 - B2012, 1 - 13 (in Russian).

[2]. J. Chadwick, The existence of a neutron, Proc. Roy. Soc. (London) **136** (1932) 692 - 708.

[3]. H. Yukawa, On the interaction of elementary particles, Proc. Phys. Math. Soc. (Japan) 17 (1935) 8 – 57.

[4]. National Nuclear Center, http://www.nndc.bnl.gov.nudat2/

[5]. F.O. Barut, Unification based on electromagnetism, Annalen Phys. (Leipzig) **98** (1986). 83 – 92.

[6]. R. Hofstadter and R. Herman, Electric and magnetic structure of the proton and neutron, Phys. Rev. Lett. **6** (1961) 293 - 296.

[7]. R.M. Littauer, H.F. Schopper and R.R. Wilson, Structure of proton and neutron, ibid **7** (1961) 1 - 17.

[8]. A. Gell - Mann, A schematic model of baryons and mesons, Phys. Lett. **8** (1964) 214 - 215,

[9]. G. Zweig, An SU(3) model for strong interaction symmetry and its breaking, CERN - NH - 0 (1964).

[10]. G. Griffiths, Introduction to Elementary Particles, Wiley - VCH, Weinheim (2008).

[11]. D.H. Perkins, Introduction to High Energy Physics, Cambridge University Press, Cambridge, (2000).

[12]. C.D. Roberts, Empirical consequences of emergent mass, Symmetry **12** (2020) 1468 - 2004

[13]. .S. - X. Qin, C.D. Roberts, .M. Schmidt, Spectrum of light and heavy - baryons, Few - Body Systems **60** (2019) 26 - 44

[14]. M.Yu. Barabanov, M.A. Bedolla, W.K. Brooks et al., Diquark correlations in hadron physics: origin, impact and evidence, ArXiv /hep - ph/ 2008.07630, (2020). 113 pp.

[15]. V.G. Plekhanov, Isotope effect - a macroscopically manifestation of a strong nuclear long - range interaction, Atomic Energy **131** (2022) 121 – 126.

[16]. G. Eichman, H. Sandis - Alepuz, R. Williams et al., Baryon as relativistic three - quark bound states, ArXiv/ hep - ph/ 1606.09602 (2016) 140 pp.

[17]. R.D. Woods and D.S. Saxon, Diffuse surface optical model for nucleon – nuclei scattering Phys. Rev. **95** (1954) 577 – 578.

[18]. R.V. Reid, Local phenomenological nucleon - nucleon scattering, Annals of Phys. **50** (1968) 411 - 448.

[19]. J.R. Christman, The strong interaction, Michigan State University (2001).

[20]. R.M. Santilli, Representation of the anomalous magnetic moment of the muon via EPR completion of quantum into hadronic mechanics, Prog. Phys. **17** (2021)210 – 216.

[21]. V.G. Plekhanov, Isotope - induced energy - spectrum renormalization of the Wannier - Mott exciton in LiH, Phys. Rev. B**54** (1996) 3869 - 3877

[22]. V.G. Plekhanov, Fundamentals and applications of isotope effect in solids, Prog. Mat. Sci. **51** (2006) 287 – 426.

[23]. V.G. Plekhanov, Modern View of the Origin of Isotope Effect, LAMBERT Academic Publishing, Saarbrucken, Germany (2018).

[24]. D. Pines, Elementary Excitations in Solids, W.A. Benjamin Inc., New York (1963).

[25]. V.G. Plekhanov, Giant Isotope Effect in Solids, Stefan University Press, La Jola, USA (2004).

[26]. V.G. Plekhanov, Necessity addition, Phys. - Uspekhi (Moscow) **61** (2019) 49 – 50.

[27]. M. Born and H. Kun, Dynamical Theory of Crystal Lattices, Clarendon Press, Oxford (1954).

[28]. V.G. Plekhanov, Measurements of the wide value range of strong interaction coupling constant, SSRG - IJAP **6** (2019) 32 - 37

[29]. A. Deur, S.J. Brodsky, G.F. Teramond, The QCD running coupling constant, Prog. Part. Nucl. Phys. **90** (2016) 1 – 74.

[30]. E.U. Condon, Note on electron - neutron interaction, Phys. Rev. **49** (1936) 59 – 61.

[31]. L.L. Foldy, Neutron - electron interaction, Rev. Mod. Phys. **30** (1958) 71 – 81.

[32]. V.G. Plekhanov, Elementary excitations in isotope - mixed crystals, Phys. Reports **410** (2005) 1 – 235.

[33]. B. Schaeffer, Electric and magnetic Coulomb potentials in the deuteron, Adv. Electromagnet. **2** (2013) 69 – 72.

[34]. B. Povh, K. Rith, Ch. Scholz, F. Zetsche, Particles and Nuclei, Springer, Heidelberg, 2006.

[35]. N.L. Bowen, The electromagnetic considerations of the nuclear force, J. Cond. Matt. Nucl. Sci. **33** (2020) 198 – 223.

[36]. A.H. Compton, The size and shape of the electron, Phys. Rev. **14** (1919) 247 – 259.

[37]. L.D. Landau, About fundamental problems, in, Selected Papers, Vol.2, Science, Moscow (1969) pp. 431 - 434 (in Russian).

[38]. V.G. Plekhanov, J.G. Buitrago, Evidence of residual strong interaction in nuclear atomic level via isotopic shoft in LiH - Lid crystals, Prog. Phys. **15** (2019) 68 – 71.

[39]. G. Breit, Theory of Isotope Shift, Rev. Mod. Phys. **30** (1958) 507 – 517.

HADRONIC JOURNAL 46, 157 - 206 (2023)
DOI 10.29083/HJ.46.02.2023/SC157

TRUE DEFINITION OF COSMIC RED SHIFT AND A REVIEW ON COSMIC EXPANSION BASED ON MICROSCOPIC PHYSICAL CONSTANTS AND TRUE RED SHIFT

U. V. S. Seshavatharam
Honorary faculty, I-SERVE, Survey no-42, Hitech City
Hyderabad-84, Telangana, India
seshavatharam.uvs@gmail.com

S. Lakshminarayana
Department of Nuclear Physics, Andhra University
Visakhapatnam-03, AP, India
lnsrirama@gmail.com

Received April 29, 2023
Revised May 16, 2023

Abstract

Considering our recently proposed light speed expanding Hubble-Hawking Universe and considering the recent paper pertaining to cosmic halt authored by Cosmin Andrei, Anna Ijjas, and Paul J. Steinhardt and reviewed by Saul Perlmutter, in this paper we propose a very simple model of universe having early stage light speed expansion and current stage quantum halt accompanied by light speed rotation. Representing early cosmic expansion and rotation as an outward spiral, Hubble's law can be considered as a representation of current cosmic rotation having no further expansion. Proceeding further, we would like to emphasize the point that, traditional definition of cosmic red shift is absolutely wrong. Based on photon energy, true cosmic red shift must be defined as the ratio of change in wavelength to the observed wavelength of photon. Halting state of the current universe can be understood with a combined study of the gravitational potential energy of proton and electron separated by a distance of 0.84 fermi and half the product of reduced Planck's constant and current Hubble parameter.

Keywords: Planck ball; Quantum cosmology; Hubble-Hawking universe; Light speed expansion; Light speed rotation; Cosmic halt with quantum physics;

1. Introduction

It is very surprising to note that, after 20 years of a strong footing, based on 'quintessence' driven universe, within coming 100 million years, universe is coming to a halt and slowly getting contraction to form a big crunch [1]. This technical paper has been reviewed by one of the co-founders of the accelerating universe, Saul Perlmutter [2] and got published in the Proceedings of the National Academy of Sciences of USA in April 2022. It is certain that this paper will bring a radical change among mainstream cosmologists and engineers. As per the papers published in Astronomical Journal 2012 [3] and Nature-Scientific Reports 2016 [4], data pertaining to 580 to 740 super novae clearly reveal that, universe is expanding at an uniform rate. In 2018-2019, the same result has been obtained by a student Lisa Goh Wan Khee of National University of Singapore supervised by Cindy Ng [5]. This information can be considered as a base for current non-accelerating universe.

Mainstream cosmologists are strongly believing that, current expanding universe is having no center and no rotation [6]. Scientists who are strongly believing in cosmic rotation suggest that, current magnitude of cosmic angular velocity is very small in magnitude and is beyond the scope of observations [7,8,9]. Unfortunately, applications of cosmic angular velocity are also lagging in acquiring a strong foundation in constructing workable models of rotating cosmologies. In this context, we emphasize the following facts.

1) Quantum cosmology [10] point of view, in a theoretical approach, Spin or Rotation can be given a chance in developing quantum models of cosmology.
2) Current model of Lambda cosmology [11] is badly failing in incorporating quantum gravity concepts.
3) Very few cosmologists are working on quantum cosmology models.
4) Clearly speaking, no cosmologist is having a clear vision of quantum models of cosmology.

Keeping these points in view, we can confidently say that, models of cosmology without cosmic rotation cannot be considered as standard models

of cosmology. In support of this statement, we propose the following logical points.

1) Important point to be noted is that, to have rotation, universe should have a closed or positive curvature. Three most recent technical papers [12,13,14] published in three very high impact journals seem to support a closed universe. In this context, we would like to recall the views of Di Valentino, Melchiorri and Silk [12]. According their analysis and interpretation, observed enhanced lensing amplitude of cosmic microwave background radiation can be explained with a positive curvature of the universe at 99% confidence level. According to George Ellis and Julien Larena [13], the possibility that the universe might be positively curved, although it would not solve all the existing tensions at once, opens exciting theoretical possibilities for cosmology. Proceeding further, according to Will Handley [14] - In light of the inconsistency between Planck, CMB lensing and BAO data in the context of curved universes, cosmologists can no longer conclude that observations support a flat universe.
2) Hubble's observations [15] can also be studied with rotating and expanding models of cosmology. In a rotating frame, quantitatively Hubble's law resembles cosmic light speed rotation concept.
3) General theory of relativity is no way against to cosmic rotation [16]. In a non-accelerating universe, considering red shift as a measure of galactic distances and revolving speeds, references [3,4,5] can be considered as a supporting data for a rotating universe.
4) Without a radial in-flow of matter in all directions towards one specific point, one cannot expect a big crunch and without a big crunch, one cannot expect a big bang. Really if there was a "big bang" in the past, with reference to formation of big bang as predicted by GTR and with reference to the cosmic rate of expansion that might have taken place simultaneously in all directions at a "naturally selected rate" about the point of big bang: "point" of big bang can be considered as the characteristic reference point of cosmic expansion in all directions. Thinking in this way, either the point of big bang or baby Planck ball can be considered as a possible centre of cosmic evolution.

5) If observed universe is assumed to be associated with only one big bang, then 'point of big bang' can certainly be considered as the characteristic reference point of cosmic evolution in all directions.
6) If currently believed cosmic big bang is really a 'singularity', it seems more logical to depend on Planck scale rather than big bang. It may be noted that, in general, gravitational singularities are not clear about "Where, When and How" like essential points that are believed to be the basics of developing any workable physical model.
7) No model of cosmology is clear about the origin of cosmic thermal radiation. Even though big bang model is giving lot of information on cosmic thermal evolution, origin point of view, initial conditions are beyond the scope of big bang.
8) Both, Planck scale and big bang are being implemented simultaneously in understanding cosmic initial conditions leading to an ambiguous situation on whether to consider only big bang or only Planck scale.
9) Modern cosmological observations are providing strong evidences for the existence of mysterious rotational features of large cosmic filaments [17].
10) Current Hubble's constant can be considered as a limiting magnitude of current cosmic angular velocity. Similarly, light speed can be considered as a limiting magnitude of current cosmic rotation speed.
11) Current Hubble mass can be considered as a characteristic mass limit of current universe having a closed curvature.
12) So far, on large scale distances, physically,
    a) No galaxy is confirmed to have super-luminal speeds.
    b) No verification for actual galactic receding speeds.

2. Hubble-Hawking cosmology

Based on light speed expansion, modified red shift formula, scaled Hawking's black hole temperature formula, super gravity of galactic baryon matter and baby Planck ball – in our recent publications, we have clearly established a novel model of quantum cosmology [18-28]. This paper is a modified version of our recent paper [28] and the key change is that, we consider current cosmic halt and light speed rotation in place of assumed

current light speed expansion. Here we would like to appeal that, a new model of cosmology, that follows Hubble's notion of expansion and Hawking's notion of black hole structure having thermal radiation can be called as Hubble–Hawking model of cosmology. We continue this section with the need of considering light speed expansion and rotation.

2.1 Need of considering light speed expansion and rotation

Technical publications that are having very high impact on science community are raising many new ideas and doubts on dark energy and dark matter. Now it is very clear hat, there is a disagreement between main stream cosmologists and other researchers. Cosmological observations are not straight forward. For the same data, different interpretations are coming into picture with a great diversity. Right now it is not at all possible to prove the exact nature of cosmic expansion whether it is accelerating or decelerating. In this very ambiguous situation, it seems interesting to take the help of 'light speed' as a tool. There is a possibility for considering light speed radial expansion as well as light speed rotation. We would like to emphasize that,

1) All cosmological observations and physical studies & research are being accomplished with 'light speed' only.
2) So far no single experiment or no single observation confirmed super luminal physical results.
3) It is well confirmed that, gravitons are also moving with speed of light.
4) In one sentence, 'without light', there is no cosmology and there is no physics.

2.2 Present cosmic critical density, volume and mass

Currently believed cosmic critical density is, $\rho_0 \cong \left(3H_0^2/8\pi G\right)$. Considering the product of currently believed cosmic critical density and Hubble volume, $V_0 \cong \left(\frac{4\pi}{3}\right)\left(c/H_0\right)^3$, it is possible to show that, $M_0 \cong \left(c^3/2GH_0\right)$. On re-arranging this mass expression, $2GM_0/c^2 \cong c/H_0 \cong R_0$. It clearly indicates something new about the current universe in terms of current cosmic black hole mass, radius and expansion speed or rotation speed. We interpret this relation as, at present, $R_0 \cong \left(c/H_0\right) \cong 2GM_0/c^2$.

2.3 Present cosmic temperature

Currently believed cosmic temperature T_0 seems to be equal to the geometric mean of Hawking temperature [29] of Planck mass, $T_{M_{pl}} \cong \frac{\hbar c^3}{8\pi k_B G M_{pl}}$ and Hawking temperature of current cosmic Hubble mass, $T_{M_0} \cong \frac{\hbar c^3}{8\pi k_B G M_0}$. In a simplified form, it can be expressed as, $T_0 \cong \frac{\hbar c^3}{8\pi k_B G\sqrt{M_{pl} M_0}}$. It clearly indicates something new about the current cosmic temperature in terms of Hawking's Black hole physics. We interpret this relation as, with respect to Planck scale, $T_0 \cong \frac{\hbar c^3}{8\pi k_B G\sqrt{M_{pl} M_0}} \cong \frac{\hbar\sqrt{H_0 H_{pl}}}{4\pi k_B}$ where $M_0 \cong \frac{c^3}{2GH_0}$, $M_{pl} \cong \sqrt{\frac{\hbar c}{G}}$ and $H_{pl} \cong \frac{1}{2}\sqrt{\frac{c^5}{G\hbar}}$.

For an observed value of $T_0 \cong 2.72548$ K, estimated $H_0 \cong 2.167867 \times 10^{-18}$ sec^{-1} $\cong 66.89$ km/sec/Mpc. We would like to emphasize the point that, based on Hawking's black hole temperature formula, geometric mean of Planck mass and the so called Hubble mass, seems to play a crucial role in estimating the observed cosmic microwave back ground temperature, (CMBR) [30]. This kind of relation is missing in Lambda cosmology and to a great extent, currently observed discrepancy or tension in estimating the Hubble parameter can be eliminated. Proceeding further currently believed Baryon acoustic bubble radius [31] can be fitted with a simple relation of the form, $(R_{BAO})_0 \cong \sqrt{\frac{T_0}{T_{\text{Recombination}}}} * \left(\frac{c}{H_0}\right) \cong \sqrt{\frac{2.725 \text{ K}}{3000 \text{ K}}} * \left(\frac{c}{H_0}\right) \cong \frac{c}{H_{\text{Recomb}}^{1/4} H_0^{3/4}} \cong 135$ Mpc.

Considering both Planck mass and the Universe as 'point particles', cosmic temperature relation can be derived with three hypothetical conditions, $\frac{GM_0M_{pl}}{r_0^2} \cong \left(\frac{c^4}{8\pi G}\right)$; $r_0 \cong \left(\frac{2.898\times10^{-3}}{2\pi T_0}\right)$ and $M_0 \cong \left(\frac{c^3}{2GH_0}\right)$. Derived relation is, $T_0 \cong \frac{\hbar c^3}{24.891 k_B G\sqrt{M_{pl}M_0}}$ and the denominator coefficient 24.891 is close to $8\pi \cong 25.13274$.

2.4 Present galactic light travel distances

It may be noted that, by the time of defining the definition of galactic red shift, maximum red shift value was around 0.003. In this context, in terms of energy of photon, we would like to emphasize the point that, traditional definition of cosmic red shift is absolutely wrong. True cosmic red shift must be defined as - ratio of loss in energy of photon to the energy of photon at galaxy or lab. As a consequence, in terms of wavelength of photon, red shift can be defined as, the ratio of change in wavelength to the observed wavelength of photon. In a mathematical form, $z_{new} \cong \frac{E_{Lab} - E_{Observed}}{E_{Lab}} \cong \frac{\lambda_{Observed} - \lambda_{Lab}}{\lambda_{Observed}} \cong 1 - \frac{\lambda_{Lab}}{\lambda_{Observed}} \cong \frac{z}{z+1}$. With reference to current definition, $0 > z <$ Infinity. By following our new definition, $0 > z_{new} < 1$. It may be noted that, with our given definition, it is very easy to implement 'light speed rotation' in cosmic evolution scheme. Fig. 1 compares galactic light travel distances according to our new definition, $d_G \cong (z_{new})(c/H_0)$ (Red curve) and the conventional formula connected with dark energy density and other density fractions (Green curve). For verification, readers are encouraged to visit the URLs, http://www.atlasoftheuniverse.com/cosmodis.c and https://cosmocalc.icrar.org/. Richard Powell has written an online C program (http://www.atlasoftheuniverse.com/cosmodis.c) (version 1.1) for estimating the light travel distance [32]. See Appendix A for the C++ program. Using that program and considering a redshift of z = (0.1 to 200), we have prepared Figure 1. Green curve indicates the light travel distance in Lambda cosmology prepared with Omega matter = 0.32, Omega lambda = 0.68, Omega radiation = 0.0 and H_0 = 66.87 km/sec/Mpc. Figure 1 will certainly encourage any cosmologist to solve Einstein's field equations with a closed curvature spreading at speed of light and rotating at speed of light. As traditional redshift is increasing from 0, error in estimated light travel distance is increasing to

+8.59% at $z \cong 1.20$ and from there onwards, error is reaching to 0% at $z \cong 11.5$ to 11.55. Proceeding further, error is reaching to -5.14% at $z \cong 200.0$. By considering $z_{new}c$ as the revolving speed of galaxy (about cosmic axis if it exists), Hubble's law [15] can be expressed as, $v_G \cong H_0 d_G$.

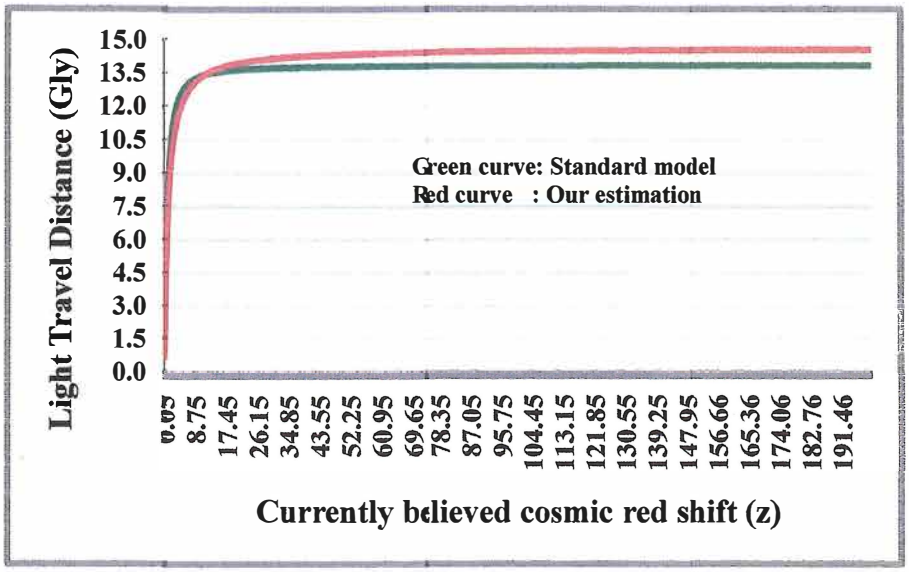

Figure 1. Comparison of standard and estimated light travel distances

3. Our 6 basic assumptions pertaining to cosmic structure and galactic structure

Based on the above points and logics proposed in sections (1) and (2),

1) We emphasize the point that, without a radial in-flow of matter in all directions towards any one specific point, it may not be possible to have a big crunch and discussing on center-less universe having a big bang or big bounce seems to be meaningless.
2) Considering the evolving universe as a growing black hole or simply a white hole [20,21], it seems natural to expect cosmic rotation.

In this section, considering the current Hubble's constant as an index of current cosmic angular velocity, we propose a simple model of light speed expanding and light speed rotating model of cosmology. It needs a review at fundamental level. Out of 6 assumptions, first four assumptions are associated with cosmic structure and expansion and the last two assumptions are associated with dark matter and galactic structure.

Assumption-1: At present, cosmic angular velocity is equal to the present Hubble constant. Mathematically, at present,

$$\begin{aligned} &\omega_0 \cong H_0 \text{ ----(1A)..Fitting with current data.} \\ &\omega_t \cong H_t \text{ ----(1B)..To be confirmed with further study for } (z+1) > 1100. \end{aligned} \tag{1}$$

Assumption-2: Universe is expanding like a black hole with initial light speed expansion and rotation and finally halted with light speed rotation. Mathematically, at present,

$$R_0 \cong \frac{2GM_0}{c^2} \cong \frac{c}{\omega_0} \tag{2}$$

Assumption-3: Universe is expanding like a black hole with a scaled Hawking's black hole temperature formula. Mathematically, it can be expressed as,

$$T_0 \cong \frac{\hbar c^3}{8\pi k_B G\sqrt{M_{pl}M_0}} \cong \frac{\hbar\sqrt{\omega_0\omega_{pl}}}{4\pi k_B} \tag{3}$$

$$\text{where } M_0 \cong \frac{c^3}{2G\omega_0},\ M_{pl} \cong \sqrt{\frac{\hbar c}{G}} \text{ and } \omega_{pl} \cong \frac{1}{2}\sqrt{\frac{c^5}{G\hbar}}.$$

It may be noted that, this assumption certainly helps in eliminating the tension in estimating the magnitude of Hubble parameter.

Assumption-4: Following light speed rotation, at present cosmic expansion is coming to a halt. Considering proton and electron rest masses, in a quantum mechanical approach it can be understood as,

$$\frac{Gm_p m_e}{R_p \omega_0} \equiv \frac{\hbar}{2} \tag{4}$$

where $R_p \cong (0.84184 \text{ to } 0.87680)$ fm is the root mean square radius of proton [33].

Assumption-5: There exists no dark matter [34-38] and when baryon mass of any galaxy crosses (180 to 200) million solar masses, galaxy 'as a whole' experiences super gravity [22,26] in such a way that its effective or total mass can be expressed as,

$$\begin{aligned}(M_{Total})_G &\cong \left\{(M_{baryon})_G + \left[\frac{(M_{baryon})_G^{3/2}}{\sqrt{(M_{\text{limit}})_0}}\right]\right\} \ldots.(\text{without dark matter}) \\ &\cong \left\{(M_{baryon})_G + (M_{dark})_G\right\} \ldots\ldots(\text{if there exists dark matter})\end{aligned} \tag{5}$$

$$\text{where, } \begin{cases} (M_{\text{limit}})_0 \cong \text{Current mass limit of ordinary gravity} \\ \qquad = 180 \text{ to } 200 \text{ solar masses} \cong (3.6 \text{ to } 4.0)\times 10^{38} \text{ kg.} \\ (M_{baryon})_G = \text{Galactic baryon mass.} \\ (M_{dark})_G = \text{Galactic dark mass.} \\ (M_{Total})_G = \text{Total mass of Galaxy.} \end{cases}$$

Starting from the recombination period, for $(M_{\text{limit}})_0$, its current cosmological mass expression can be expressed as,

$$\frac{M_0}{(M_{\text{limit}})_0} \cong \exp\left(\sqrt{\frac{T_{\text{Recomb}}}{T_0}}\right)$$

$$\text{where } M_0 \cong \frac{c^3}{2G\omega_0} \text{ and } \frac{T_{\text{Recomb}}}{T_0} \cong \frac{\text{Recombination temperature}}{\text{Current cosmic temperature}} \cong \frac{3000 \text{ K}}{2.725 \text{ K}}.$$

Assumption-6: Current cosmic mass plays a vital role in understanding the observed galactic flat rotation speeds in such a way that,

$$\frac{V_G}{c} \cong \frac{1}{4}\left[\frac{(M_{Total})_G}{M_0}\right]^{1/4} \tag{6}$$

$$V_G \cong 0.2973\left[G(M_{Total})_G(c\omega_0)\right]^{1/4} \tag{7}$$

It may be noted that, this relation is very similar to the famous MOND's formula [33]. Interesting point to be noted is that $(c\omega_0)$ can be considered as the upper limit of current cosmic acceleration. In addition to that, MOND's concept of weak gravity can be studied in terms of Mach's view on the universal role of cosmic distance back ground [39]. See Fig. 2 for the estimated galactic flat rotation speeds.

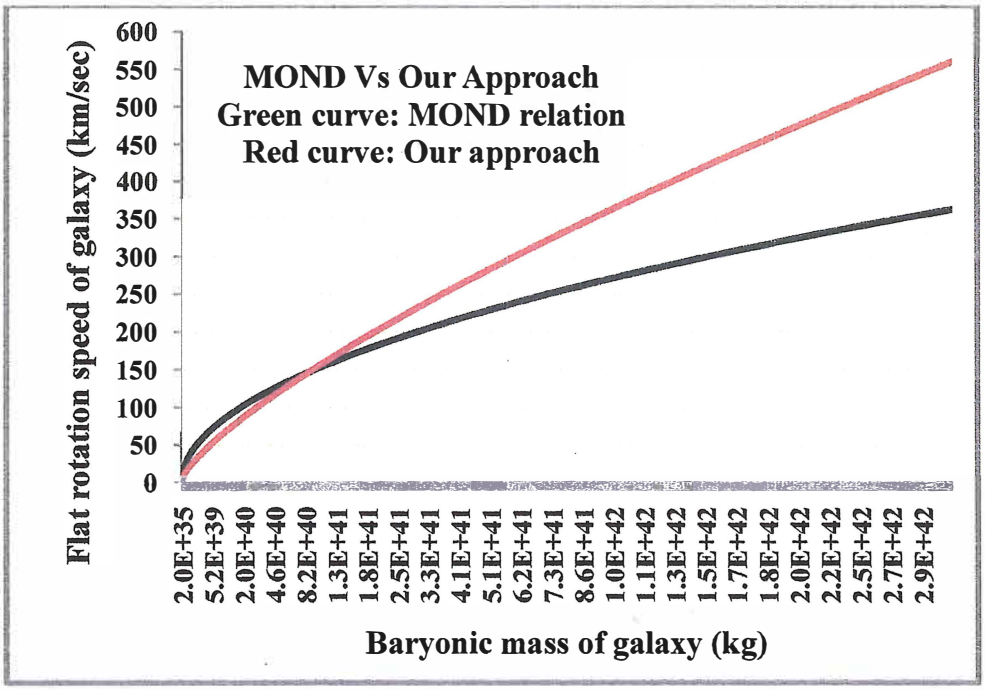

Figure 2: Galactic flat rotation speeds

Flat rotation speeds from 10 km/sec to 500km/sec can be understood in this way. Our proposal is in line with newly discovered dark matter deficient galaxies [40] and large massive galaxies having high flat rotation speeds [41]. Another interesting feature is that, Sun's estimated equivalent dark mass is

around $1.5x10^{26}$ kg and its effect seems to be negligible. It needs observational and experimental confirmation. To some extent, considering the estimated Virial mass of Sun and based on the theory of light bending, our proposal can be confirmed. Nucleons estimated equivalent dark mass is around 10^{-60} kg and it needs experimental verification.

4. Discussion on present cosmic rotation

Historically, Godel, Gamow, Whittakar, Hawking, Narlikar, Nodland, Ralston, Rubin, Birch, Korotky, Obukhov, Chechin, Sivaram, Magueijo and Longo like many cosmologists expressed their positive opinion on cosmic rotation [7-9],[42-47]. Recent observations on cosmic anisotropy [48] and galactic spin directions seem to support the possible existence of cosmic rotation [49]. Most recent references [12,13,14] seem to shed light on the necessity of considering cosmic positive curvature which is a major prerequisite for cosmic rotation. Even though cosmological principle [50,51] is having 100 years of strong footing, at present, it is being suspected and examined in many directions seriously. It may also be noted that, the argument that the Universe does not rotate is not based on observational evidence, but is merely an assumption that became popular.

It may be noted that, by considering 'light speed rotation' and ignoring 'light speed expansion', Einstein's static universe can be made stable dynamically. There seems no need to introduce the 'Lambda term'. Against to the strongly believed current cosmic acceleration [2], if current universe is having a trend of deceleration as proposed by Paul J. Steinhardt et al and reviewed by Perlmutter S. [1] – by considering light speed rotation throughout the cosmic history- there is a scope for developing light speed rotating and decelerating models of cosmology [18]. We are working on understanding and validating the dual role of light speed in cosmic expansion and rotation. With ongoing observations, whether it is cosmic light speed expansion or light speed rotation - can be explored in all possible ways.

5. Discussion on present cosmic halt

Based on ref. [1], it seems very clear to say that, dark energy is taking a new turn and making the universe to decelerate and within 100 million years, universe is coming to a halt. Here it is very important to note that, so far no

single observation or no single experiment has shown a signal for the existence of dark energy. Cosmologists are somehow making attempts to understand the expanding nature of current universe in terms of dark energy for acceleration as well as deceleration. If it is really true that, in near future, universe is going to a halt, based on assumptions (1) to (4), it can be understood in terms of unification of atomic and cosmic physical constants [52-56]. Relation (4) can be re-written as,

$$\frac{Gm_p m_e}{R_p} \equiv \frac{1}{2}\hbar\omega_0 \quad ---(8A)$$

$$\frac{2Gm_p m_e}{\hbar R_p} \equiv \omega_0 \cong (67.88 \text{ to } 70.69)\,\text{km/sec/Mpc} ---(8B) \qquad (8)$$

where $R_p \cong (0.84184 \text{ to } 0.87680)$ fm

Here in this expression, LHS is a representation of gravitational potential energy of proton and electron separated by a distance equal to the root mean square radius of proton. RHS seems to be a representation of ground state quantum of energy associated with cosmic angular velocity and characteristic quantum constant.

Following relation (4), quantum of orbiting electron's areal velocity can be expressed as,

$$\frac{dA}{dt} \cong \frac{1}{2}vr \cong \frac{Gm_p}{R_p\omega_0} \qquad (9)$$

Based on our 4G model of unification [57-60], we noticed that [61],

$$R_p \cong \sqrt{\frac{\alpha_s}{\alpha}}\left(\frac{\hbar}{m_p c}\right) \cong \sqrt{\frac{0.115 \text{ to } 0.12}{0.0073}}\left(\frac{\hbar}{m_p c}\right) \cong (4 \mp 0.05)\left(\frac{\hbar}{m_p c}\right) \cong 4\left(\frac{\hbar}{m_p c}\right) \qquad (10)$$

where α_s is the strong coupling constant and α is the fine structure ratio.
Hence, it is also possible to write another two relations in the following way.

$$\sqrt{\frac{Gm_p^2 m_e c}{2\omega_0}} \cong \hbar \text{---(11A)}$$

$$\frac{Gm_p^2 m_e c}{2\hbar^2} \cong \omega_0 \cong 70.75 \text{ km/sec/Mpc---(11B)} \tag{11}$$

Another very interesting relation is associated with fine structure ratio. For $\omega_0 \cong H_0 \cong 76.266$ km/sec/Mpc,

$$\frac{1}{\alpha} \cong \ln \sqrt{\frac{(E_T)_0/2}{(E_{em})_0}} \cong \ln \sqrt{\frac{4\pi\varepsilon_0 c^6}{23040\pi G\omega_0^2 e^2}} \cong 137.036 \tag{12}$$

where

$(E_T)_0 \cong aT_0^4 \left(\frac{4\pi}{3} \left(\frac{c}{\omega_0} \right)^3 \right) \cong$ Current thermal energy within the current Hubble volume.

$(E_T)_0 / 2 \cong$ Half of $aT_0^4 \left(\frac{4\pi}{3} \left(\frac{c}{\omega_0} \right)^3 \right)$

$\cong$ Current thermal energy within the current hemi spherical or dipole Hubble volume.

$(E_{em})_0 \cong \frac{e^2}{4\pi\varepsilon_0 (c/\omega_0)} \cong$ Electromagnetic potential assocaited with current Hubble radius.

Readers are encouraged to refer the URL for various values of the current Hubble parameter estimated with various methods: https://en.wikipedia.org/wiki/Hubble%27s_law. From the data it is clear that, $H_0 \cong$ (67.6 to 76.2) km/sec/Mpc. Relation (12) seems to give a nice picture of the current cosmic closed or positive curvature and it needs a very special study at fundamental level.

6. General discussion on quantum cosmology

Quantum cosmology point of view, our assumptions are very clear and seem to incorporate Planck scale in current cosmic observations. Our assumptions (1) to (4) are giving a very nice explanation for the origin of current cosmic temperature and its observed isotropy on large scales. Proceeding further,

halting of the universe with atomic, nuclear and quantum physical constants seem to open a new branch of cosmology associated with microscopic physics. We are working on finding other such relations. It is well believed that, Hawking's findings about black holes and the universe [62] are the most important contributions to physics in recent decades. Proposed Hawking's scaled black hole temperature formula can be given a chance in understanding and refining the views of Hawking's multi universal paradigm.

1. General discussion on Hubble's law in view of cosmic rotation

Following section (2.4), if one is willing to consider cosmic red shift definition as,

$$z_{new} \cong \frac{\lambda_{Observed} - \lambda_{Lab}}{\lambda_{Observed}} \cong 1 - \frac{\lambda_{Lab}}{\lambda_{Observed}} \cong \frac{z}{z+1} \tag{13}$$

It will certainly help in understanding and resolving the issues connected with cosmic acceleration and dark energy. Based on this new definition of cosmic red shift, observed farthest galaxies distance can be estimated very easily. For example, see the following Table 1. We sincerely appeal that, on cosmological scales, 2.5% is not yet all a 'serious' error. We would like to emphasize the point that, conceptually, we are no way deviating from the basic idea of cosmic expansion. Only thing is that, we are confining to 'initial light speed expansion and rotation' and 'present light speed rotation with no further expansion'. Whether current/future universe is expanding or not can be understood with,

a) Rate of decrease in cosmic temperature.
b) Rate of decrease in Hubble parameter.

Based on the data presented in Tab. 1 Hubble's law for cosmic rotation applicable to whole Hubble volume can be expressed as,

$$d_G \omega_0 \cong \left(\frac{z}{z+1}\right) c \cong (z_{new})\, c \tag{14}$$

Cosmic scale factor seems to be associated with time and temperature rather than red shift. Scale factor can be expressed as,

$$1+z \cong \sqrt{\exp(\gamma_0 - \gamma_t)} \cong \frac{T_t}{T_0} \tag{15}$$

where $\gamma_0 \cong 1+\ln\left(\frac{\omega_{pl}}{\omega_0}\right)$ and $\gamma_t \cong 1+\ln\left(\frac{\omega_{pl}}{\omega_t}\right)$

$T_t, T_0 \cong$ Past and current cosmic temperatures.

Table-1: To estimate and fit the distances of farthest galaxies

Galaxy	Redshift	Standard Light travel distance (Gly)	Estimated Light travel distance (Gly)	%Error
GN-z11	11.09	13.39	13.41	-0.15
MACS1149-JD1	9.11	13.26	13.17	0.65
EGSY8p7	8.68	13.23	13.11	0.91
A2744 YD4	8.38	13.2	13.06	1.05
EGS-zs8-1	7.73	13.13	12.95	1.41
z7 GSD 3811	7.66	13.11	12.93	1.36
z8_GND_5296	7.51	13.1	12.9	1.51
SXDF-NB1006-2	7.215	13.17	12.84	2.5
GN-108036	7.213	13.07	12.84	2.5
BDF-3299	7.109	13.05	12.84	2.5
A1703 zD6	7.014	13.04	12.84	2.5
BDF-521	7.008	13.04	12.84	2.5
G2-1408	6.972	13.03	12.84	2.5
IOK-1	6.964	13.03	12.84	2.5

Following our approach, currently believed cosmic time scale up to $1+z=1100$ can be expressed as,

$$t\omega_t \cong \sqrt{1+z} \tag{16}$$

It is an accurate fit and needs a careful review for its strange matching. We are working in this direction. If so,

$$t \cong \left(\frac{1}{1+z}\right)^{\frac{3}{2}}\left(\frac{1}{H_0}\right) \cong \left(\frac{1}{1+z}\right)^{\frac{3}{2}}\left(\frac{1}{\omega_0}\right) \cong \frac{\sqrt{1+z}}{\omega_t} \cong \frac{\left[\exp(\gamma_0 - \gamma_t)\right]^{\frac{1}{4}}}{\omega_t} \tag{17}$$

where $\omega_t \cong \left(\frac{1}{\omega_{pl}}\right)\left(\frac{4\pi k_B T_t}{\hbar}\right)^2 \cong 2\sqrt{\frac{G\hbar}{c^5}}\left(\frac{4\pi k_B T_t}{\hbar}\right)^2$.

Interesting observation to be noted is that,

$$\frac{\omega_t}{\omega_0} \cong \exp(\gamma_0 - \gamma_t) \cong (1+z)^2 \tag{18}$$

8. Estimation of distances associated with galactic flat rotation speeds

Following assumptions (5) and (6), we suggest the following points for further study and observation.

1) Galactic total mass can be considered as the sum of galactic baryonic mass and dark mass.
2) As galactic total mass increases, galactic flat rotation speed as well as the distance associated with flat rotation speed increases.
3) Galactic core radius seems to depend on galactic baryon mass, current cosmic Hubble mass and the ratio of galactic baryon mass to total mass.
4) Galactic flat rotation distance seems to depend on galactic total mass, current cosmic Hubble mass and the ratio of galactic baryon mass to total mass.

Based on these points, we noticed a very simple relation for galactic flat rotation distances. It can be expressed as,

$$\begin{aligned} r_f &\cong \frac{2G\sqrt{\left(M_{baryon}\right)_G M_0}}{c^2} \\ &\cong \sqrt{\left(\frac{2G\left(M_{baryon}\right)_G}{c^2}\right)\left(\frac{c}{\omega_0}\right)} \cong \sqrt{\frac{2G\left(M_{baryon}\right)_G}{c\omega_0}} \end{aligned} \tag{19}$$

where $\begin{cases} r_f = \text{Distance from galactic center associated with flat rotation speed.} \\ M_0 \cong \dfrac{c^3}{2G\omega_0} = \text{Current cosmic Hubble mass.} \end{cases}$

Galactic core radius can be expressed as,

$$r_c \cong \sqrt{\frac{M_0}{(M_{Total})_G}}\left(\frac{2G(M_{baryon})_G}{c^2}\right) \tag{20}$$

Based on relations (19) and (20),

$$\frac{r_f}{r_c} \cong \frac{\text{Distance from galactic center associated with flat rotation speed}}{\text{Galactic core radius}} \cong \sqrt{\frac{(M_{Total})_G}{(M_{baryon})_G}} \cong \sqrt{1+\frac{(M_{dark})_G}{(M_{baryon})_G}} \tag{21}$$

Interesting point to be noted is that, by knowing the galactic flat rotation speed and flat rotation distance, galactic baryon mass, galactic total mass and hence galactic dark mass can be estimated in a unified approach. This is for observational test. Galactic whole radius can be expressed as,

$$R_G \cong \frac{G(M_{Total})_G}{V_G^2} \cong \left(\frac{16G\sqrt{(M_{Total})_G M_0}}{c^2}\right) \cong \sqrt{\frac{128G(M_{Total})_G}{c\omega_0}} \tag{22}$$

It may be noted that, based on relations (19) to (22), galactic masses, flat rotation speeds and corresponding distances can be studied in a unified approach. Estimated baryon and dark masses can be compared with existing methods. Advantage of our approach is that, current cosmic Hubble mass can be considered as a key tool in exploring the structural secrets of galaxies.

See Tab. 2 for galactic masses, flat rotation speeds and working radii. See Fig. 3 for estimated galactic flat rotation distances. Galactic rotation curves for $r \geq r_c$ can be approximated with the following relations. It needs a fine tuning based on the actual curve [63].

Table 2. Galactic masses, flat rotation speeds and working radii						
Assumed baryon mass $M_\odot$	**Estimated dark mass $M_\odot$**	**Estimated total mass $M_\odot$**	**Estimated flat rotation speed (km/sec)**	**Estimated core radius (kpc)**	**Estimated flat rotation distance (kpc)**	**Estimated whole radius (kpc)**
5.03E+05	2.51E+04	5.28E+05	4.34	0.014	0.015	0.120
7.54E+05	4.62E+04	8.00E+05	4.82	0.017	0.018	0.148
1.13E+06	8.48E+04	1.22E+06	5.35	0.021	0.022	0.183
1.70E+06	1.56E+05	1.85E+06	5.95	0.026	0.027	0.225
2.55E+06	2.86E+05	2.83E+06	6.61	0.031	0.033	0.279
3.82E+06	5.26E+05	4.34E+06	7.36	0.038	0.040	0.345
5.73E+06	9.66E+05	6.69E+06	8.20	0.046	0.049	0.428
8.59E+06	1.78E+06	1.04E+07	9.15	0.055	0.061	0.533
1.29E+07	3.26E+06	1.61E+07	10.22	0.066	0.074	0.665
1.93E+07	5.99E+06	2.53E+07	11.43	0.079	0.091	0.833
2.90E+07	1.10E+07	4.00E+07	12.82	0.095	0.111	1.047
4.35E+07	2.02E+07	6.37E+07	14.40	0.113	0.136	1.321
6.52E+07	3.72E+07	1.02E+08	16.21	0.133	0.167	1.675
9.78E+07	6.83E+07	1.66E+08	18.30	0.157	0.204	2.134
1.47E+08	1.25E+08	2.72E+08	20.70	0.184	0.250	2.731
2.20E+08	2.30E+08	4.51E+08	23.48	0.214	0.307	3.514
3.30E+08	4.23E+08	7.53E+08	26.71	0.249	0.376	4.544
4.95E+08	7.77E+08	1.27E+09	30.45	0.287	0.460	5.906
7.43E+08	1.43E+09	2.17E+09	34.80	0.330	0.563	7.714
1.11E+09	2.62E+09	3.74E+09	39.86	0.377	0.690	10.122
1.67E+09	4.82E+09	6.49E+09	45.76	0.429	0.845	13.339
2.51E+09	8.86E+09	1.14E+10	52.63	0.486	1.035	17.647
3.76E+09	1.63E+10	2.00E+10	60.64	0.549	1.268	23.430
5.64E+09	2.99E+10	3.55E+10	69.98	0.619	1.553	31.205
8.46E+09	5.49E+10	6.34E+10	80.88	0.695	1.902	41.674
1.27E+10	1.01E+11	1.14E+11	93.57	0.779	2.329	55.789
1.90E+10	1.85E+11	2.04E+11	108.38	0.871	2.852	74.837
2.86E+10	3.40E+11	3.69E+11	125.63	0.972	3.493	100.564
4.28E+10	6.25E+11	6.68E+11	145.74	1.083	4.279	135.333
6.43E+10	1.15E+12	1.21E+12	169.17	1.206	5.240	182.348
9.64E+10	2.11E+12	2.21E+12	196.48	1.341	6.418	245.951
1.45E+11	3.88E+12	4.02E+12	228.28	1.490	7.860	332.024
2.17E+11	7.12E+12	7.34E+12	265.33	1.655	9.627	448.539
3.25E+11	1.31E+13	1.34E+13	308.48	1.836	11.790	606.300
4.88E+11	2.40E+13	2.45E+13	358.74	2.037	14.440	819.950
7.32E+11	4.42E+13	4.49E+13	417.27	2.258	17.685	1109.333
1.10E+12	8.11E+13	8.22E+13	485.43	2.503	21.660	1501.342
1.65E+12	1.49E+14	1.51E+14	564.80	2.773	26.528	2032.429
2.47E+12	2.74E+14	2.76E+14	657.21	3.072	32.490	2751.996

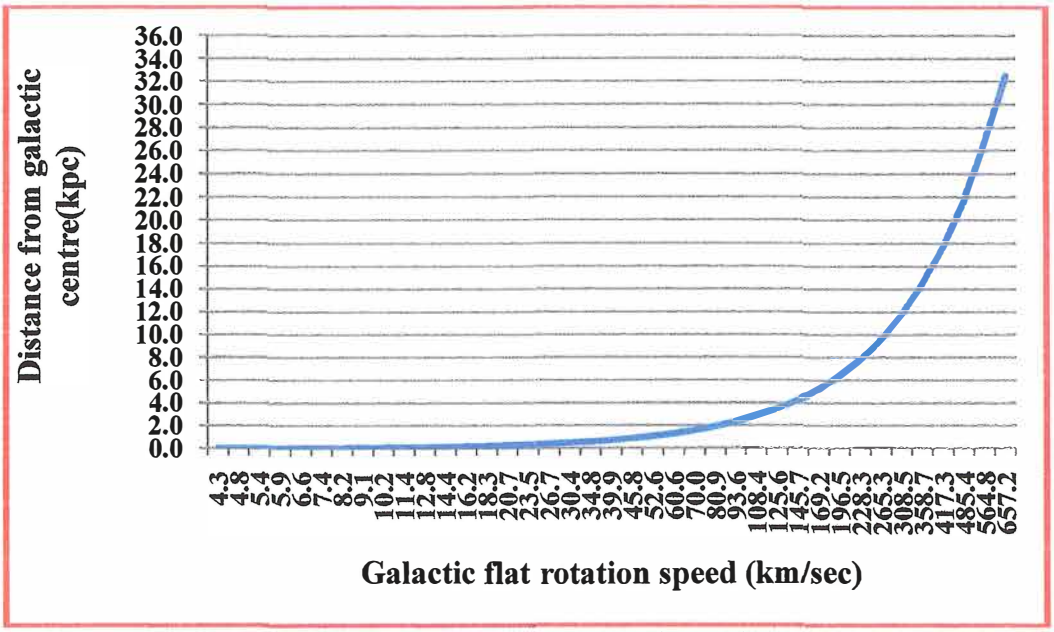

Figure 3: Galactic flat rotation speeds Vs distances

$$\left.\begin{aligned} V_r &\cong \frac{1}{3}\left[1+\ln\left(\frac{r}{r_c}\right)+\frac{1}{2}\ln\left(\frac{(M_{Total})_G}{(M_{baryon})_G}\right)\right]\left[\frac{G(M_{Total})_G V_{Ref}^2}{r}\right]^{\frac{1}{4}} \quad ---(23A)\\ V_r &\cong \frac{1}{3}\left[1+\ln\left(\frac{r}{r_c}\right)+\frac{1}{3}\ln\left(\frac{(M_{Total})_G}{M_{(M_{baryon})_G}}\right)\right]\left[\frac{G(M_{Total})_G V_{Ref}^2}{r}\right]^{\frac{1}{4}} \quad ---(23B)\end{aligned}\right\} \quad (23)$$

$$\text{where} \begin{cases} V_{\text{Ref}} \cong \left[\dfrac{G(M_{\text{Ref}})_0\, c\omega_0}{128}\right]^{1/4} \cong 19.2 \text{ km/sec} \\ (M_{\text{limit}})_0 \cong 4\times10^{38}\,\text{kg} = 200 \text{ million solar masses} \end{cases}$$

Thus, the proposed reference mass unit of 200 million solar masses seems to play a crucial role in deciding galactic structures.

See the following Fig. 4 pertaining to estimated Milky Way rotation Curves for 1.4 kpc to 319 kpc [64]. Estimated baryon mass, dark mass and total mass of Milky Way are, $1.2\times10^{11}M_{\odot}$, $2.94\times10^{12}M_{\odot}$ and $3.06\times10^{12}M_{\odot}$ respectively.

Based on relation (23), in terms of galactic core radius and flat rotation distance, galactic rotation curve can be re-expressed as,

$$\left.\begin{aligned} V_r &\cong \frac{1}{3}\left[1+\ln\left(\frac{r}{r_c}\right)+\ln\left(\frac{r_f}{r_c}\right)\right]\left[\frac{G\left(M_{Total}\right)_G V_{Ref}^2}{r}\right]^{\frac{1}{4}} \quad ----(24\text{A}) \\ V_r &\cong \frac{1}{3}\left[1+\ln\left(\frac{r}{r_c}\right)+\frac{2}{3}\ln\left(\frac{r_f}{r_c}\right)\right]\left[\frac{G\left(M_{Total}\right)_G V_{Ref}^2}{r}\right]^{\frac{1}{4}} \quad ---(24\text{B}) \end{aligned}\right\} \qquad (24)$$

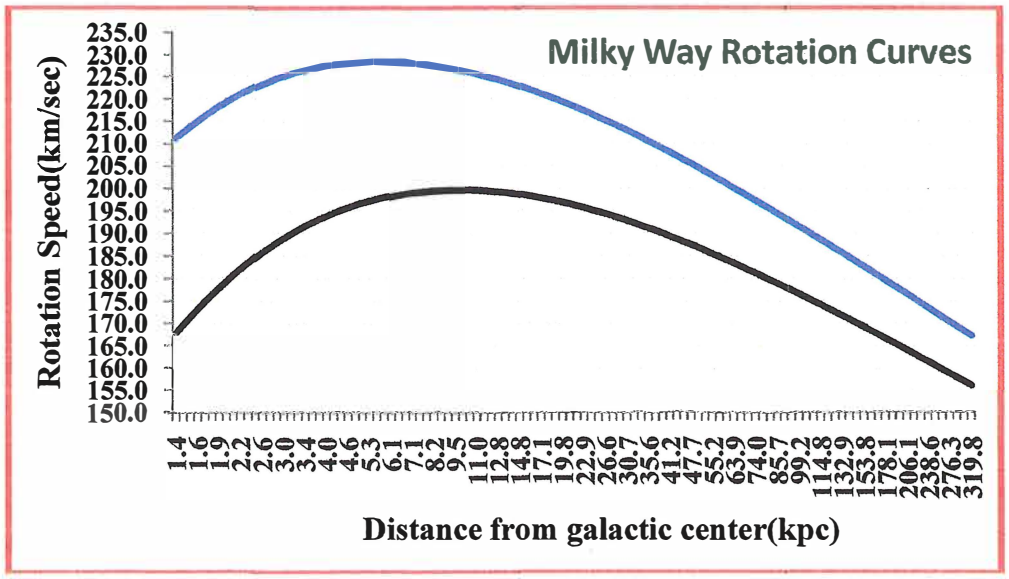

Figure 4: Estimated Milky Way Rotation Curves

Considering relations (19) and (20) and by knowing the galactic flat rotation speeds, galactic total masses and galactic radii can be estimated without the need of currently believed 'dark matter halo' concepts and their complicated analytical procedures.

Based on relations (19) to (24), one can understand the potential applications of current cosmic angular velocity or rotation speed in exploring the constructional secrets of galaxies. It needs further study.

It may be noted that, considering a rotating and expanding model of cosmology, it seems possible to say that,

1) Galaxies seem to follow an outward spiral path.
2) Galaxies can be seemed to be arranged in a systematic order.
3) Even though present universe is believed to be accelerating, as current expansion rate is very small, increase in separation distance between neighboring galaxies seems to be negligible. Hence, distance between neighboring galaxies seems to be approximately fixed.

Based on the new red shift definition as discussed in section (7), various distances associated with galactic light can be understood in the following way.

Light Travel Distance can be approximated with,

$$LTD \cong z_{new}\left(\frac{c}{\omega_0}\right) \tag{25}$$

Comoving Distance can be approximated with,

$$CD \cong \exp(z_{new}) * LTD \tag{26}$$

Hence, Hubble's law for galactic comoving distances can be expressed as,

$$CD_{gal} \cong z_{new}\exp(z_{new}) * \left(\frac{c}{\omega_0}\right) \text{ where } z_{new} \leq 1 \tag{27}$$

For Lambda model of cosmology, corresponding receding speed of a galaxy can be expressed as, $V_{gal} \cong [z_{new}\exp(z_{new})]c \cong \left[\left(\frac{z}{1+z}\right)\exp\left(\frac{z}{1+z}\right)\right]c$

For $z_{new} \cong 1$, $CD_{gal} \cong \exp(1) * \left(\frac{c}{\omega_0}\right) \cong 2.7183\left(\frac{c}{\omega_0}\right) \cong 39.74$ Gly.

It may be noted that, according to Lambda model of cosmology, radius of observable universe is around 45 Gly.

Luminosity Distance can be approximated with,

$$LD \cong \frac{CD}{1-z_{new}} \cong \left(\frac{z_{new}\exp(z_{new})}{1-z_{new}}\right)\left(\frac{c}{\omega_0}\right) \tag{28}$$

See Fig. 5 and Table 3. See Appendix A for the C++ program.

Column Details of Table 3

Column-1: Red shift
Column-2: Modified Red shift
Column-3: Light travel distance as per Lambda Cosmology (Gly)
Column-4: Light travel distance in Hubble-Hawking Cosmology (Gly)
Column-5: % error in Light travel distance (Blue curve in the graph)
Column-6: Comoving distance as per Lambda Cosmology (Gly)
Column-7: Comoving distance in Hubble-Hawking Cosmology (Gly)
Column-8: % error in Comoving distance (Red curve in the graph)
Column-9: Luminosity distance as per Lambda Cosmology (Gly)
Column-10: Luminosity distance in Hubble-Hawking Cosmology (Gly)
Column-11: % error in Luminosity distance (Red curve in the graph)

Note-1: LC = Lambda cosmology and HHC = Hubble-Hawking cosmology
Note-2: Numerically, columns 8 and 11 are almost same.

Data values: H_0 = 66.89 km/sec/Mpc;
Matter density %= 0.32%;
Dark energy density %= 0.68%

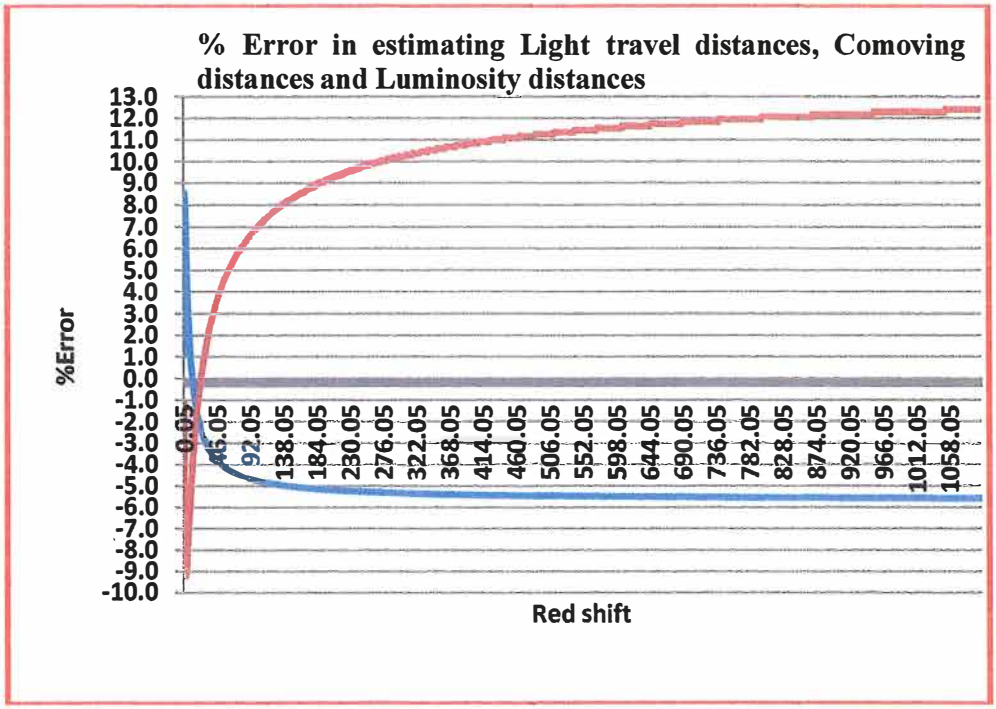

Figure 5: Comparative study of various cosmological distances

Table 3: Various cosmological distances estimated with true cosmic red shift

Z	z/(1+z)	LTD_LC	LTD_HHC	%Error	CD_LC	CD_HHC	%Error	LD_LC	LD_HHC	%Error
(1)	(2)	(3)	(4)	(5)	(6)	(7)	(8)	(9)	(10)	(11)
0.05	0.048	0.704	0.696	1.174	0.722	0.730	-1.149	0.76	0.767	-1.149
1.05	0.512	8.188	7.487	8.558	11.545	12.495	-8.233	23.67	25.616	-8.233
2.05	0.672	10.643	9.825	7.685	17.618	19.241	-9.211	53.74	58.685	-9.211
3.05	0.753	11.735	11.008	6.197	21.435	23.376	-9.059	86.81	94.674	-9.059
4.05	0.802	12.324	11.723	4.875	24.085	26.142	-8.537	121.63	132.014	-8.537
5.05	0.835	12.681	12.201	3.784	26.056	28.114	-7.898	157.64	170.088	-7.898
6.05	0.858	12.918	12.544	2.894	27.599	29.589	-7.210	194.57	208.602	-7.210
7.05	0.876	13.083	12.802	2.152	28.842	30.733	-6.556	232.18	247.403	-6.556
8.05	0.890	13.204	13.002	1.528	29.873	31.646	-5.936	270.35	286.400	-5.936
9.05	0.900	13.296	13.163	1.000	30.748	32.392	-5.344	309.02	325.537	-5.344
10.05	0.910	13.367	13.295	0.545	31.501	33.012	-4.794	348.09	364.778	-4.794
11.05	0.917	13.424	13.404	0.149	32.158	33.535	-4.283	387.50	404.098	-4.283
12.05	0.923	13.471	13.497	-0.196	32.742	33.983	-3.790	427.28	443.479	-3.790
13.05	0.929	13.509	13.577	-0.505	33.254	34.371	-3.357	467.22	482.909	-3.357
14.05	0.934	13.541	13.646	-0.775	33.726	34.710	-2.916	507.58	522.378	-2.916
15.05	0.938	13.568	13.707	-1.022	34.143	35.008	-2.535	547.99	561.879	-2.535
16.05	0.941	13.591	13.760	-1.245	34.520	35.273	-2.182	588.57	601.407	-2.182
17.05	0.945	13.611	13.808	-1.443	34.876	35.510	-1.818	629.51	640.957	-1.818
18.05	0.948	13.629	13.850	-1.626	35.198	35.723	-1.493	670.52	680.526	-1.493
19.05	0.950	13.644	13.888	-1.794	35.494	35.916	-1.189	711.65	720.111	-1.189
20.05	0.952	13.657	13.923	-1.946	35.774	36.091	-0.886	753.04	759.711	-0.886
21.05	0.955	13.669	13.955	-2.089	36.025	36.250	-0.626	794.35	799.321	-0.626
22.05	0.957	13.680	13.983	-2.218	36.269	36.397	-0.351	836.01	838.943	-0.351
23.05	0.958	13.689	14.010	-2.340	36.494	36.531	-0.101	877.69	878.574	-0.101
24.05	0.960	13.698	14.034	-2.451	36.711	36.655	0.152	919.61	918.213	0.152
25.05	0.962	13.706	14.056	-2.557	36.906	36.770	0.369	961.41	957.859	0.369
26.05	0.963	13.713	14.077	-2.656	37.092	36.877	0.580	1003.33	997.511	0.580
27.05	0.964	13.719	14.096	-2.749	37.267	36.976	0.782	1045.35	1037.170	0.782
28.05	0.966	13.726	14.114	-2.832	37.446	37.068	1.009	1087.81	1076.830	1.009

Z	z/(1+z)	LTD_LC	LTD_HHC	%Error	CD_LC	CD_HHC	%Error	LD_LC	LD_HHC	%Error
(1)	(2)	(3)	(4)	(5)	(6)	(7)	(8)	(9)	(10)	(11)
29.05	0.967	13.731	14.131	-2.915	37.600	37.155	1.184	1129.87	1116.500	1.184
30.05	0.968	13.736	14.147	-2.991	37.756	37.236	1.378	1172.33	1156.170	1.378
31.05	0.969	13.740	14.161	-3.064	37.901	37.312	1.553	1214.71	1195.850	1.553
32.05	0.970	13.744	14.175	-3.134	38.033	37.384	1.706	1256.98	1235.530	1.706
33.05	0.971	13.748	14.188	-3.198	38.167	37.451	1.874	1299.57	1275.210	1.874
34.05	0.971	13.752	14.200	-3.258	38.303	37.515	2.056	1342.50	1314.900	2.056
35.05	0.972	13.756	14.212	-3.316	38.425	37.575	2.212	1385.23	1354.590	2.212
36.05	0.973	13.759	14.223	-3.373	38.534	37.632	2.340	1427.69	1394.280	2.340
37.05	0.974	13.762	14.233	-3.426	38.644	37.686	2.479	1470.41	1433.970	2.479
38.05	0.974	13.765	14.243	-3.476	38.756	37.738	2.627	1513.42	1473.660	2.627
39.05	0.975	13.767	14.252	-3.525	38.853	37.787	2.744	1556.05	1513.360	2.744
40.05	0.976	13.770	14.261	-3.572	38.951	37.833	2.869	1598.93	1553.060	2.869
41.05	0.976	13.772	14.270	-3.615	39.050	37.878	3.002	1642.06	1592.760	3.002
42.05	0.977	13.774	14.278	-3.656	39.151	37.920	3.143	1685.44	1632.460	3.143
43.05	0.977	13.776	14.286	-3.698	39.235	37.961	3.249	1728.32	1672.160	3.249
44.05	0.978	13.778	14.293	-3.737	39.321	37.999	3.361	1771.41	1711 870	3.361
45.05	0.978	13.780	14.300	-3.773	39.408	38.036	3.480	1814.72	1751.580	3.480
46.05	0.979	13.782	14.307	-3.811	39.478	38.072	3.561	1857.43	1791.280	3.561
47.05	0.979	13.783	14.313	-3.844	39.566	38.106	3.690	1901.15	1830.990	3.691
48.05	0.980	13.785	14.319	-3.878	39.638	38.139	3.782	1944.23	1870.700	3.782
49.05	0.980	13.786	14.325	-3.910	39.710	38.170	3.878	1987.48	1910.410	3.878
50.05	0.980	13.788	14.331	-3.941	39.783	38.200	3.978	2030.91	1950.120	3.978
51.05	0.981	13.789	14.337	-3.970	39.856	38.229	4.082	2074.53	1989.830	4.083
52.05	0.981	13.790	14.342	-4.000	39.912	38.257	4.146	2117.34	2029.550	4.146
53.05	0.981	13.792	14.347	-4.026	39.987	38.284	4.259	2161.31	2069.260	4.259
54.05	0.982	13.793	14.352	-4.054	40.044	38.310	4.330	2204.42	2108.980	4.329
55.05	0.982	13.794	14.357	-4.078	40.120	38.335	4.449	2248.75	2148.690	4.449
56.05	0.982	13.795	14.361	-4.104	40.178	38.360	4.527	2292.17	2188.410	4.527
57.05	0.983	13.796	14.366	-4.128	40.237	38.383	4.607	2335.73	2228.130	4.607
58.05	0.983	13.797	14.370	-4.151	40.296	38.405	4.690	2379.45	2267.840	4.690
59.05	0.983	13.798	14.374	-4.176	40.335	38.427	4.730	2422.12	2307.560	4.729
60.05	0.984	13.799	14.378	-4.198	40.395	38.448	4.818	2466.10	2347.280	4.818
61.05	0.984	13.800	14.382	-4.218	40.455	38.469	4.909	2510.23	2387.000	4.909
62.05	0.984	13.800	14.386	-4.240	40.496	38.489	4.955	2553.24	2426.710	4.955
63.05	0.984	13.801	14.389	-4.259	40.557	38.508	5.051	2597.66	2466.440	5.051
64.05	0.985	13.802	14.393	-4.280	40.598	38.527	5.102	2640.89	2506 150	5.102
65.05	0.985	13.803	14.396	-4.297	40.660	38.545	5.202	2685.59	2545.870	5.202
66.05	0.985	13.804	14.399	-4.317	40.702	38.562	5.257	2729.05	2585.600	5.256
67.05	0.985	13.804	14.403	-4.335	40.744	38.579	5.313	2772.62	2625.320	5.312
68.05	0.986	13.805	14.406	-4.353	40.786	38.596	5.370	2816.29	2665.040	5.370
69.05	0.986	13.805	14.409	-4.370	40.829	38.612	5.430	2860.06	2704.770	5.430
70.05	0.986	13.806	14.412	-4.387	40.872	38.628	5.491	2903.94	2744.480	5.491
71.05	0.986	13.807	14.415	-4.403	40.915	38.643	5.554	2947.92	2784.210	5.554
72.05	0.986	13.807	14.417	-4.419	40.959	38.658	5.618	2992.02	2823.930	5.618
73.05	0.986	13.808	14.420	-4.434	41.002	38.672	5.684	3036.22	2863.650	5.684
74.05	0.987	13.808	14.423	-4.448	41.047	38.686	5.751	3080.54	2903.380	5.751
75.05	0.987	13.809	14.425	-4.462	41.091	38.700	5.820	3124.97	2943.100	5.820
76.05	0.987	13.809	14.428	-4.478	41.113	38.713	5.839	3167.79	2982.820	5.839
77.05	0.987	13.810	14.430	-4.491	41.158	38.726	5.910	3212.41	3022.550	5.910
78.05	0.987	13.810	14.433	-4.506	41.181	38.739	5.931	3255.36	3062.280	5.931
79.05	0.988	13.811	14.435	-4.519	41.227	38.751	6.005	3300.18	3102.000	6.005
80.05	0.988	13.811	14.437	-4.531	41.272	38.763	6.081	3345.13	3141.730	6.080
81.05	0.988	13.812	14.439	-4.544	41.296	38.775	6.105	3388.29	3181.440	6.105
82.05	0.988	13.812	14.441	-4 556	41.342	38.786	6.182	3433.44	3221.180	6.182
83.05	0.988	13.812	14.444	-4.569	41.365	38.797	6.208	3476.75	3260.900	6.208
84.05	0.988	13.813	14.446	-4.582	41.389	38.808	6.235	3520.11	3300.630	6.235
85.05	0.988	13.813	14.448	-4.592	41.436	38.819	6.316	3565.56	3340 350	6.316
86.05	0.989	13.814	14.450	-4.604	41.460	38.829	6.345	3609.06	3380.080	6.345
87.05	0.989	13.814	14.451	-4.616	41.484	38.839	6.374	3652.62	3419.810	6.374
88.05	0.989	13.814	14.453	-4.625	41.532	38.849	6.458	3698.38	3459.540	6.458
89.05	0.989	13.815	14.455	-4.636	41.556	38.859	6.489	3742.08	3499.260	6.489
90.05	0.989	13.815	14.457	-4.647	41.580	38.869	6.521	3785.85	3538.980	6.521
91.05	0.989	13.815	14.459	-4.658	41.604	38.878	6.553	3829.67	3578.710	6.553
92.05	0.989	13.816	14.460	-4.666	41.653	38.887	6.641	3875.84	3618.450	6.641
93.05	0.989	13.816	14.462	-4.676	41.678	38.896	6.675	3919.82	3658.170	6.675
94.05	0.989	13.816	14.464	-4.686	41.703	38.905	6.710	3963.85	3697.910	6.709
95.05	0.990	13.817	14.465	-4.696	41.728	38.913	6.745	4007.95	3737.620	6.745

Z	z/(1+z)	LTD_LC	LTD_HHC	%Error	CD_LC	CD_HHC	%Error	LD_LC	LD_HHC	%Error
(1)	(2)	(3)	(4)	(5)	(6)	(7)	(8)	(9)	(10)	(11)
96.05	0.990	13.817	14.467	-4.705	41.753	38.922	6.781	4052.11	3777.350	6.781
97.05	0.990	13.817	14.468	-4.714	41.778	38.930	6.817	4096.33	3817.080	6.817
98.05	0.990	13.817	14.470	-4.723	41.803	38.938	6.854	4140.61	3856.820	6.854
99.05	0.990	13.818	14.471	-4.732	41.829	38.946	6.892	4184.96	3896.550	6.892
100.05	0.990	13.818	14.473	-4.740	41.854	38.954	6.930	4229.37	3936.260	6.930
101.05	0.990	13.818	14.474	-4.749	41.880	38.961	6.969	4273.84	3975.990	6.969
102.05	0.990	13.818	14.476	-4.757	41.906	38.969	7.008	4318.38	4015.710	7.009
103.05	0.990	13.819	14.477	-4.765	41.932	38.976	7.049	4362.98	4055.450	7.049
104.05	0.990	13.819	14.478	-4.773	41.958	38.983	7.089	4407.65	4095.180	7.089
105.05	0.991	13.819	14.480	-4.780	41.984	38.990	7.130	4452.38	4134.910	7.130
106.05	0.991	13.819	14.481	-4.788	42.010	38.997	7.172	4497.18	4174.640	7.172
107.05	0.991	13.819	14.482	-4.797	42.010	39.004	7.156	4539.19	4214.360	7.156
108.05	0.991	13.820	14.483	-4.804	42.037	39.011	7.199	4584.08	4254.090	7.199
109.05	0.991	13.820	14.485	-4.811	42.063	39.017	7.242	4629.05	4293.820	7.242
110.05	0.991	13.820	14.486	-4.818	42.090	39.024	7.285	4674.08	4333.560	7.285
111.05	0.991	13.820	14.487	-4.824	42.117	39.030	7.330	4719.18	4373.280	7.330
112.05	0.991	13.821	14.488	-4.831	42.144	39.036	7.374	4764.35	4413.020	7.374
113.05	0.991	13.821	14.489	-4.839	42.144	39.042	7.360	4806.50	4452.750	7.360
114.05	0.991	13.821	14.490	-4.845	42.171	39.048	7.405	4851.77	4492.490	7.405
115.05	0.991	13.821	14.492	-4.851	42.198	39.054	7.451	4897.11	4532.200	7.451
116.05	0.991	13.821	14.493	-4.857	42.226	39.060	7.498	4942.52	4571.930	7.498
117.05	0.992	13.821	14.494	-4.865	42.226	39.065	7.485	4984.75	4611.650	7.485
118.05	0.992	13.821	14.495	-4.871	42.253	39.071	7.532	5030.26	4651.390	7.532
119.05	0.992	13.822	14.496	-4.877	42.281	39.076	7.580	5075.85	4691.120	7.580
120.05	0.992	13.822	14.497	-4.884	42.281	39.082	7.567	5118.14	4730.870	7.567
121.05	0.992	13.822	14.498	-4.889	42.309	39.087	7.615	5163.83	4770.580	7.615
122.05	0.992	13.822	14.499	-4.895	42.337	39.092	7.664	5209.60	4810.310	7.665
123.05	0.992	13.822	14.500	-4.901	42.337	39.098	7.652	5251.94	4850.030	7.653
124.05	0.992	13.822	14.501	-4.907	42.366	39.103	7.702	5297.81	4889.780	7.702
125.05	0.992	13.823	14.502	-4.912	42.394	39.108	7.752	5343.76	4929.500	7.752
126.05	0.992	13.823	14.502	-4.918	42.394	39.113	7.741	5386.16	4969.240	7.741
127.05	0.992	13.823	14.503	-4.923	42.423	39.117	7.791	5432.22	5008.960	7.792
128.05	0.992	13.823	14.504	-4.928	42.451	39.122	7.843	5478.36	5048.680	7.843
129.05	0.992	13.823	14.505	-4.934	42.451	39.127	7.832	5520.81	5088.430	7.832
130.05	0.992	13.823	14.506	-4.938	42.480	39.131	7.884	5567.06	5128.180	7.884
131.05	0.992	13.823	14.507	-4.945	42.480	39.136	7.873	5609.54	5167.890	7.873
132.05	0.992	13.823	14.508	-4.949	42.510	39.140	7.926	5655.90	5207.620	7.926
133.05	0.993	13.823	14.508	-4.955	42.510	39.145	7.916	5698.41	5247.370	7.915
134.05	0.993	13.824	14.509	-4.959	42.539	39.149	7.969	5744.89	5287.070	7.969
135.05	0.993	13.824	14.510	-4.965	42.539	39.153	7.959	5787.43	5326.800	7.959
136.05	0.993	13.824	14.511	-4.969	42.569	39.158	8.013	5834.02	5366.540	8.013
137.05	0.993	13.824	14.512	-4.973	42.598	39.162	8.067	5880.69	5406.280	8.067
138.05	0.993	13.824	14.512	-4.978	42.598	39.166	8.058	5923.29	5446.010	8.058
139.05	0.993	13.824	14.513	-4.982	42.628	39.170	8.113	5970.08	5485.760	8.112
140.05	0.993	13.824	14.514	-4.987	42.628	39.174	8.104	6012.71	5525.480	8.103
141.05	0.993	13.825	14.515	-4.991	42.658	39.178	8.159	6059.62	5565.190	8.159
142.05	0.993	13.825	14.515	-4.996	42.658	39.182	8.150	6102.28	5604.940	8.150
143.05	0.993	13.825	14.516	-5.000	42.689	39.186	8.207	6149.31	5644.670	8.207
144.05	0.993	13.825	14.517	-5.005	42.689	39.189	8.198	6192.00	5684.400	8.198
145.05	0.993	13.825	14.517	-5.008	42.719	39.193	8.255	6239.16	5724.130	8.255
146.05	0.993	13.825	14.518	-5.013	42.719	39.197	8.246	6281.88	5763.860	8.246
147.05	0.993	13.825	14.519	-5.018	42.719	39.200	8.238	6324.60	5803.610	8.238
148.05	0.993	13.825	14.519	-5.021	42.750	39.204	8.296	6371.90	5843.320	8.296
149.05	0.993	13.825	14.520	-5.026	42.750	39.207	8.287	6414.65	5883.050	8.287
150.05	0.993	13.825	14.521	-5.029	42.781	39.211	8.346	6462.09	5922.770	8.346
151.05	0.993	13.825	14.521	-5.034	42.781	39.214	8.338	6504.87	5962.520	8.338
152.05	0.993	13.826	14.522	-5.037	42.812	39.218	8.397	6552.43	6002.260	8.396
153.05	0.994	13.826	14.523	-5.041	42.812	39.221	8.389	6595.24	6041.960	8.389
154.05	0.994	13.826	14.523	-5.044	42.844	39.224	8.448	6642.94	6081.720	8.448
155.05	0.994	13.826	14.524	-5.048	42.844	39.228	8.441	6685.78	6121.430	8.441
156.05	0.994	13.826	14.524	-5.053	42.844	39.231	8.433	6728.62	6161.190	8.433
157.05	0.994	13.826	14.525	-5.055	42.876	39.234	8.494	6776.48	6200.930	8.493
158.05	0.994	13.826	14.526	-5.060	42.876	39.237	8.486	6819.35	6240.640	8.486
159.05	0.994	13.826	14.526	-5.062	42.908	39.240	8.547	6867.34	6280.360	8.547
160.05	0.994	13.826	14.527	-5.066	42.908	39.243	8.540	6910.25	6320.100	8.540
161.05	0.994	13.826	14.527	-5.070	42.908	39.246	8.533	6953.16	6359.840	8.533
162.05	0.994	13.826	14.528	-5.073	42.940	39.249	8.595	7001.31	6399.580	8.595

Z	z/(1+z)	LTD_LC	LTD_HHC	%Error	CD_LC	CD_HHC	%Error	LD_LC	LD_HHC	%Error
(1)	(2)	(3)	(4)	(5)	(6)	(7)	(8)	(9)	(10)	(11)
163.05	0.994	13.826	14.528	-5.077	42.940	39.252	8.588	7044.25	6439.300	8.588
164.05	0.994	13.826	14.529	-5.081	42.940	39.255	8.581	7087.19	6479.050	8.581
165.05	0.994	13.827	14.529	-5.083	42.972	39.258	8.643	7135.52	6518.770	8.643
166.05	0.994	13.827	14.530	-5.087	42.972	39.261	8.637	7178.49	6558.520	8.637
167.05	0.994	13.827	14.530	-5.091	42.972	39.264	8.630	7221.46	6598.210	8.631
168.05	0.994	13.827	14.531	-5.093	43.005	39.266	8.693	7269.96	6637.970	8.693
169.05	0.994	13.827	14.532	-5.097	43.005	39.269	8.687	7312.97	6677.730	8.687
170.05	0.994	13.827	14.532	-5.099	43.038	39.272	8.751	7361.61	6717.400	8.751
171.05	0.994	13.827	14.533	-5.102	43.038	39.274	8.744	7404.65	6757.130	8.745
172.05	0.994	13.827	14.533	-5.106	43.038	39.277	8.738	7447.69	6796.900	8.738
173.05	0.994	13.827	14.533	-5.108	43.071	39.280	8.803	7496.51	6836.630	8.803
174.05	0.994	13.827	14.534	-5.112	43.071	39.282	8.797	7539.58	6876.390	8.796
175.05	0.994	13.827	14.534	-5.115	43.071	39.285	8.791	7582.65	6916.090	8.791
176.05	0.994	13.827	14.535	-5.117	43.105	39.287	8.856	7631.66	6955.800	8.856
177.05	0.994	13.827	14.535	-5.120	43.105	39.290	8.850	7674.76	6995.520	8.850
178.05	0.994	13.827	14.536	-5.124	43.105	39.292	8.844	7717.87	7035.310	8.844
179.05	0.994	13.827	14.536	-5.127	43.105	39.295	8.839	7760.97	7075.010	8.839
180.05	0.994	13.828	14.537	-5.129	43.138	39.297	8.904	7810.20	7114.760	8.904
181.05	0.995	13.828	14.537	-5.132	43.138	39.300	8.899	7853.34	7154.500	8.899
182.05	0.995	13.828	14.538	-5.135	43.138	39.302	8.893	7896.47	7194.190	8.894
183.05	0.995	13.828	14.538	-5.137	43.172	39.304	8.960	7945.89	7233.930	8.960
184.05	0.995	13.828	14.538	-5.140	43.172	39.307	8.955	7989.06	7273.690	8.954
185.05	0.995	13.828	14.539	-5.143	43.172	39.309	8.949	8032.23	7313.400	8.949
186.05	0.995	13.828	14.539	-5.145	43.207	39.311	9.016	8081.84	7353.120	9.017
187.05	0.995	13.828	14.540	-5.148	43.207	39.313	9.011	8125.05	7392.860	9.012
188.05	0.995	13.828	14.540	-5.151	43.207	39.316	9.006	8168.25	7432.600	9.006
189.05	0.995	13.828	14.541	-5.153	43.207	39.318	9.001	8211.46	7472.330	9.001
190.05	0.995	13.828	14.541	-5.155	43.242	39.320	9.069	8261.30	7512.060	9.069
191.05	0.995	13.828	14.541	-5.158	43.242	39.322	9.064	8304.54	7551.770	9.065
192.05	0.995	13.828	14.542	-5.161	43.242	39.324	9.059	8347.78	7591.550	9.059
193.05	0.995	13.828	14.542	-5.164	43.242	39.326	9.054	8391.02	7631.290	9.054
194.05	0.995	13.828	14.543	-5.165	43.277	39.328	9.123	8441.10	7671.000	9.123
195.05	0.995	13.828	14.543	-5.168	43.277	39.331	9.118	8484.37	7710.760	9.118
196.05	0.995	13.828	14.543	-5.170	43.277	39.333	9.114	8527.65	7750.460	9.114
197.05	0.995	13.828	14.544	-5.172	43.312	39.335	9.183	8577.93	7790.210	9.183
198.05	0.995	13.828	14.544	-5.175	43.312	39.337	9.179	8621.24	7829.980	9.178
199.05	0.995	13.828	14.544	-5.177	43.312	39.339	9.174	8664.55	7869.680	9.174
200.05	0.995	13.828	14.545	-5.180	43.312	39.341	9.169	8707.86	7909.400	9.169
201.05	0.995	13.829	14.545	-5.181	43.348	39.342	9.240	8758.39	7949.130	9.240
202.05	0.995	13.829	14.545	-5.184	43.348	39.344	9.235	8801.73	7988.870	9.235
203.05	0.995	13.829	14.546	-5.186	43.348	39.346	9.231	8845.08	8028.610	9.231
204.05	0.995	13.829	14.546	-5.189	43.348	39.348	9.227	8888.43	8068.350	9.226
205.05	0.995	13.829	14.547	-5.191	43.348	39.350	9.222	8931.78	8108.070	9.222
206.05	0.995	13.829	14.547	-5.192	43.384	39.352	9.293	8982.58	8147.780	9.294
207.05	0.995	13.829	14.547	-5.195	43.384	39.354	9.289	9025.97	8187.560	9.289
208.05	0.995	13.829	14.548	-5.197	43.384	39.356	9.285	9069.35	8227.220	9.285
209.05	0.995	13.829	14.548	-5.200	43.384	39.357	9.281	9112.73	8267.050	9.280
210.05	0.995	13.829	14.548	-5.201	43.420	39.359	9.353	9163.80	8306.730	9.353
211.05	0.995	13.829	14.549	-5.203	43.420	39.361	9.349	9207.22	8346.480	9.349
212.05	0.995	13.829	14.549	-5.205	43.420	39.363	9.345	9250.64	8386.170	9.345
213.05	0.995	13.829	14.549	-5.208	43.420	39.364	9.341	9294.06	8425.920	9.341
214.05	0.995	13.829	14.549	-5.210	43.420	39.366	9.337	9337.48	8465.710	9.336
215.05	0.995	13.829	14.550	-5.211	43.457	39.368	9.410	9388.84	8505.430	9.409
216.05	0.995	13.829	14.550	-5.213	43.457	39.369	9.406	9432.30	8545.080	9.406
217.05	0.995	13.829	14.550	-5.216	43.457	39.371	9.402	9475.75	8584.870	9.402
218.05	0.995	13.829	14.551	-5.218	43.457	39.373	9.398	9519.21	8624.570	9.398
219.05	0.995	13.829	14.551	-5.219	43.494	39.374	9.472	9570.84	8664.300	9.472
220.05	0.995	13.829	14.551	-5.221	43.494	39.376	9.468	9614.33	8704.040	9.468
221.05	0.995	13.829	14.552	-5.223	43.494	39.378	9.464	9657.82	8743.800	9.464
222.05	0.996	13.829	14.552	-5.225	43.494	39.379	9.460	9701.32	8783.560	9.460
223.05	0.996	13.829	14.552	-5.227	43.494	39.381	9.457	9744.81	8823.210	9.457
224.05	0.996	13.830	14.553	-5.228	43.531	39.382	9.531	9796.75	8862.970	9.531
225.05	0.996	13.830	14.553	-5.230	43.531	39.384	9.528	9840.28	8902.730	9.528
226.05	0.996	13.830	14.553	-5.232	43.531	39.385	9.524	9883.81	8942.480	9.524
227.05	0.996	13.830	14.553	-5.234	43.531	39.387	9.521	9927.34	8982.210	9.521
228.05	0.996	13.830	14.554	-5.236	43.531	39.389	9.517	9970.88	9021.920	9.517
229.05	0.996	13.830	14.554	-5.237	43.569	39.390	9.593	10023.10	9061.600	9.593

Z	z/(1+z)	LTD_LC	LTD_HHC	%Error	CD_LC	CD_HHC	%Error	LD_LC	LD_HHC	%Error
(1)	(2)	(3)	(4)	(5)	(6)	(7)	(8)	(9)	(10)	(11)
230.05	0.996	13.830	14.554	-5.239	43.569	39.391	9.589	10066.70	9101.380	9.589
231.05	0.996	13.830	14.554	-5.241	43.569	39.393	9.586	10110.30	9141.120	9.586
232.05	0.996	13.830	14.555	-5.243	43.569	39.394	9.582	10153.80	9180.830	9.583
233.05	0.996	13.830	14.555	-5.245	43.569	39.396	9.579	10197.40	9220.620	9.579
234.05	0.996	13.830	14.555	-5.247	43.569	39.397	9.576	10241.00	9260.350	9.575
235.05	0.996	13.830	14.556	-5.247	43.608	39.399	9.652	10293.60	9300.040	9.652
236.05	0.996	13.830	14.556	-5.249	43.608	39.400	9.649	10337.20	9339.790	9.649
237.05	0.996	13.830	14.556	-5.251	43.608	39.402	9.646	10380.80	9379.480	9.646
238.05	0.996	13.830	14.556	-5.253	43.608	39.403	9.642	10424.40	9419.240	9.643
239.05	0.996	13.830	14.557	-5.255	43.608	39.404	9.639	10468.00	9458.920	9.640
240.05	0.996	13.830	14.557	-5.255	43.647	39.406	9.716	10521.00	9498.660	9.717
241.05	0.996	13.830	14.557	-5.257	43.647	39.407	9.713	10564.60	9538.460	9.713
242.05	0.996	13.830	14.557	-5.259	43.647	39.408	9.710	10608.30	9578.170	9.710
243.05	0.996	13.830	14.558	-5.261	43.647	39.410	9.707	10651.90	9617.920	9.707
244.05	0.996	13.830	14.558	-5.263	43.647	39.411	9.704	10695.60	9657.720	9.703
245.05	0.996	13.830	14.558	-5.264	43.647	39.412	9.701	10739.20	9697.420	9.701
246.05	0.996	13.830	14.558	-5.265	43.686	39.414	9.779	10792.50	9737.150	9.779
247.05	0.996	13.830	14.559	-5.267	43.686	39.415	9.776	10836.20	9776.920	9.776
248.05	0.996	13.830	14.559	-5.268	43.686	39.416	9.773	10879.90	9816.570	9.774
249.05	0.996	13.830	14.559	-5.270	43.686	39.417	9.770	10923.60	9856.390	9.770
250.05	0.996	13.830	14.559	-5.272	43.686	39.419	9.768	10967.30	9896.080	9.767
251.05	0.996	13.830	14.559	-5.273	43.686	39.420	9.765	11011.00	9935.800	9.765
252.05	0.996	13.830	14.560	-5.275	43.686	39.421	9.762	11054.70	9975.520	9.762
253.05	0.996	13.830	14.560	-5.276	43.725	39.422	9.841	11108.40	10015.300	9.841
254.05	0.996	13.830	14.560	-5.277	43.725	39.424	9.838	11152.10	10055.000	9.838
255.05	0.996	13.830	14.560	-5.279	43.725	39.425	9.835	11195.90	10094.800	9.835
256.05	0.996	13.830	14.561	-5.280	43.725	39.426	9.833	11239.60	10134.500	9.832
257.05	0.996	13.830	14.561	-5.282	43.725	39.427	9.830	11283.30	10174.200	9.829
258.05	0.996	13.830	14.561	-5.284	43.725	39.428	9.827	11327.00	10214.000	9.827
259.05	0.996	13.830	14.561	-5.284	43.766	39.430	9.907	11381.20	10253.700	9.907
260.05	0.996	13.830	14.561	-5.285	43.766	39.431	9.905	11425.00	10293.400	9.904
261.05	0.996	13.830	14.562	-5.287	43.766	39.432	9.902	11468.70	10333.100	9.902
262.05	0.996	13.830	14.562	-5.289	43.766	39.433	9.899	11512.50	10372.800	9.900
263.05	0.996	13.830	14.562	-5.290	43.766	39.434	9.897	11556.30	10412.600	9.897
264.05	0.996	13.830	14.562	-5.292	43.766	39.435	9.894	11600.00	10452.400	9.894
265.05	0.996	13.830	14.563	-5.293	43.766	39.436	9.892	11643.80	10492.100	9.891
266.05	0.996	13.831	14.563	-5.293	43.806	39.438	9.973	11698.40	10531.800	9.972
267.05	0.996	13.831	14.563	-5.295	43.806	39.439	9.970	11742.20	10571.500	9.970
268.05	0.996	13.831	14.563	-5.296	43.806	39.440	9.968	11786.00	10611.300	9.967
269.05	0.996	13.831	14.563	-5.298	43.806	39.441	9.965	11829.80	10651.000	9.965
270.05	0.996	13.831	14.564	-5.299	43.806	39.442	9.963	11873.60	10690.700	9.962
271.05	0.996	13.831	14.564	-5.301	43.806	39.443	9.960	11917.50	10730.400	9.961
272.05	0.996	13.831	14.564	-5.302	43.806	39.444	9.958	11961.30	10770.100	9.958
273.05	0.996	13.831	14.564	-5.302	43.847	39.445	10.040	12016.30	10809.800	10.041
274.05	0.996	13.831	14.564	-5.304	43.847	39.446	10.037	12060.20	10849.700	10.038
275.05	0.996	13.831	14.565	-5.305	43.847	39.447	10.035	12104.00	10889.400	10.035
276.05	0.996	13.831	14.565	-5.307	43.847	39.448	10.033	12147.90	10929.100	10.033
277.05	0.996	13.831	14.565	-5.308	43.847	39.449	10.030	12191.70	10968.800	10.031
278.05	0.996	13.831	14.565	-5.309	43.847	39.450	10.028	12235.60	11008.500	10.029
279.05	0.996	13.831	14.565	-5.311	43.847	39.451	10.026	12279.40	11048.300	10.026
280.05	0.996	13.831	14.565	-5.312	43.847	39.452	10.023	12323.30	11088.000	10.024
281.05	0.996	13.831	14.566	-5.312	43.889	39.453	10.107	12378.90	11127.800	10.106
282.05	0.996	13.831	14.566	-5.314	43.889	39.454	10.104	12422.80	11167.500	10.104
283.05	0.996	13.831	14.566	-5.315	43.889	39.455	10.102	12466.70	11207.300	10.102
284.05	0.996	13.831	14.566	-5.316	43.889	39.456	10.100	12510.50	11247.000	10.100
285.05	0.997	13.831	14.566	-5.317	43.889	39.457	10.098	12554.40	11286.800	10.097
286.05	0.997	13.831	14.567	-5.319	43.889	39.458	10.096	12598.30	11326.500	10.096
287.05	0.997	13.831	14.567	-5.320	43.889	39.459	10.093	12642.20	11366.200	10.093
288.05	0.997	13.831	14.567	-5.321	43.889	39.460	10.091	12686.10	11405.900	10.092
289.05	0.997	13.831	14.567	-5.321	43.931	39.461	10.175	12742.20	11445.800	10.175
290.05	0.997	13.831	14.567	-5.323	43.931	39.462	10.173	12786.20	11485.300	10.174
291.05	0.997	13.831	14.567	-5.324	43.931	39.463	10.171	12830.10	11525.200	10.171
292.05	0.997	13.831	14.568	-5.325	43.931	39.464	10.169	12874.00	11564.900	10.169
293.05	0.997	13.831	14.568	-5.326	43.931	39.465	10.167	12918.00	11604.500	10.168
294.05	0.997	13.831	14.568	-5.328	43.931	39.466	10.165	12961.90	11644.400	10.165
295.05	0.997	13.831	14.568	-5.329	43.931	39.467	10.163	13005.80	11684.100	10.163
296.05	0.997	13.831	14.568	-5.330	43.931	39.467	10.161	13049.80	11723.900	10.160

Z	z/(1+z)	LTD_LC	LTD_HHC	%Error	CD_LC	CD_HHC	%Error	LD_LC	LD_HHC	%Error
(1)	(2)	(3)	(4)	(5)	(6)	(7)	(8)	(9)	(10)	(11)
297.05	0.997	13.831	14.568	-5.331	43.931	39.468	10.159	13093.70	11763.500	10.159
298.05	0.997	13.831	14.569	-5.331	43.974	39.469	10.244	13150.40	11803.200	10.245
299.05	0.997	13.831	14.569	-5.332	43.974	39.470	10.242	13194.40	11842.900	10.243
300.05	0.997	13.831	14.569	-5.334	43.974	39.471	10.240	13238.40	11882.700	10.240
301.05	0.997	13.831	14.569	-5.335	43.974	39.472	10.238	13282.30	11922.400	10.239
302.05	0.997	13.831	14.569	-5.336	43.974	39.473	10.236	13326.30	11962.200	10.236
303.05	0.997	13.831	14.569	-5.337	43.974	39.474	10.234	13370.30	12002.000	10.234
304.05	0.997	13.831	14.570	-5.338	43.974	39.474	10.232	13414.30	12041.700	10.232
305.05	0.997	13.831	14.570	-5.339	43.974	39.475	10.231	13458.20	12081.300	10.231
306.05	0.997	13.831	14.570	-5.341	43.974	39.476	10.229	13502.20	12121.100	10.229
307.05	0.997	13.831	14.570	-5.341	44.017	39.477	10.315	13559.60	12160.800	10.316
308.05	0.997	13.831	14.570	-5.342	44.017	39.478	10.313	13603.60	12200.700	10.313
309.05	0.997	13.831	14.570	-5.343	44.017	39.479	10.311	13647.60	12240.400	10.311
310.05	0.997	13.831	14.570	-5.344	44.017	39.479	10.310	13691.60	12280.100	10.309
311.05	0.997	13.831	14.571	-5.345	44.017	39.480	10.308	13735.60	12319.700	10.309
312.05	0.997	13.831	14.571	-5.346	44.017	39.481	10.306	13779.60	12359.500	10.306
313.05	0.997	13.831	14.571	-5.347	44.017	39.482	10.304	13823.70	12399.300	10.304
314.05	0.997	13.831	14.571	-5.348	44.017	39.483	10.302	13867.70	12438.900	10.303
315.05	0.997	13.831	14.571	-5.349	44.017	39.483	10.300	13911.70	12478.700	10.300
316.05	0.997	13.831	14.571	-5.350	44.017	39.484	10.299	13955.70	12518.400	10.299
317.05	0.997	13.831	14.572	-5.350	44.061	39.485	10.387	14013.70	12558.300	10.386
318.05	0.997	13.831	14.572	-5.351	44.061	39.486	10.385	14057.80	12597.900	10.385
319.05	0.997	13.831	14.572	-5.352	44.061	39.487	10.383	14101.90	12637.600	10.384
320.05	0.997	13.831	14.572	-5.353	44.061	39.487	10.381	14145.90	12677.500	10.381
321.05	0.997	13.831	14.572	-5.354	44.061	39.488	10.380	14190.00	12717.200	10.379
322.05	0.997	13.831	14.572	-5.355	44.061	39.489	10.378	14234.00	12756.800	10.378
323.05	0.997	13.831	14.572	-5.356	44.061	39.490	10.376	14278.10	12796.500	10.377
324.05	0.997	13.831	14.573	-5.357	44.061	39.490	10.374	14322.20	12836.400	10.374
325.05	0.997	13.831	14.573	-5.358	44.061	39.491	10.373	14366.20	12876.100	10.373
326.05	0.997	13.831	14.573	-5.359	44.061	39.492	10.371	14410.30	12915.700	10.372
327.05	0.997	13.832	14.573	-5.359	44.106	39.493	10.460	14469.00	12955.600	10.460
328.05	0.997	13.832	14.573	-5.360	44.106	39.493	10.458	14513.10	12995.200	10.459
329.05	0.997	13.832	14.573	-5.361	44.106	39.494	10.457	14557.20	13035.100	10.456
330.05	0.997	13.832	14.573	-5.362	44.106	39.495	10.455	14601.30	13074.700	10.456
331.05	0.997	13.832	14.573	-5.363	44.106	39.496	10.454	14645.40	13114.500	10.453
332.05	0.997	13.832	14.574	-5.364	44.106	39.496	10.452	14689.50	13154.300	10.451
333.05	0.997	13.832	14.574	-5.365	44.106	39.497	10.450	14733.70	13193.900	10.451
334.05	0.997	13.832	14.574	-5.366	44.106	39.498	10.449	14777.80	13233.600	10.449
335.05	0.997	13.832	14.574	-5.367	44.106	39.498	10.447	14821.90	13273.300	10.448
336.05	0.997	13.832	14.574	-5.368	44.106	39.499	10.446	14866.00	13313.000	10.446
337.05	0.997	13.832	14.574	-5.369	44.106	39.500	10.444	14910.10	13353.000	10.443
338.05	0.997	13.832	14.574	-5.369	44.152	39.500	10.534	14969.60	13392.600	10.534
339.05	0.997	13.832	14.574	-5.370	44.152	39.501	10.533	15013.70	13432.500	10.532
340.05	0.997	13.832	14.575	-5.371	44.152	39.502	10.531	15057.90	13472.000	10.532
341.05	0.997	13.832	14.575	-5.372	44.152	39.502	10.530	15102.00	13511.800	10.530
342.05	0.997	13.832	14.575	-5.372	44.152	39.503	10.528	15146.20	13551.600	10.528
343.05	0.997	13.832	14.575	-5.373	44.152	39.504	10.527	15190.30	13591.200	10.527
344.05	0.997	13.832	14.575	-5.374	44.152	39.505	10.525	15234.50	13630.900	10.526
345.05	0.997	13.832	14.575	-5.375	44.152	39.505	10.524	15278.60	13670.800	10.524
346.05	0.997	13.832	14.575	-5.376	44.152	39.506	10.522	15322.80	13710.600	10.522
347.05	0.997	13.832	14.575	-5.377	44.152	39.506	10.521	15366.90	13750.300	10.520
348.05	0.997	13.832	14.576	-5.378	44.152	39.507	10.519	15411.10	13790.100	10.519
349.05	0.997	13.832	14.576	-5.379	44.152	39.508	10.518	15455.20	13829.700	10.518
350.05	0.997	13.832	14.576	-5.378	44.198	39.508	10.610	15515.60	13869.300	10.611
351.05	0.997	13.832	14.576	-5.379	44.198	39.509	10.608	15559.80	13909.100	10.609
352.05	0.997	13.832	14.576	-5.380	44.198	39.510	10.607	15604.00	13948.800	10.607
353.05	0.997	13.832	14.576	-5.381	44.198	39.510	10.605	15648.20	13988.500	10.606
354.05	0.997	13.832	14.576	-5.382	44.198	39.511	10.604	15692.40	14028.400	10.604
355.05	0.997	13.832	14.576	-5.383	44.198	39.512	10.603	15736.60	14068.200	10.602
356.05	0.997	13.832	14.577	-5.384	44.198	39.512	10.601	15780.70	14107.900	10.600
357.05	0.997	13.832	14.577	-5.384	44.198	39.513	10.600	15824.90	14147.600	10.599
358.05	0.997	13.832	14.577	-5.385	44.198	39.513	10.598	15869.10	14187.200	10.599
359.05	0.997	13.832	14.577	-5.386	44.198	39.514	10.597	15913.30	14227.000	10.597
360.05	0.997	13.832	14.577	-5.387	44.198	39.515	10.596	15957.50	14266.700	10.596
361.05	0.997	13.832	14.577	-5.388	44.198	39.515	10.594	16001.70	14306.300	10.595
362.05	0.997	13.832	14.577	-5.388	44.198	39.516	10.593	16045.90	14346.200	10.593
363.05	0.997	13.832	14.577	-5.388	44.244	39.516	10.686	16107.20	14385.900	10.686

Z	z/(1+z)	LTD_LC	LTD_HHC	%Error	CD_LC	CD_HHC	%Error	LD_LC	LD_HHC	%Error
(1)	(2)	(3)	(4)	(5)	(6)	(7)	(8)	(9)	(10)	(11)
364.05	0.997	13.832	14.577	-5.389	44.244	39.517	10.685	16151.40	14425.600	10.685
365.05	0.997	13.832	14.578	-5.390	44.244	39.518	10.683	16195.70	14465.500	10.683
366.05	0.997	13.832	14.578	-5.391	44.244	39.518	10.682	16239.90	14505.200	10.682
367.05	0.997	13.832	14.578	-5.391	44.244	39.519	10.681	16284.20	14544.900	10.681
368.05	0.997	13.832	14.578	-5.392	44.244	39.519	10.679	16328.40	14584.500	10.680
369.05	0.997	13.832	14.578	-5.393	44.244	39.520	10.678	16372.70	14624.300	10.679
370.05	0.997	13.832	14.578	-5.394	44.244	39.521	10.677	16416.90	14663.900	10.678
371.05	0.997	13.832	14.578	-5.394	44.244	39.521	10.676	16461.10	14703.800	10.676
372.05	0.997	13.832	14.578	-5.395	44.244	39.522	10.674	16505.40	14743.600	10.674
373.05	0.997	13.832	14.578	-5.396	44.244	39.522	10.673	16549.60	14783.300	10.673
374.05	0.997	13.832	14.578	-5.397	44.244	39.523	10.672	16593.90	14823.100	10.671
375.05	0.997	13.832	14.579	-5.398	44.244	39.523	10.670	16638.10	14862.900	10.670
376.05	0.997	13.832	14.579	-5.398	44.244	39.524	10.669	16682.40	14902.500	10.669
377.05	0.997	13.832	14.579	-5.398	44.292	39.525	10.764	16744.60	14942.300	10.763
378.05	0.997	13.832	14.579	-5.399	44.292	39.525	10.763	16788.90	14982.000	10.762
379.05	0.997	13.832	14.579	-5.399	44.292	39.526	10.762	16833.20	15021.600	10.762
380.05	0.997	13.832	14.579	-5.400	44.292	39.526	10.760	16877.50	15061.400	10.760
381.05	0.997	13.832	14.579	-5.401	44.292	39.527	10.759	16921.80	15101.000	10.760
382.05	0.997	13.832	14.579	-5.402	44.292	39.527	10.758	16966.10	15140.900	10.758
383.05	0.997	13.832	14.579	-5.402	44.292	39.528	10.757	17010.40	15180.600	10.757
384.05	0.997	13.832	14.580	-5.403	44.292	39.528	10.755	17054.70	15220.200	10.756
385.05	0.997	13.832	14.580	-5.404	44.292	39.529	10.754	17098.90	15260.000	10.755
386.05	0.997	13.832	14.580	-5.405	44.292	39.529	10.753	17143.20	15300.000	10.752
387.05	0.997	13.832	14.580	-5.405	44.292	39.530	10.752	17187.50	15339.500	10.753
388.05	0.997	13.832	14.580	-5.406	44.292	39.530	10.751	17231.80	15379.100	10.752
389.05	0.997	13.832	14.580	-5.407	44.292	39.531	10.749	17276.10	15419.000	10.749
390.05	0.997	13.832	14.580	-5.407	44.292	39.531	10.748	17320.40	15458.800	10.748
391.05	0.997	13.832	14.580	-5.408	44.292	39.532	10.747	17364.70	15498.300	10.748
392.05	0.997	13.832	14.580	-5.408	44.341	39.533	10.844	17428.00	15538.100	10.844
393.05	0.997	13.832	14.580	-5.408	44.341	39.533	10.842	17472.40	15578.100	10.842
394.05	0.997	13.832	14.580	-5.409	44.341	39.534	10.841	17516.70	15617.600	10.842
395.05	0.997	13.832	14.581	-5.410	44.341	39.534	10.840	17561.10	15657.600	10.839
396.05	0.997	13.832	14.581	-5.410	44.341	39.535	10.839	17605.40	15697.000	10.840
397.05	0.997	13.832	14.581	-5.411	44.341	39.535	10.838	17649.70	15736.700	10.839
398.05	0.997	13.832	14.581	-5.412	44.341	39.536	10.837	17694.10	15776.600	10.837
399.05	0.998	13.832	14.581	-5.412	44.341	39.536	10.836	17738.40	15816.300	10.836
400.05	0.998	13.832	14.581	-5.413	44.341	39.537	10.834	17782.80	15856.200	10.834
401.05	0.998	13.832	14.581	-5.414	44.341	39.537	10.833	17827.10	15895.900	10.833
402.05	0.998	13.832	14.581	-5.414	44.341	39.538	10.832	17871.40	15935.400	10.833
403.05	0.998	13.832	14.581	-5.415	44.341	39.538	10.831	17915.80	15975.200	10.832
404.05	0.998	13.832	14.581	-5.416	44.341	39.538	10.830	17960.10	16015.100	10.830
405.05	0.998	13.832	14.581	-5.416	44.341	39.539	10.829	18004.50	16054.800	10.829
406.05	0.998	13.832	14.582	-5.417	44.341	39.539	10.828	18048.80	16094.400	10.829
407.05	0.998	13.832	14.582	-5.418	44.341	39.540	10.827	18093.10	16134.100	10.828
408.05	0.998	13.832	14.582	-5.417	44.390	39.540	10.925	18157.70	16174.000	10.925
409.05	0.998	13.832	14.582	-5.418	44.390	39.541	10.924	18202.10	16213.700	10.924
410.05	0.998	13.832	14.582	-5.419	44.390	39.541	10.923	18246.40	16253.300	10.924
411.05	0.998	13.832	14.582	-5.419	44.390	39.542	10.922	18290.80	16293.400	10.921
412.05	0.998	13.832	14.582	-5.420	44.390	39.542	10.921	18335.20	16332.900	10.921
413.05	0.998	13.832	14.582	-5.420	44.390	39.543	10.920	18379.60	16372.600	10.920
414.05	0.998	13.832	14.582	-5.421	44.390	39.543	10.919	18424.00	16412.400	10.918
415.05	0.998	13.832	14.582	-5.422	44.390	39.544	10.918	18468.40	16452.100	10.918
416.05	0.998	13.832	14.582	-5.422	44.390	39.544	10.916	18512.80	16492.000	10.916
417.05	0.998	13.832	14.583	-5.423	44.390	39.545	10.915	18557.20	16531.600	10.915
418.05	0.998	13.832	14.583	-5.424	44.390	39.545	10.914	18601.60	16571.400	10.914
419.05	0.998	13.832	14.583	-5.424	44.390	39.545	10.913	18646.00	16611.100	10.913
420.05	0.998	13.832	14.583	-5.425	44.390	39.546	10.912	18690.30	16650.800	10.912
421.05	0.998	13.832	14.583	-5.425	44.390	39.546	10.911	18734.70	16690.400	10.912
422.05	0.998	13.832	14.583	-5.426	44.390	39.547	10.910	18779.10	16730.200	10.911
423.05	0.998	13.832	14.583	-5.426	44.390	39.547	10.909	18823.50	16770.100	10.909
424.05	0.998	13.832	14.583	-5.427	44.390	39.548	10.908	18867.90	16809.800	10.908
425.05	0.998	13.833	14.583	-5.427	44.440	39.548	11.008	18933.70	16849.200	11.009
426.05	0.998	13.833	14.583	-5.427	44.440	39.549	11.007	18978.10	16889.300	11.007
427.05	0.998	13.833	14.583	-5.428	44.440	39.549	11.006	19022.60	16928.700	11.007
428.05	0.998	13.833	14.583	-5.428	44.440	39.549	11.005	19067.00	16968.700	11.005
429.05	0.998	13.833	14.583	-5.429	44.440	39.550	11.004	19111.50	17008.500	11.004
430.05	0.998	13.833	14.584	-5.430	44.440	39.550	11.003	19155.90	17048.000	11.004

Z	z/(1+z)	LTD_LC	LTD_HHC	%Error	CD_LC	CD_HHC	%Error	LD_LC	LD_HHC	%Error
(1)	(2)	(3)	(4)	(5)	(6)	(7)	(8)	(9)	(10)	(11)
431.05	0.998	13.833	14.584	-5.430	44.440	39.551	11.002	19200.30	17087.700	11.003
432.05	0.998	13.833	14.584	-5.431	44.440	39.551	11.001	19244.80	17127.600	11.001
433.05	0.998	13.833	14.584	-5.431	44.440	39.552	11.001	19289.20	17167.200	11.001
434.05	0.998	13.833	14.584	-5.432	44.440	39.552	11.000	19333.70	17207.000	11.000
435.05	0.998	13.833	14.584	-5.432	44.440	39.552	10.999	19378.10	17247.000	10.998
436.05	0.998	13.833	14.584	-5.433	44.440	39.553	10.998	19422.60	17286.700	10.997
437.05	0.998	13.833	14.584	-5.434	44.440	39.553	10.997	19467.00	17326.200	10.997
438.05	0.998	13.833	14.584	-5.434	44.440	39.554	10.996	19511.40	17365.800	10.997
439.05	0.998	13.833	14.584	-5.435	44.440	39.554	10.995	19555.90	17405.600	10.996
440.05	0.998	13.833	14.584	-5.435	44.440	39.554	10.994	19600.30	17445.600	10.993
441.05	0.998	13.833	14.584	-5.436	44.440	39.555	10.993	19644.80	17485.300	10.993
442.05	0.998	13.833	14.584	-5.436	44.440	39.555	10.992	19689.20	17524.700	10.993
443.05	0.998	13.833	14.585	-5.437	44.440	39.556	10.991	19733.60	17564.800	10.991
444.05	0.998	13.833	14.585	-5.436	44.491	39.556	11.093	19800.90	17604.600	11.092
445.05	0.998	13.833	14.585	-5.437	44.491	39.556	11.092	19845.40	17644.100	11.092
446.05	0.998	13.833	14.585	-5.438	44.491	39.557	11.091	19889.90	17683.700	11.092
447.05	0.998	13.833	14.585	-5.438	44.491	39.557	11.090	19934.30	17723.600	11.090
448.05	0.998	13.833	14.585	-5.439	44.491	39.558	11.089	19978.80	17763.100	11.090
449.05	0.998	13.833	14.585	-5.439	44.491	39.558	11.088	20023.30	17802.900	11.089
450.05	0.998	13.833	14.585	-5.440	44.491	39.558	11.088	20067.80	17842.800	11.088
451.05	0.998	13.833	14.585	-5.440	44.491	39.559	11.087	20112.30	17882.400	11.088
452.05	0.998	13.833	14.585	-5.441	44.491	39.559	11.086	20156.80	17922.100	11.086
453.05	0.998	13.833	14.585	-5.441	44.491	39.560	11.085	20201.30	17962.100	11.085
454.05	0.998	13.833	14.585	-5.442	44.491	39.560	11.084	20245.80	18001.700	11.084
455.05	0.998	13.833	14.585	-5.442	44.491	39.560	11.083	20290.30	18041.500	11.083
456.05	0.998	13.833	14.585	-5.443	44.491	39.561	11.082	20334.80	18081.000	11.083
457.05	0.998	13.833	14.586	-5.443	44.491	39.561	11.081	20379.30	18121.200	11.080
458.05	0.998	13.833	14.586	-5.444	44.491	39.561	11.081	20423.80	18160.500	11.081
459.05	0.998	13.833	14.586	-5.444	44.491	39.562	11.080	20468.20	18200.500	11.079
460.05	0.998	13.833	14.586	-5.445	44.491	39.562	11.079	20512.70	18240.200	11.079
461.05	0.998	13.833	14.586	-5.445	44.491	39.563	11.078	20557.20	18280.100	11.077
462.05	0.998	13.833	14.586	-5.446	44.491	39.563	11.077	20601.70	18319.600	11.077
463.05	0.998	13.833	14.586	-5.446	44.491	39.563	11.076	20646.20	18359.300	11.077
464.05	0.998	13.833	14.586	-5.447	44.491	39.564	11.076	20690.70	18399.200	11.075
465.05	0.998	13.833	14.586	-5.446	44.544	39.564	11.179	20759.60	18438.700	11.180
466.05	0.998	13.833	14.586	-5.447	44.544	39.564	11.178	20804.10	18478.400	11.179
467.05	0.998	13.833	14.586	-5.447	44.544	39.565	11.178	20848.60	18518.200	11.178
468.05	0.998	13.833	14.586	-5.448	44.544	39.565	11.177	20893.20	18557.800	11.178
469.05	0.998	13.833	14.586	-5.448	44.544	39.566	11.176	20937.70	18598.000	11.175
470.05	0.998	13.833	14.586	-5.449	44.544	39.566	11.175	20982.30	18637.300	11.176
471.05	0.998	13.833	14.587	-5.449	44.544	39.566	11.174	21026.80	18677.300	11.174
472.05	0.998	13.833	14.587	-5.450	44.544	39.567	11.174	21071.40	18717.000	11.173
473.05	0.998	13.833	14.587	-5.450	44.544	39.567	11.173	21115.90	18756.800	11.172
474.05	0.998	13.833	14.587	-5.451	44.544	39.567	11.172	21160.40	18796.300	11.173
475.05	0.998	13.833	14.587	-5.451	44.544	39.568	11.171	21205.00	18835.900	11.172
476.05	0.998	13.833	14.587	-5.452	44.544	39.568	11.170	21249.50	18875.700	11.171
477.05	0.998	13.833	14.587	-5.452	44.544	39.568	11.170	21294.10	18915.700	11.169
478.05	0.998	13.833	14.587	-5.452	44.544	39.569	11.169	21338.60	18955.300	11.169
479.05	0.998	13.833	14.587	-5.453	44.544	39.569	11.168	21383.20	18995.000	11.168
480.05	0.998	13.833	14.587	-5.453	44.544	39.569	11.167	21427.70	19035.000	11.167
481.05	0.998	13.833	14.587	-5.454	44.544	39.570	11.167	21472.30	19074.500	11.167
482.05	0.998	13.833	14.587	-5.454	44.544	39.570	11.166	21516.80	19114.200	11.166
483.05	0.998	13.833	14.587	-5.455	44.544	39.570	11.165	21561.30	19154.100	11.165
484.05	0.998	13.833	14.587	-5.455	44.544	39.571	11.164	21605.90	19193.600	11.165
485.05	0.998	13.833	14.587	-5.456	44.544	39.571	11.163	21650.40	19233.800	11.162
486.05	0.998	13.833	14.587	-5.456	44.544	39.571	11.163	21695.00	19273.000	11.164
487.05	0.998	13.833	14.588	-5.456	44.597	39.572	11.268	21765.60	19313.000	11.268
488.05	0.998	13.833	14.588	-5.456	44.597	39.572	11.268	21810.20	19352.500	11.268
489.05	0.998	13.833	14.588	-5.457	44.597	39.572	11.267	21854.80	19392.300	11.268
490.05	0.998	13.833	14.588	-5.457	44.597	39.573	11.266	21899.40	19432.200	11.266
491.05	0.998	13.833	14.588	-5.457	44.597	39.573	11.265	21944.00	19471.700	11.266
492.05	0.998	13.833	14.588	-5.458	44.597	39.573	11.265	21988.60	19511.900	11.264
493.05	0.998	13.833	14.588	-5.458	44.597	39.574	11.264	22033.20	19551.100	11.265
494.05	0.998	13.833	14.588	-5.459	44.597	39.574	11.263	22077.70	19591.100	11.263
495.05	0.998	13.833	14.588	-5.459	44.597	39.574	11.262	22122.30	19630.600	11.263
496.05	0.998	13.833	14.588	-5.460	44.597	39.575	11.262	22166.90	19670.300	11.263
497.05	0.998	13.833	14.588	-5.460	44.597	39.575	11.261	22211.50	19710.200	11.262

Z	z/(1+z)	LTD_LC	LTD_HHC	%Error	CD_LC	CD_HHC	%Error	LD_LC	LD_HHC	%Error
(1)	(2)	(3)	(4)	(5)	(6)	(7)	(8)	(9)	(10)	(11)
498.05	0.998	13.833	14.588	-5.460	44.597	39.575	11.260	22256.10	19750.200	11.259
499.05	0.998	13.833	14.588	-5.461	44.597	39.576	11.260	22300.70	19789.800	11.259
500.05	0.998	13.833	14.588	-5.461	44.597	39.576	11.259	22345.30	19829.600	11.259
501.05	0.998	13.833	14.588	-5.462	44.597	39.576	11.258	22389.90	19869.500	11.257
502.05	0.998	13.833	14.588	-5.462	44.597	39.577	11.257	22434.50	19909.000	11.257
503.05	0.998	13.833	14.588	-5.463	44.597	39.577	11.257	22479.10	19948.600	11.257
504.05	0.998	13.833	14.589	-5.463	44.597	39.577	11.256	22523.70	19988.400	11.256
505.05	0.998	13.833	14.589	-5.463	44.597	39.578	11.255	22568.30	20028.300	11.255
506.05	0.998	13.833	14.589	-5.464	44.597	39.578	11.255	22612.90	20067.800	11.255
507.05	0.998	13.833	14.589	-5.464	44.597	39.578	11.254	22657.50	20107.500	11.255
508.05	0.998	13.833	14.589	-5.465	44.597	39.578	11.253	22702.10	20147.300	11.254
509.05	0.998	13.833	14.589	-5.465	44.597	39.579	11.253	22746.70	20187.300	11.252
510.05	0.998	13.833	14.589	-5.465	44.597	39.579	11.252	22791.30	20226.800	11.252
511.05	0.998	13.833	14.589	-5.466	44.597	39.579	11.251	22835.90	20266.500	11.252
512.05	0.998	13.833	14.589	-5.465	44.652	39.580	11.359	22908.50	20306.300	11.359
513.05	0.998	13.833	14.589	-5.466	44.652	39.580	11.358	22953.10	20346.200	11.357
514.05	0.998	13.833	14.589	-5.466	44.652	39.580	11.358	22997.80	20385.800	11.358
515.05	0.998	13.833	14.589	-5.467	44.652	39.581	11.357	23042.40	20425.400	11.357
516.05	0.998	13.833	14.589	-5.467	44.652	39.581	11.356	23087.10	20465.200	11.356
517.05	0.998	13.833	14.589	-5.467	44.652	39.581	11.356	23131.70	20505.200	11.355
518.05	0.998	13.833	14.589	-5.468	44.652	39.581	11.355	23176.40	20544.700	11.355
519.05	0.998	13.833	14.589	-5.468	44.652	39.582	11.354	23221.00	20584.300	11.355
520.05	0.998	13.833	14.589	-5.469	44.652	39.582	11.354	23265.70	20624.100	11.354
521.05	0.998	13.833	14.589	-5.469	44.652	39.582	11.353	23310.30	20664.000	11.353
522.05	0.998	13.833	14.590	-5.469	44.652	39.583	11.352	23355.00	20703.500	11.353
523.05	0.998	13.833	14.590	-5.470	44.652	39.583	11.352	23399.70	20743.100	11.353
524.05	0.998	13.833	14.590	-5.470	44.652	39.583	11.351	23444.30	20782.800	11.352
525.05	0.998	13.833	14.590	-5.471	44.652	39.583	11.350	23489.00	20822.700	11.351
526.05	0.998	13.833	14.590	-5.471	44.652	39.584	11.350	23533.60	20862.800	11.349
527.05	0.998	13.833	14.590	-5.471	44.652	39.584	11.349	23578.30	20902.300	11.349
528.05	0.998	13.833	14.590	-5.472	44.652	39.584	11.349	23622.90	20942.000	11.349
529.05	0.998	13.833	14.590	-5.472	44.652	39.585	11.348	23667.60	20981.900	11.348
530.05	0.998	13.833	14.590	-5.472	44.652	39.585	11.347	23712.20	21021.200	11.349
531.05	0.998	13.833	14.590	-5.473	44.652	39.585	11.347	23756.90	21061.400	11.346
532.05	0.998	13.833	14.590	-5.473	44.652	39.585	11.346	23801.50	21101.000	11.346
533.05	0.998	13.833	14.590	-5.474	44.652	39.586	11.345	23846.20	21140.800	11.345
534.05	0.998	13.833	14.590	-5.474	44.652	39.586	11.345	23890.80	21180.700	11.344
535.05	0.998	13.833	14.590	-5.474	44.652	39.586	11.344	23935.50	21220.100	11.345
536.05	0.998	13.833	14.590	-5.475	44.652	39.587	11.344	23980.10	21259.600	11.345
537.05	0.998	13.833	14.590	-5.475	44.652	39.587	11.343	24024.80	21299.300	11.344
538.05	0.998	13.833	14.590	-5.475	44.652	39.587	11.342	24069.40	21339.200	11.343
539.05	0.998	13.833	14.590	-5.476	44.652	39.587	11.342	24114.10	21379.200	11.342
540.05	0.998	13.833	14.590	-5.475	44.707	39.588	11.452	24188.90	21418.600	11.453
541.05	0.998	13.833	14.591	-5.476	44.707	39.588	11.451	24233.60	21458.900	11.450
542.05	0.998	13.833	14.591	-5.476	44.707	39.588	11.451	24278.30	21498.600	11.449
543.05	0.998	13.833	14.591	-5.476	44.707	39.588	11.450	24323.00	21537.800	11.451
544.05	0.998	13.833	14.591	-5.477	44.707	39.589	11.449	24367.80	21577.800	11.449
545.05	0.998	13.833	14.591	-5.477	44.707	39.589	11.449	24412.50	21617.300	11.450
546.05	0.998	13.833	14.591	-5.477	44.707	39.589	11.448	24457.20	21656.900	11.450
547.05	0.998	13.833	14.591	-5.478	44.707	39.590	11.448	24501.90	21696.700	11.449
548.05	0.998	13.833	14.591	-5.478	44.707	39.590	11.447	24546.60	21736.600	11.448
549.05	0.998	13.833	14.591	-5.478	44.707	39.590	11.446	24591.30	21776.700	11.446
550.05	0.998	13.833	14.591	-5.479	44.707	39.590	11.446	24636.00	21816.100	11.446
551.05	0.998	13.833	14.591	-5.479	44.707	39.591	11.445	24680.70	21855.800	11.446
552.05	0.998	13.833	14.591	-5.480	44.707	39.591	11.445	24725.40	21895.500	11.445
553.05	0.998	13.833	14.591	-5.480	44.707	39.591	11.444	24770.10	21935.400	11.444
554.05	0.998	13.833	14.591	-5.480	44.707	39.591	11.444	24814.80	21975.500	11.442
555.05	0.998	13.833	14.591	-5.481	44.707	39.592	11.443	24859.50	22015.000	11.443
556.05	0.998	13.833	14.591	-5.481	44.707	39.592	11.442	24904.20	22054.600	11.442
557.05	0.998	13.833	14.591	-5.481	44.707	39.592	11.442	24949.00	22094.300	11.442
558.05	0.998	13.833	14.591	-5.482	44.707	39.592	11.441	24993.70	22134.200	11.441
559.05	0.998	13.833	14.591	-5.482	44.707	39.593	11.441	25038.40	22173.500	11.442
560.05	0.998	13.833	14.591	-5.482	44.707	39.593	11.440	25083.10	22213.700	11.439
561.05	0.998	13.833	14.591	-5.483	44.707	39.593	11.440	25127.80	22253.300	11.439
562.05	0.998	13.833	14.592	-5.483	44.707	39.593	11.439	25172.50	22293.000	11.439
563.05	0.998	13.833	14.592	-5.483	44.707	39.594	11.438	25217.20	22332.900	11.438
564.05	0.998	13.833	14.592	-5.484	44.707	39.594	11.438	25261.90	22372.200	11.439

Z	z/(1+z)	LTD_LC	LTD_HHC	%Error	CD_LC	CD_HHC	%Error	LD_LC	LD_HHC	%Error
(1)	(2)	(3)	(4)	(5)	(6)	(7)	(8)	(9)	(10)	(11)
565.05	0.998	13.833	14.592	-5.484	44.707	39.594	11.437	25306.60	22412.300	11.437
566.05	0.998	13.833	14.592	-5.484	44.707	39.594	11.437	25351.30	22451.800	11.437
567.05	0.998	13.833	14.592	-5.485	44.707	39.595	11.436	25396.00	22491.500	11.437
568.05	0.998	13.833	14.592	-5.485	44.707	39.595	11.436	25440.70	22531.300	11.436
569.05	0.998	13.833	14.592	-5.485	44.707	39.595	11.435	25485.40	22571.300	11.435
570.05	0.998	13.833	14.592	-5.486	44.707	39.595	11.435	25530.10	22610.600	11.436
571.05	0.998	13.833	14.592	-5.485	44.765	39.596	11.547	25607.60	22650.800	11.546
572.05	0.998	13.833	14.592	-5.485	44.765	39.596	11.547	25652.30	22690.400	11.546
573.05	0.998	13.833	14.592	-5.486	44.765	39.596	11.546	25697.10	22730.100	11.546
574.05	0.998	13.833	14.592	-5.486	44.765	39.596	11.546	25741.90	22770.000	11.545
575.05	0.998	13.833	14.592	-5.486	44.765	39.597	11.545	25786.60	22809.200	11.546
576.05	0.998	13.833	14.592	-5.487	44.765	39.597	11.544	25831.40	22849.400	11.544
577.05	0.998	13.833	14.592	-5.487	44.765	39.597	11.544	25876.10	22888.900	11.545
578.05	0.998	13.833	14.592	-5.487	44.765	39.597	11.543	25920.90	22928.500	11.544
579.05	0.998	13.833	14.592	-5.488	44.765	39.597	11.543	25965.70	22968.300	11.544
580.05	0.998	13.833	14.592	-5.488	44.765	39.598	11.542	26010.40	23008.200	11.542
581.05	0.998	13.833	14.592	-5.488	44.765	39.598	11.542	26055.20	23048.200	11.541
582.05	0.998	13.833	14.592	-5.489	44.765	39.598	11.541	26100.00	23087.600	11.542
583.05	0.998	13.833	14.592	-5.489	44.765	39.598	11.541	26144.70	23127.200	11.542
584.05	0.998	13.833	14.592	-5.489	44.765	39.599	11.540	26189.50	23166.800	11.542
585.05	0.998	13.833	14.593	-5.490	44.765	39.599	11.540	26234.30	23206.600	11.541
586.05	0.998	13.833	14.593	-5.490	44.765	39.599	11.539	26279.00	23246.500	11.540
587.05	0.998	13.833	14.593	-5.490	44.765	39.599	11.539	26323.80	23286.600	11.538
588.05	0.998	13.833	14.593	-5.490	44.765	39.600	11.538	26368.60	23326.000	11.539
589.05	0.998	13.833	14.593	-5.491	44.765	39.600	11.538	26413.30	23365.500	11.539
590.05	0.998	13.833	14.593	-5.491	44.765	39.600	11.537	26458.10	23405.900	11.536
591.05	0.998	13.833	14.593	-5.491	44.765	39.600	11.537	26502.80	23445.700	11.535
592.05	0.998	13.833	14.593	-5.492	44.765	39.600	11.536	26547.60	23484.800	11.537
593.05	0.998	13.833	14.593	-5.492	44.765	39.601	11.536	26592.40	23524.900	11.535
594.05	0.998	13.833	14.593	-5.492	44.765	39.601	11.535	26637.10	23564.200	11.536
595.05	0.998	13.833	14.593	-5.493	44.765	39.601	11.535	26681.90	23604.500	11.534
596.05	0.998	13.833	14.593	-5.493	44.765	39.601	11.534	26726.70	23644.100	11.534
597.05	0.998	13.833	14.593	-5.493	44.765	39.602	11.534	26771.40	23683.900	11.533
598.05	0.998	13.833	14.593	-5.493	44.765	39.602	11.533	26816.20	23723.800	11.532
599.05	0.998	13.833	14.593	-5.494	44.765	39.602	11.533	26861.00	23762.900	11.534
600.05	0.998	13.833	14.593	-5.494	44.765	39.602	11.532	26905.70	23803.100	11.532
601.05	0.998	13.833	14.593	-5.494	44.765	39.602	11.532	26950.50	23842.500	11.532
602.05	0.998	13.833	14.593	-5.495	44.765	39.603	11.531	26995.30	23882.000	11.533
603.05	0.998	13.833	14.593	-5.495	44.765	39.603	11.531	27040.00	23921.700	11.532
604.05	0.998	13.833	14.593	-5.495	44.765	39.603	11.530	27084.80	23961.500	11.531
605.05	0.998	13.833	14.593	-5.495	44.765	39.603	11.530	27129.60	24001.500	11.530
606.05	0.998	13.833	14.593	-5.495	44.823	39.604	11.645	27209.90	24041.600	11.644
607.05	0.998	13.833	14.593	-5.495	44.823	39.604	11.645	27254.70	24080.900	11.645
608.05	0.998	13.833	14.593	-5.496	44.823	39.604	11.644	27299.50	24120.400	11.646
609.05	0.998	13.833	14.594	-5.496	44.823	39.604	11.644	27344.40	24160.900	11.642
610.05	0.998	13.833	14.594	-5.496	44.823	39.604	11.643	27389.20	24200.600	11.642
611.05	0.998	13.833	14.594	-5.496	44.823	39.605	11.643	27434.00	24239.600	11.644
612.05	0.998	13.833	14.594	-5.497	44.823	39.605	11.642	27478.80	24279.500	11.643
613.05	0.998	13.833	14.594	-5.497	44.823	39.605	11.642	27523.70	24319.700	11.641
614.05	0.998	13.833	14.594	-5.497	44.823	39.605	11.641	27568.50	24359.000	11.642
615.05	0.998	13.833	14.594	-5.498	44.823	39.605	11.641	27613.30	24398.500	11.642
616.05	0.998	13.833	14.594	-5.498	44.823	39.606	11.640	27658.10	24439.000	11.639
617.05	0.998	13.833	14.594	-5.498	44.823	39.606	11.640	27703.00	24478.800	11.639
618.05	0.998	13.833	14.594	-5.498	44.823	39.606	11.639	27747.80	24517.700	11.641
619.05	0.998	13.833	14.594	-5.499	44.823	39.606	11.639	27792.60	24557.700	11.639
620.05	0.998	13.833	14.594	-5.499	44.823	39.607	11.638	27837.40	24597.800	11.638
621.05	0.998	13.833	14.594	-5.499	44.823	39.607	11.638	27882.20	24637.200	11.638
622.05	0.998	13.833	14.594	-5.499	44.823	39.607	11.638	27927.10	24676.700	11.639
623.05	0.998	13.833	14.594	-5.500	44.823	39.607	11.637	27971.90	24717.200	11.636
624.05	0.998	13.833	14.594	-5.500	44.823	39.607	11.637	28016.70	24756.900	11.635
625.05	0.998	13.833	14.594	-5.500	44.823	39.608	11.636	28061.50	24795.800	11.638
626.05	0.998	13.833	14.594	-5.501	44.823	39.608	11.636	28106.40	24835.800	11.636
627.05	0.998	13.833	14.594	-5.501	44.823	39.608	11.635	28151.20	24875.900	11.635
628.05	0.998	13.833	14.594	-5.501	44.823	39.608	11.635	28196.00	24915.200	11.636
629.05	0.998	13.833	14.594	-5.501	44.823	39.608	11.634	28240.80	24955.600	11.633
630.05	0.998	13.833	14.594	-5.502	44.823	39.609	11.634	28285.70	24995.100	11.633
631.05	0.998	13.833	14.594	-5.502	44.823	39.609	11.633	28330.50	25034.800	11.633

Z	z/(1+z)	LTD_LC	LTD_HHC	%Error	CD_LC	CD_HHC	%Error	LD_LC	LD_HHC	%Error
(1)	(2)	(3)	(4)	(5)	(6)	(7)	(8)	(9)	(10)	(11)
632.05	0.998	13.833	14.594	-5.502	44.823	39.609	11.633	28375.30	25074.600	11.632
633.05	0.998	13.833	14.594	-5.502	44.823	39.609	11.633	28420.10	25114.500	11.631
634.05	0.998	13.833	14.594	-5.503	44.823	39.609	11.632	28465.00	25153.600	11.633
635.05	0.998	13.833	14.594	-5.503	44.823	39.610	11.632	28509.80	25193.800	11.631
636.05	0.998	13.833	14.595	-5.503	44.823	39.610	11.631	28554.60	25233.100	11.632
637.05	0.998	13.833	14.595	-5.503	44.823	39.610	11.631	28599.40	25272.600	11.632
638.05	0.998	13.833	14.595	-5.504	44.823	39.610	11.630	28644.20	25313.200	11.629
639.05	0.998	13.833	14.595	-5.504	44.823	39.610	11.630	28689.10	25352.900	11.629
640.05	0.998	13.833	14.595	-5.504	44.823	39.610	11.630	28733.90	25392.700	11.628
641.05	0.998	13.833	14.595	-5.505	44.823	39.611	11.629	28778.70	25431.700	11.630
642.05	0.998	13.833	14.595	-5.505	44.823	39.611	11.629	28823.50	25471.800	11.628
643.05	0.998	13.833	14.595	-5.505	44.823	39.611	11.628	28868.40	25511.000	11.630
644.05	0.998	13.833	14.595	-5.505	44.823	39.611	11.628	28913.20	25551.400	11.627
645.05	0.998	13.833	14.595	-5.505	44.883	39.611	11.746	28996.90	25590.900	11.746
646.05	0.998	13.833	14.595	-5.505	44.883	39.612	11.746	29041.80	25630.500	11.746
647.05	0.998	13.833	14.595	-5.505	44.883	39.612	11.745	29086.70	25670.200	11.746
648.05	0.998	13.833	14.595	-5.506	44.883	39.612	11.745	29131.50	25710.000	11.745
649.05	0.998	13.833	14.595	-5.506	44.883	39.612	11.744	29176.40	25750.000	11.744
650.05	0.998	13.833	14.595	-5.506	44.883	39.612	11.744	29221.30	25790.100	11.742
651.05	0.998	13.833	14.595	-5.506	44.883	39.613	11.743	29266.20	25829.300	11.744
652.05	0.998	13.833	14.595	-5.507	44.883	39.613	11.743	29311.10	25868.600	11.745
653.05	0.998	13.833	14.595	-5.507	44.883	39.613	11.743	29356.00	25909.100	11.742
654.05	0.998	13.833	14.595	-5.507	44.883	39.613	11.742	29400.80	25948.700	11.742
655.05	0.998	13.833	14.595	-5.507	44.883	39.613	11.742	29445.70	25988.400	11.742
656.05	0.998	13.833	14.595	-5.508	44.883	39.614	11.741	29490.60	26028.200	11.741
657.05	0.998	13.833	14.595	-5.508	44.883	39.614	11.741	29535.50	26068.100	11.740
658.05	0.998	13.833	14.595	-5.508	44.883	39.614	11.741	29580.40	26107.100	11.742
659.05	0.998	13.833	14.595	-5.508	44.883	39.614	11.740	29625.30	26147.300	11.740
660.05	0.998	13.833	14.595	-5.509	44.883	39.614	11.740	29670.10	26186.600	11.741
661.05	0.998	13.833	14.595	-5.509	44.883	39.614	11.739	29715.00	26227.000	11.738
662.05	0.998	13.833	14.595	-5.509	44.883	39.615	11.739	29759.90	26266.500	11.739
663.05	0.998	13.833	14.595	-5.509	44.883	39.615	11.739	29804.80	26306.200	11.739
664.05	0.998	13.833	14.595	-5.509	44.883	39.615	11.738	29849.70	26345.900	11.738
665.05	0.998	13.833	14.596	-5.510	44.883	39.615	11.738	29894.60	26385.800	11.737
666.05	0.999	13.833	14.596	-5.510	44.883	39.615	11.737	29939.40	26425.700	11.736
667.05	0.999	13.833	14.596	-5.510	44.883	39.615	11.737	29984.30	26464.800	11.738
668.05	0.999	13.833	14.596	-5.510	44.883	39.616	11.737	30029.20	26505.000	11.736
669.05	0.999	13.833	14.596	-5.511	44.883	39.616	11.736	30074.10	26544.300	11.737
670.05	0.999	13.833	14.596	-5.511	44.883	39.616	11.736	30119.00	26584.800	11.734
671.05	0.999	13.833	14.596	-5.511	44.883	39.616	11.735	30163.90	26624.300	11.735
672.05	0.999	13.833	14.596	-5.511	44.883	39.616	11.735	30208.70	26663.900	11.734
673.05	0.999	13.833	14.596	-5.512	44.883	39.617	11.735	30253.60	26703.700	11.734
674.05	0.999	13.833	14.596	-5.512	44.883	39.617	11.734	30298.50	26743.600	11.733
675.05	0.999	13.833	14.596	-5.512	44.883	39.617	11.734	30343.40	26782.500	11.735
676.05	0.999	13.833	14.596	-5.512	44.883	39.617	11.733	30388.30	26822.600	11.734
677.05	0.999	13.833	14.596	-5.513	44.883	39.617	11.733	30433.20	26862.800	11.732
678.05	0.999	13.833	14.596	-5.513	44.883	39.617	11.733	30478.00	26902.100	11.733
679.05	0.999	13.833	14.596	-5.513	44.883	39.618	11.732	30522.90	26941.400	11.734
680.05	0.999	13.833	14.596	-5.513	44.883	39.618	11.732	30567.80	26982.000	11.731
681.05	0.999	13.833	14.596	-5.513	44.883	39.618	11.731	30612.70	27021.600	11.731
682.05	0.999	13.833	14.596	-5.514	44.883	39.618	11.731	30657.60	27061.300	11.730
683.05	0.999	13.833	14.596	-5.514	44.883	39.618	11.731	30702.50	27101.200	11.730
684.05	0.999	13.833	14.596	-5.514	44.883	39.618	11.730	30747.30	27141.100	11.729
685.05	0.999	13.833	14.596	-5.514	44.883	39.619	11.730	30792.20	27180.100	11.731
686.05	0.999	13.833	14.596	-5.515	44.883	39.619	11.730	30837.10	27220.300	11.729
687.05	0.999	13.833	14.596	-5.515	44.883	39.619	11.729	30882.00	27259.500	11.730
688.05	0.999	13.833	14.596	-5.515	44.883	39.619	11.729	30926.90	27299.900	11.728
689.05	0.999	13.833	14.596	-5.515	44.945	39.619	11.850	31014.50	27339.300	11.850
690.05	0.999	13.833	14.596	-5.515	44.945	39.619	11.850	31059.40	27378.800	11.850
691.05	0.999	13.833	14.596	-5.515	44.945	39.620	11.849	31104.40	27418.500	11.850
692.05	0.999	13.833	14.596	-5.515	44.945	39.620	11.849	31149.30	27458.200	11.850
693.05	0.999	13.833	14.596	-5.515	44.945	39.620	11.849	31194.20	27498.100	11.849
694.05	0.999	13.833	14.596	-5.516	44.945	39.620	11.848	31239.20	27538.100	11.848
695.05	0.999	13.833	14.596	-5.516	44.945	39.620	11.848	31284.10	27578.200	11.846
696.05	0.999	13.833	14.596	-5.516	44.945	39.620	11.847	31329.10	27617.300	11.848
697.05	0.999	13.833	14.597	-5.516	44.945	39.621	11.847	31374.00	27657.600	11.846
698.05	0.999	13.833	14.597	-5.517	44.945	39.621	11.847	31419.00	27696.900	11.847

Z	z/(1+z)	LTD_LC	LTD_HHC	%Error	CD_LC	CD_HHC	%Error	LD_LC	LD_HHC	%Error
(1)	(2)	(3)	(4)	(5)	(6)	(7)	(8)	(9)	(10)	(11)
699.05	0.999	13.833	14.597	-5.517	44.945	39.621	11.846	31463.90	27736.300	11.847
700.05	0.999	13.833	14.597	-5.517	44.945	39.621	11.846	31508.90	27775.800	11.848
701.05	0.999	13.833	14.597	-5.517	44.945	39.621	11.846	31553.80	27816.600	11.844
702.05	0.999	13.833	14.597	-5.517	44.945	39.621	11.845	31598.80	27856.300	11.844
703.05	0.999	13.833	14.597	-5.518	44.945	39.622	11.845	31643.70	27895.000	11.847
704.05	0.999	13.833	14.597	-5.518	44.945	39.622	11.845	31688.60	27935.000	11.845
705.05	0.999	13.833	14.597	-5.518	44.945	39.622	11.844	31733.60	27975.100	11.844
706.05	0.999	13.833	14.597	-5.518	44.945	39.622	11.844	31778.50	28015.300	11.842
707.05	0.999	13.833	14.597	-5.518	44.945	39.622	11.844	31823.50	28054.400	11.844
708.05	0.999	13.833	14.597	-5.519	44.945	39.622	11.843	31868.40	28093.700	11.845
709.05	0.999	13.833	14.597	-5.519	44.945	39.623	11.843	31913.40	28134.200	11.842
710.05	0.999	13.833	14.597	-5.519	44.945	39.623	11.842	31958.30	28173.700	11.843
711.05	0.999	13.833	14.597	-5.519	44.945	39.623	11.842	32003.30	28213.200	11.843
712.05	0.999	13.833	14.597	-5.520	44.945	39.623	11.842	32048.20	28252.900	11.843
713.05	0.999	13.833	14.597	-5.520	44.945	39.623	11.841	32093.10	28292.700	11.842
714.05	0.999	13.833	14.597	-5.520	44.945	39.623	11.841	32138.10	28332.600	11.841
715.05	0.999	13.833	14.597	-5.520	44.945	39.623	11.841	32183.00	28372.600	11.840
716.05	0.999	13.833	14.597	-5.520	44.945	39.624	11.840	32228.00	28411.500	11.842
717.05	0.999	13.833	14.597	-5.521	44.945	39.624	11.840	32272.90	28451.800	11.840
718.05	0.999	13.833	14.597	-5.521	44.945	39.624	11.840	32317.90	28492.100	11.838
719.05	0.999	13.833	14.597	-5.521	44.945	39.624	11.839	32362.80	28531.400	11.839
720.05	0.999	13.833	14.597	-5.521	44.945	39.624	11.839	32407.80	28570.700	11.840
721.05	0.999	13.833	14.597	-5.521	44.945	39.624	11.839	32452.70	28610.200	11.840
722.05	0.999	13.833	14.597	-5.522	44.945	39.625	11.838	32497.70	28651.000	11.837
723.05	0.999	13.833	14.597	-5.522	44.945	39.625	11.838	32542.60	28690.600	11.837
724.05	0.999	13.833	14.597	-5.522	44.945	39.625	11.838	32587.50	28730.400	11.836
725.05	0.999	13.833	14.597	-5.522	44.945	39.625	11.837	32632.50	28769.100	11.839
726.05	0.999	13.833	14.597	-5.522	44.945	39.625	11.837	32677.40	28809.100	11.838
727.05	0.999	13.833	14.597	-5.523	44.945	39.625	11.837	32722.40	28849.200	11.837
728.05	0.999	13.833	14.597	-5.523	44.945	39.625	11.836	32767.30	28889.400	11.835
729.05	0.999	13.833	14.597	-5.523	44.945	39.626	11.836	32812.30	28928.500	11.836
730.05	0.999	13.833	14.597	-5.523	44.945	39.626	11.836	32857.20	28969.000	11.834
731.05	0.999	13.833	14.598	-5.523	44.945	39.626	11.835	32902.20	29008.200	11.835
732.05	0.999	13.833	14.598	-5.524	44.945	39.626	11.835	32947.10	29047.600	11.836
733.05	0.999	13.833	14.598	-5.524	44.945	39.626	11.835	32992.10	29087.200	11.836
734.05	0.999	13.833	14.598	-5.524	44.945	39.626	11.834	33037.00	29126.800	11.836
735.05	0.999	13.833	14.598	-5.524	44.945	39.626	11.834	33081.90	29166.500	11.836
736.05	0.999	13.833	14.598	-5.524	44.945	39.627	11.834	33126.90	29206.300	11.835
737.05	0.999	13.833	14.598	-5.525	44.945	39.627	11.833	33171.80	29246.200	11.834
738.05	0.999	13.833	14.598	-5.525	44.945	39.627	11.833	33216.80	29286.300	11.833
739.05	0.999	13.833	14.598	-5.525	44.945	39.627	11.833	33261.70	29326.500	11.831
740.05	0.999	13.834	14.598	-5.524	45.009	39.627	11.957	33353.90	29365.400	11.958
741.05	0.999	13.834	14.598	-5.525	45.009	39.627	11.957	33398.90	29405.800	11.956
742.05	0.999	13.834	14.598	-5.525	45.009	39.627	11.957	33443.90	29445.000	11.957
743.05	0.999	13.834	14.598	-5.525	45.009	39.628	11.956	33488.90	29484.200	11.958
744.05	0.999	13.834	14.598	-5.525	45.009	39.628	11.956	33533.90	29524.900	11.955
745.05	0.999	13.834	14.598	-5.525	45.009	39.628	11.956	33578.90	29564.400	11.955
746.05	0.999	13.834	14.598	-5.526	45.009	39.628	11.955	33624.00	29604.000	11.956
747.05	0.999	13.834	14.598	-5.526	45.009	39.628	11.955	33669.00	29643.700	11.955
748.05	0.999	13.834	14.598	-5.526	45.009	39.628	11.955	33714.00	29683.600	11.955
749.05	0.999	13.834	14.598	-5.526	45.009	39.628	11.954	33759.00	29723.500	11.954
750.05	0.999	13.834	14.598	-5.526	45.009	39.629	11.954	33804.00	29763.500	11.953
751.05	0.999	13.834	14.598	-5.527	45.009	39.629	11.954	33849.00	29802.300	11.955
752.05	0.999	13.834	14.598	-5.527	45.009	39.629	11.954	33894.00	29842.500	11.953
753.05	0.999	13.834	14.598	-5.527	45.009	39.629	11.953	33939.00	29882.900	11.951
754.05	0.999	13.834	14.598	-5.527	45.009	39.629	11.953	33984.00	29922.000	11.953
755.05	0.999	13.834	14.598	-5.527	45.009	39.629	11.953	34029.00	29961.200	11.954
756.05	0.999	13.834	14.598	-5.527	45.009	39.629	11.952	34074.00	30001.900	11.951
757.05	0.999	13.834	14.598	-5.528	45.009	39.630	11.952	34119.10	30041.300	11.952
758.05	0.999	13.834	14.598	-5.528	45.009	39.630	11.952	34164.10	30080.800	11.952
759.05	0.999	13.834	14.598	-5.528	45.009	39.630	11.951	34209.10	30120.400	11.952
760.05	0.999	13.834	14.598	-5.528	45.009	39.630	11.951	34254.10	30160.100	11.952
761.05	0.999	13.834	14.598	-5.528	45.009	39.630	11.951	34299.10	30200.000	11.951
762.05	0.999	13.834	14.598	-5.529	45.009	39.630	11.950	34344.10	30239.900	11.950
763.05	0.999	13.834	14.598	-5.529	45.009	39.630	11.950	34389.10	30279.900	11.949
764.05	0.999	13.834	14.598	-5.529	45.009	39.631	11.950	34434.10	30318.700	11.952
765.05	0.999	13.834	14.598	-5.529	45.009	39.631	11.950	34479.10	30359.000	11.950

Z	z/(1+z)	LTD_LC	LTD_HHC	%Error	CD_LC	CD_HHC	%Error	LD_LC	LD_HHC	%Error
(1)	(2)	(3)	(4)	(5)	(6)	(7)	(8)	(9)	(10)	(11)
766.05	0.999	13.834	14.598	-5.529	45.009	39.631	11.949	34524.10	30399.300	11.948
767.05	0.999	13.834	14.598	-5.529	45.009	39.631	11.949	34569.10	30438.400	11.949
768.05	0.999	13.834	14.598	-5.530	45.009	39.631	11.949	34614.20	30477.600	11.951
769.05	0.999	13.834	14.598	-5.530	45.009	39.631	11.948	34659.20	30518.200	11.948
770.05	0.999	13.834	14.599	-5.530	45.009	39.631	11.948	34704.20	30557.600	11.948
771.05	0.999	13.834	14.599	-5.530	45.009	39.631	11.948	34749.20	30597.100	11.949
772.05	0.999	13.834	14.599	-5.530	45.009	39.632	11.947	34794.20	30636.700	11.949
773.05	0.999	13.834	14.599	-5.531	45.009	39.632	11.947	34839.20	30676.300	11.949
774.05	0.999	13.834	14.599	-5.531	45.009	39.632	11.947	34884.20	30716.100	11.948
775.05	0.999	13.834	14.599	-5.531	45.009	39.632	11.947	34929.20	30756.000	11.948
776.05	0.999	13.834	14.599	-5.531	45.009	39.632	11.946	34974.20	30796.000	11.947
777.05	0.999	13.834	14.599	-5.531	45.009	39.632	11.946	35019.20	30836.100	11.945
778.05	0.999	13.834	14.599	-5.531	45.009	39.632	11.946	35064.20	30876.300	11.944
779.05	0.999	13.834	14.599	-5.532	45.009	39.633	11.945	35109.30	30915.100	11.946
780.05	0.999	13.834	14.599	-5.532	45.009	39.633	11.945	35154.30	30955.500	11.944
781.05	0 999	13.834	14.599	-5.532	45.009	39.633	11.945	35199.30	30994.600	11.945
782.05	0.999	13.834	14.599	-5.532	45.009	39.633	11.945	35244.30	31035.200	11.943
783.05	0.999	13.834	14.599	-5.532	45.009	39.633	11.944	35289.30	31074.500	11.944
784.05	0.999	13.834	14.599	-5.532	45.009	39.633	11.944	35334.30	31113.800	11.944
785.05	0.999	13.834	14.599	-5.533	45.009	39.633	11.944	35379.30	31153.300	11.945
786.05	0.999	13.834	14.599	-5.533	45.009	39.633	11.943	35424.30	31192.800	11.945
787.05	0.999	13.834	14.599	-5.533	45.009	39.634	11.943	35469.30	31232.500	11.945
788.05	0.999	13.834	14.599	-5.533	45.009	39.634	11.943	35514.30	31272.300	11.945
789.05	0.999	13.834	14.599	-5.533	45.009	39.634	11.943	35559.30	31312.100	11.944
790.05	0.999	13.834	14.599	-5.533	45.009	39.634	11.942	35604.40	31352.100	11.943
791.05	0.999	13.834	14.599	-5.534	45.009	39.634	11.942	35649.40	31392.200	11.942
792.05	0.999	13.834	14.599	-5.534	45.009	39.634	11.942	35694.40	31432.300	11.940
793.05	0.999	13.834	14.599	-5.534	45.009	39.634	11.941	35739.40	31471.100	11.943
794.05	0.999	13.834	14.599	-5.534	45.009	39.634	11.941	35784.40	31511.500	11.941
795.05	0.999	13.834	14.599	-5.534	45.009	39.635	11.941	35829.40	31550.400	11.943
796.05	0.999	13.834	14.599	-5.534	45.009	39.635	11.941	35874.40	31591.000	11.940
797.05	0.999	13.834	14.599	-5.535	45.009	39.635	11.940	35919.40	31630.200	11.941
798.05	0.999	13.834	14.599	-5.535	45.009	39.635	11.940	35964.40	31671.000	11.938
799.05	0.999	13.834	14.599	-5.534	45.075	39.635	12.068	36062.10	31710.300	12.067
800.05	0.999	13.834	14.599	-5.535	45.075	39.635	12.068	36107.10	31749.800	12.068
801.05	0 999	13.834	14.599	-5.535	45.075	39.635	12.068	36152.20	31789.400	12.068
802.05	0.999	13.834	14.599	-5.535	45.075	39.635	12.067	36197.30	31829.000	12.068
803.05	0.999	13.834	14.599	-5.535	45.075	39.636	12.067	36242.40	31868.800	12.068
804.05	0.999	13.834	14.599	-5.535	45.075	39.636	12.067	36287.40	31908.600	12.067
805.05	0.999	13.834	14.599	-5.535	45.075	39.636	12.067	36332.50	31948.600	12.066
806.05	0.999	13.834	14.599	-5.535	45.075	39.636	12.066	36377.60	31988.600	12.065
807.05	0.999	13.834	14.599	-5.536	45.075	39.636	12.066	36422.70	32027.300	12.068
808.05	0.999	13.834	14.599	-5.536	45.075	39.636	12.066	36467.70	32067.500	12.066
809.05	0.999	13.834	14.599	-5.536	45.075	39.636	12.066	36512.80	32107.900	12.064
810.05	0.999	13.834	14.599	-5.536	45.075	39.636	12.065	36557.90	32146.800	12.066
811.05	0.999	13.834	14.599	-5.536	45.075	39.637	12.065	36603.00	32187.300	12.064
812.05	0.999	13.834	14.599	-5.536	45.075	39.637	12.065	36648.00	32226.400	12.065
813.05	0.999	13.834	14.600	-5.537	45.075	39.637	12.065	36693.10	32265.600	12.066
814.05	0.999	13.834	14.600	-5.537	45.075	39.637	12.064	36738.20	32306.500	12.063
815.05	0.999	13.834	14.600	-5.537	45.075	39.637	12.064	36783.30	32345.800	12.064
816.05	0.999	13.834	14.600	-5.537	45.075	39.637	12.064	36828.30	32385.300	12.064
817.05	0.999	13.834	14.600	-5.537	45.075	39.637	12.063	36873.40	32424.900	12.064
818.05	0.999	13.834	14.600	-5.537	45.075	39.637	12.063	36918.50	32464.600	12.064
819.05	0.999	13.834	14.600	-5.538	45.075	39.637	12.063	36963.60	32504.300	12.064
820.05	0.999	13.834	14.600	-5.538	45.075	39.638	12.063	37008.60	32544.200	12.063
821.05	0.999	13.834	14.600	-5.538	45.075	39.638	12.062	37053.70	32584.200	12.062
822.05	0.999	13.834	14.600	-5.538	45.075	39.638	12.062	37098.80	32624.200	12.061
823.05	0.999	13.834	14.600	-5.538	45.075	39.638	12.062	37143.90	32664.400	12.060
824.05	0.999	13.834	14.600	-5.538	45.075	39.638	12.062	37188.90	32703.000	12.063
825.05	0.999	13.834	14.600	-5.538	45.075	39.638	12.061	37234.00	32743.400	12.061
826.05	0.999	13.834	14.600	-5.539	45.075	39.638	12.061	37279.10	32782.200	12.063
827.05	0.999	13.834	14.600	-5.539	45.075	39.638	12.061	37324.20	32822.800	12.060
828.05	0.999	13.834	14.600	-5.539	45.075	39.639	12.061	37369.20	32861.800	12.062
829.05	0.999	13.834	14.600	-5.539	45.075	39.639	12.060	37414.30	32902.500	12.059
830.05	0.999	13.834	14.600	-5.539	45.075	39.639	12.060	37459.40	32941.700	12.060
831.05	0.999	13.834	14.600	-5.539	45.075	39.639	12.060	37504.50	32981.000	12.061
832.05	0.999	13.834	14.600	-5.540	45.075	39.639	12.060	37549.50	33020.400	12.062

Z	z/(1+z)	LTD_LC	LTD_HHC	%Error	CD_LC	CD_HHC	%Error	LD_LC	LD_HHC	%Error
(1)	(2)	(3)	(4)	(5)	(6)	(7)	(8)	(9)	(10)	(11)
833.05	0.999	13.834	14.600	-5.540	45.075	39.639	12.059	37594.60	33061.600	12.058
834.05	0.999	13.834	14.600	-5.540	45.075	39.639	12.059	37639.70	33101.100	12.058
835.05	0.999	13.834	14.600	-5.540	45.075	39.639	12.059	37684.80	33140.800	12.058
836.05	0.999	13.834	14.600	-5.540	45.075	39.639	12.059	37729.80	33180.600	12.057
837.05	0.999	13.834	14.600	-5.540	45.075	39.640	12.058	37774.90	33220.500	12.057
838.05	0.999	13.834	14.600	-5.540	45.075	39.640	12.058	37820.00	33260.500	12.056
839.05	0.999	13.834	14.600	-5.541	45.075	39.640	12.058	37865.10	33298.900	12.059
840.05	0.999	13.834	14.600	-5.541	45.075	39.640	12.058	37910.10	33339.000	12.058
841.05	0.999	13.834	14.600	-5.541	45.075	39.640	12.057	37955.20	33379.300	12.056
842.05	0.999	13.834	14.600	-5.541	45.075	39.640	12.057	38000.30	33417.900	12.059
843.05	0.999	13.834	14.600	-5.541	45.075	39.640	12.057	38045.30	33458.400	12.057
844.05	0.999	13.834	14.600	-5.541	45.075	39.640	12.057	38090.40	33497.200	12.059
845.05	0.999	13.834	14.600	-5.542	45.075	39.640	12.056	38135.50	33537.900	12.056
846.05	0.999	13.834	14.600	-5.542	45.075	39.641	12.056	38180.60	33576.900	12.058
847.05	0.999	13.834	14.600	-5.542	45.075	39.641	12.056	38225.60	33617.700	12.055
848.05	0.999	13.834	14.600	-5.542	45.075	39.641	12.056	38270.70	33657.000	12.056
849.05	0.999	13.834	14.600	-5.542	45.075	39.641	12.055	38315.80	33696.300	12.057
850.05	0.999	13.834	14.600	-5.542	45.075	39.641	12.055	38360.90	33735.700	12.057
851.05	0.999	13.834	14.600	-5.542	45.075	39.641	12.055	38405.90	33776.900	12.053
852.05	0.999	13.834	14.600	-5.543	45.075	39.641	12.055	38451.00	33816.500	12.053
853.05	0.999	13.834	14.600	-5.543	45.075	39.641	12.054	38496.10	33856.200	12.053
854.05	0.999	13.834	14.600	-5.543	45.075	39.641	12.054	38541.20	33896.000	12.053
855.05	0.999	13.834	14.600	-5.543	45.075	39.642	12.054	38586.20	33935.800	12.052
856.05	0.999	13.834	14.600	-5.543	45.075	39.642	12.054	38631.30	33974.100	12.056
857.05	0.999	13.834	14.600	-5.543	45.075	39.642	12.053	38676.40	34014.100	12.055
858.05	0.999	13.834	14.600	-5.543	45.075	39.642	12.053	38721.50	34054.300	12.053
859.05	0.999	13.834	14.600	-5.544	45.075	39.642	12.053	38766.50	34094.500	12.052
860.05	0.999	13.834	14.600	-5.544	45.075	39.642	12.053	38811.60	34133.100	12.055
861.05	0.999	13.834	14.601	-5.544	45.075	39.642	12.052	38856.70	34173.500	12.052
862.05	0.999	13.834	14.601	-5.544	45.075	39.642	12.052	38901.80	34214.100	12.050
863.05	0.999	13.834	14.601	-5.544	45.075	39.642	12.052	38946.80	34252.900	12.052
864.05	0.999	13.834	14.601	-5.544	45.075	39.643	12.052	38991.90	34291.900	12.054
865.05	0.999	13.834	14.601	-5.544	45.075	39.643	12.052	39037.00	34332.700	12.051
866.05	0.999	13.834	14.601	-5.545	45.075	39.643	12.051	39082.10	34371.800	12.052
867.05	0.999	13.834	14.601	-5.545	45.075	39.643	12.051	39127.10	34412.800	12.049
868.05	0.999	13.834	14.601	-5.545	45.075	39.643	12.051	39172.20	34452.100	12.050
869.05	0.999	13.834	14.601	-5.544	45.143	39.643	12.183	39276.50	34491.500	12.183
870.05	0.999	13.834	14.601	-5.545	45.143	39.643	12.183	39321.60	34531.000	12.183
871.05	0.999	13.834	14.601	-5.545	45.143	39.643	12.183	39366.80	34570.500	12.183
872.05	0.999	13.834	14.601	-5.545	45.143	39.643	12.182	39411.90	34610.200	12.183
873.05	0.999	13.834	14.601	-5.545	45.143	39.643	12.182	39457.00	34650.000	12.183
874.05	0.999	13.834	14.601	-5.545	45.143	39.644	12.182	39502.20	34689.800	12.183
875.05	0.999	13.834	14.601	-5.545	45.143	39.644	12.182	39547.30	34729.800	12.182
876.05	0.999	13.834	14.601	-5.545	45.143	39.644	12.181	39592.50	34769.800	12.181
877.05	0.999	13.834	14.601	-5.545	45.143	39.644	12.181	39637.60	34809.900	12.180
878.05	0.999	13.834	14.601	-5.546	45.143	39.644	12.181	39682.80	34848.300	12.183
879.05	0.999	13.834	14.601	-5.546	45.143	39.644	12.181	39727.90	34888.600	12.181
880.05	0.999	13.834	14.601	-5.546	45.143	39.644	12.181	39773.00	34929.000	12.179
881.05	0.999	13.834	14.601	-5.546	45.143	39.644	12.180	39818.20	34967.700	12.182
882.05	0.999	13.834	14.601	-5.546	45.143	39.644	12.180	39863.30	35008.300	12.179
883.05	0.999	13.834	14.601	-5.546	45.143	39.645	12.180	39908.50	35047.100	12.181
884.05	0.999	13.834	14.601	-5.546	45.143	39.645	12.180	39953.60	35087.800	12.179
885.05	0.999	13.834	14.601	-5.547	45.143	39.645	12.179	39998.80	35126.900	12.180
886.05	0.999	13.834	14.601	-5.547	45.143	39.645	12.179	40043.90	35167.800	12.177
887.05	0.999	13.834	14.601	-5.547	45.143	39.645	12.179	40089.00	35207.000	12.178
888.05	0.999	13.834	14.601	-5.547	45.143	39.645	12.179	40134.20	35246.300	12.179
889.05	0.999	13.834	14.601	-5.547	45.143	39.645	12.179	40179.30	35285.600	12.180
890.05	0.999	13.834	14.601	-5.547	45.143	39.645	12.178	40224.50	35325.100	12.180
891.05	0.999	13.834	14.601	-5.547	45.143	39.645	12.178	40269.60	35366.500	12.176
892.05	0.999	13.834	14.601	-5.547	45.143	39.645	12.178	40314.80	35406.100	12.176
893.05	0.999	13.834	14.601	-5.548	45.143	39.646	12.178	40359.90	35445.800	12.176
894.05	0.999	13.834	14.601	-5.548	45.143	39.646	12.177	40405.00	35485.600	12.175
895.05	0.999	13.834	14.601	-5.548	45.143	39.646	12.177	40450.20	35523.600	12.179
896.05	0.999	13.834	14.601	-5.548	45.143	39.646	12.177	40495.30	35563.600	12.179
897.05	0.999	13.834	14.601	-5.548	45.143	39.646	12.177	40540.50	35603.600	12.178
898.05	0.999	13.834	14.601	-5.548	45.143	39.646	12.177	40585.60	35643.800	12.176
899.05	0.999	13.834	14.601	-5.548	45.143	39.646	12.176	40630.80	35684.000	12.175

Z	z/(1+z)	LTD_LC	LTD_HHC	%Error	CD_LC	CD_HHC	%Error	LD_LC	LD_HHC	%Error
(1)	(2)	(3)	(4)	(5)	(6)	(7)	(8)	(9)	(10)	(11)
900.05	0.999	13.834	14.601	-5.549	45.143	39.646	12.176	40675.90	35722.400	12.178
901.05	0.999	13.834	14.601	-5.549	45.143	39.646	12.176	40721.00	35762.900	12.176
902.05	0.999	13.834	14.601	-5.549	45.143	39.646	12.176	40766.20	35803.400	12.174
903.05	0.999	13.834	14.601	-5.549	45.143	39.646	12.176	40811.30	35842.100	12.176
904.05	0.999	13.834	14.601	-5.549	45.143	39.647	12.175	40856.50	35882.800	12.174
905.05	0.999	13.834	14.601	-5.549	45.143	39.647	12.175	40901.60	35921.600	12.176
906.05	0.999	13.834	14.601	-5.549	45.143	39.647	12.175	40946.80	35962.500	12.173
907.05	0.999	13.834	14.601	-5.549	45.143	39.647	12.175	40991.90	36001.500	12.174
908.05	0.999	13.834	14.601	-5.550	45.143	39.647	12.174	41037.00	36040.600	12.176
909.05	0.999	13.834	14.601	-5.550	45.143	39.647	12.174	41082.20	36081.700	12.172
910.05	0.999	13.834	14.601	-5.550	45.143	39.647	12.174	41127.30	36121.000	12.173
911.05	0.999	13.834	14.601	-5.550	45.143	39.647	12.174	41172.50	36160.400	12.173
912.05	0.999	13.834	14.601	-5.550	45.143	39.647	12.174	41217.60	36199.800	12.174
913.05	0.999	13.834	14.601	-5.550	45.143	39.647	12.173	41262.80	36239.300	12.174
914.05	0.999	13.834	14.601	-5.550	45.143	39.648	12.173	41307.90	36278.900	12.174
915.05	0.999	13.834	14.602	-5.550	45.143	39.648	12.173	41353.00	36318.700	12.174
916.05	0.999	13.834	14.602	-5.551	45.143	39.648	12.173	41398.20	36358.400	12.174
917.05	0.999	13.834	14.602	-5.551	45.143	39.648	12.173	41443.30	36398.300	12.173
918.05	0.999	13.834	14.602	-5.551	45.143	39.648	12.172	41488.50	36438.300	12.173
919.05	0.999	13.834	14.602	-5.551	45.143	39.648	12.172	41533.60	36478.300	12.172
920.05	0.999	13.834	14.602	-5.551	45.143	39.648	12.172	41578.80	36518.500	12.170
921.05	0.999	13.834	14.602	-5.551	45.143	39.648	12.172	41623.90	36556.700	12.174
922.05	0.999	13.834	14.602	-5.551	45.143	39.648	12.172	41669.00	36597.000	12.172
923.05	0.999	13.834	14.602	-5.551	45.143	39.648	12.171	41714.20	36637.400	12.170
924.05	0.999	13.834	14.602	-5.552	45.143	39.648	12.171	41759.30	36675.900	12.173
925.05	0.999	13.834	14.602	-5.552	45.143	39.649	12.171	41804.50	36716.400	12.171
926.05	0.999	13.834	14.602	-5.552	45.143	39.649	12.171	41849.60	36757.100	12.169
927.05	0.999	13.834	14.602	-5.552	45.143	39.649	12.170	41894.80	36795.800	12.171
928.05	0.999	13.834	14.602	-5.552	45.143	39.649	12.170	41939.90	36836.700	12.168
929.05	0.999	13.834	14.602	-5.552	45.143	39.649	12.170	41985.00	36875.500	12.170
930.05	0.999	13.834	14.602	-5.552	45.143	39.649	12.170	42030.20	36914.500	12.171
931.05	0.999	13.834	14.602	-5.552	45.143	39.649	12.170	42075.30	36955.600	12.168
932.05	0.999	13.834	14.602	-5.553	45.143	39.649	12.169	42120.50	36994.800	12.169
933.05	0.999	13.834	14.602	-5.553	45.143	39.649	12.169	42165.60	37034.000	12.170
934.05	0.999	13.834	14.602	-5.553	45.143	39.649	12.169	42210.80	37073.300	12.171
935.05	0.999	13.834	14.602	-5.553	45.143	39.649	12.169	42255.90	37114.700	12.167
936.05	0.999	13.834	14.602	-5.553	45.143	39.650	12.169	42301.00	37154.200	12.167
937.05	0.999	13.834	14.602	-5.553	45.143	39.650	12.168	42346.20	37193.800	12.167
938.05	0.999	13.834	14.602	-5.553	45.143	39.650	12.168	42391.30	37233.400	12.167
939.05	0.999	13.834	14.602	-5.553	45.143	39.650	12.168	42436.50	37273.100	12.167
940.05	0.999	13.834	14.602	-5.554	45.143	39.650	12.168	42481.60	37312.900	12.167
941.05	0.999	13.834	14.602	-5.554	45.143	39.650	12.168	42526.80	37352.800	12.166
942.05	0.999	13.834	14.602	-5.554	45.143	39.650	12.167	42571.90	37392.800	12.166
943.05	0.999	13.834	14.602	-5.554	45.143	39.650	12.167	42617.00	37430.700	12.170
944.05	0.999	13.834	14.602	-5.554	45.143	39.650	12.167	42662.20	37470.900	12.168
945.05	0.999	13.834	14.602	-5.554	45.143	39.650	12.167	42707.30	37511.100	12.167
946.05	0.999	13.834	14.602	-5.554	45.143	39.650	12.167	42752.50	37551.400	12.165
947.05	0.999	13.834	14.602	-5.554	45.143	39.651	12.166	42797.60	37589.700	12.169
948.05	0.999	13.834	14.602	-5.554	45.143	39.651	12.166	42842.80	37630.200	12.167
949.05	0.999	13.834	14.602	-5.555	45.143	39.651	12.166	42887.90	37670.800	12.165
950.05	0.999	13.834	14.602	-5.555	45.143	39.651	12.166	42933.00	37709.300	12.167
951.05	0.999	13.834	14.602	-5.555	45.143	39.651	12.166	42978.20	37750.000	12.165
952.05	0.999	13.834	14.602	-5.554	45.213	39.651	12.302	43090.50	37788.700	12.304
953.05	0.999	13.834	14.602	-5.554	45.213	39.651	12.302	43135.70	37829.600	12.301
954.05	0.999	13.834	14.602	-5.555	45.213	39.651	12.302	43180.90	37868.500	12.303
955.05	0.999	13.834	14.602	-5.555	45.213	39.651	12.302	43226.20	37909.600	12.300
956.05	0.999	13.834	14.602	-5.555	45.213	39.651	12.302	43271.40	37948.600	12.301
957.05	0.999	13.834	14.602	-5.555	45.213	39.651	12.302	43316.60	37987.700	12.302
958.05	0.999	13.834	14.602	-5.555	45.213	39.652	12.301	43361.80	38026.800	12.303
959.05	0.999	13.834	14.602	-5.555	45.213	39.652	12.301	43407.00	38068.300	12.299
960.05	0.999	13.834	14.602	-5.555	45.213	39.652	12.301	43452.20	38107.600	12.300
961.05	0.999	13.834	14.602	-5.555	45.213	39.652	12.301	43497.40	38147.000	12.301
962.05	0.999	13.834	14.602	-5.556	45.213	39.652	12.301	43542.60	38186.500	12.301
963.05	0.999	13.834	14.602	-5.556	45.213	39.652	12.300	43587.90	38226.100	12.301
964.05	0.999	13.834	14.602	-5.556	45.213	39.652	12.300	43633.10	38265.700	12.301
965.05	0.999	13.834	14.602	-5.556	45.213	39.652	12.300	43678.30	38305.500	12.301
966.05	0.999	13.834	14.602	-5.556	45.213	39.652	12.300	43723.50	38345.300	12.301

Z	z/(1+z)	LTD_LC	LTD_HHC	%Error	CD_LC	CD_HHC	%Error	LD_LC	LD_HHC	%Error
(1)	(2)	(3)	(4)	(5)	(6)	(7)	(8)	(9)	(10)	(11)
967.05	0.999	13.834	14.602	-5.556	45.213	39.652	12.300	43768.70	38385.200	12.300
968.05	0.999	13.834	14.602	-5.556	45.213	39.652	12.299	43813.90	38425.200	12.299
969.05	0.999	13.834	14.602	-5.556	45.213	39.652	12.299	43859.10	38465.300	12.298
970.05	0.999	13.834	14.602	-5.556	45.213	39.653	12.299	43904.40	38505.400	12.297
971.05	0.999	13.834	14.602	-5.557	45.213	39.653	12.299	43949.60	38543.400	12.301
972.05	0.999	13.834	14.602	-5.557	45.213	39.653	12.299	43994.80	38583.800	12.299
973.05	0.999	13.834	14.602	-5.557	45.213	39.653	12.299	44040.00	38624.200	12.298
974.05	0.999	13.834	14.602	-5.557	45.213	39.653	12.298	44085.20	38662.400	12.301
975.05	0.999	13.834	14.602	-5.557	45.213	39.653	12.298	44130.40	38703.000	12.299
976.05	0.999	13.834	14.603	-5.557	45.213	39.653	12.298	44175.60	38743.600	12.296
977.05	0.999	13.834	14.603	-5.557	45.213	39.653	12.298	44220.80	38782.100	12.299
978.05	0.999	13.834	14.603	-5.557	45.213	39.653	12.298	44266.10	38822.900	12.296
979.05	0.999	13.834	14.603	-5.557	45.213	39.653	12.297	44311.30	38861.600	12.299
980.05	0.999	13.834	14.603	-5.558	45.213	39.653	12.297	44356.50	38902.500	12.296
981.05	0.999	13.834	14.603	-5.558	45.213	39.653	12.297	44401.70	38941.300	12.298
982.05	0.999	13.834	14.603	-5.558	45.213	39.654	12.297	44446.90	38982.500	12.294
983.05	0.999	13.834	14.603	-5.558	45.213	39.654	12.297	44492.10	39021.400	12.296
984.05	0.999	13.834	14.603	-5.558	45.213	39.654	12.296	44537.30	39060.500	12.297
985.05	0.999	13.834	14.603	-5.558	45.213	39.654	12.296	44582.60	39099.600	12.299
986.05	0.999	13.834	14.603	-5.558	45.213	39.654	12.296	44627.80	39141.100	12.294
987.05	0.999	13.834	14.603	-5.558	45.213	39.654	12.296	44673.00	39180.300	12.295
988.05	0.999	13.834	14.603	-5.558	45.213	39.654	12.296	44718.20	39219.700	12.296
989.05	0.999	13.834	14.603	-5.559	45.213	39.654	12.296	44763.40	39259.100	12.296
990.05	0.999	13.834	14.603	-5.559	45.213	39.654	12.295	44808.60	39298.600	12.297
991.05	0.999	13.834	14.603	-5.559	45.213	39.654	12.295	44853.80	39338.200	12.297
992.05	0.999	13.834	14.603	-5.559	45.213	39.654	12.295	44899.00	39377.800	12.297
993.05	0.999	13.834	14.603	-5.559	45.213	39.654	12.295	44944.30	39417.600	12.297
994.05	0.999	13.834	14.603	-5.559	45.213	39.655	12.295	44989.50	39457.400	12.296
995.05	0.999	13.834	14.603	-5.559	45.213	39.655	12.295	45034.70	39497.300	12.296
996.05	0.999	13.834	14.603	-5.559	45.213	39.655	12.294	45079.90	39537.300	12.295
997.05	0.999	13.834	14.603	-5.559	45.213	39.655	12.294	45125.10	39577.400	12.294
998.05	0.999	13.834	14.603	-5.559	45.213	39.655	12.294	45170.30	39617.500	12.293
999.05	0.999	13.834	14.603	-5.560	45.213	39.655	12.294	45215.50	39657.700	12.292
1000.05	0.999	13.834	14.603	-5.560	45.213	39.655	12.294	45260.80	39695.700	12.296
1001.05	0.999	13.834	14.603	-5.560	45.213	39.655	12.293	45306.00	39736.100	12.294
1002.05	0.999	13.834	14.603	-5.560	45.213	39.655	12.293	45351.20	39776.500	12.292
1003.05	0.999	13.834	14.603	-5.560	45.213	39.655	12.293	45396.40	39814.700	12.296
1004.05	0.999	13.834	14.603	-5.560	45.213	39.655	12.293	45441.60	39855.300	12.293
1005.05	0.999	13.834	14.603	-5.560	45.213	39.655	12.293	45486.80	39896.000	12.291
1006.05	0.999	13.834	14.603	-5.560	45.213	39.655	12.293	45532.00	39934.400	12.294
1007.05	0.999	13.834	14.603	-5.560	45.213	39.656	12.292	45577.20	39975.300	12.291
1008.05	0.999	13.834	14.603	-5.561	45.213	39.656	12.292	45622.50	40013.800	12.294
1009.05	0.999	13.834	14.603	-5.561	45.213	39.656	12.292	45667.70	40054.900	12.291
1010.05	0.999	13.834	14.603	-5.561	45.213	39.656	12.292	45712.90	40093.600	12.293
1011.05	0.999	13.834	14.603	-5.561	45.213	39.656	12.292	45758.10	40134.800	12.289
1012.05	0.999	13.834	14.603	-5.561	45.213	39.656	12.292	45803.30	40173.600	12.291
1013.05	0.999	13.834	14.603	-5.561	45.213	39.656	12.291	45848.50	40212.500	12.293
1014.05	0.999	13.834	14.603	-5.561	45.213	39.656	12.291	45893.70	40254.000	12.289
1015.05	0.999	13.834	14.603	-5.561	45.213	39.656	12.291	45939.00	40293.100	12.290
1016.05	0.999	13.834	14.603	-5.561	45.213	39.656	12.291	45984.20	40332.200	12.291
1017.05	0.999	13.834	14.603	-5.561	45.213	39.656	12.291	46029.40	40371.500	12.292
1018.05	0.999	13.834	14.603	-5.562	45.213	39.656	12.291	46074.60	40410.800	12.293
1019.05	0.999	13.834	14.603	-5.562	45.213	39.656	12.290	46119.80	40452.600	12.288
1020.05	0.999	13.834	14.603	-5.562	45.213	39.657	12.290	46165.00	40492.100	12.288
1021.05	0.999	13.834	14.603	-5.562	45.213	39.657	12.290	46210.20	40531.600	12.289
1022.05	0.999	13.834	14.603	-5.562	45.213	39.657	12.290	46255.40	40571.300	12.289
1023.05	0.999	13.834	14.603	-5.562	45.213	39.657	12.290	46300.70	40611.000	12.289
1024.05	0.999	13.834	14.603	-5.562	45.213	39.657	12.290	46345.90	40650.700	12.288
1025.05	0.999	13.834	14.603	-5.562	45.213	39.657	12.289	46391.10	40690.600	12.288
1026.05	0.999	13.834	14.603	-5.562	45.213	39.657	12.289	46436.30	40730.500	12.287
1027.05	0.999	13.834	14.603	-5.562	45.213	39.657	12.289	46481.50	40770.500	12.287
1028.05	0.999	13.834	14.603	-5.563	45.213	39.657	12.289	46526.70	40808.100	12.291
1029.05	0.999	13.834	14.603	-5.563	45.213	39.657	12.289	46571.90	40848.300	12.290
1030.05	0.999	13.834	14.603	-5.563	45.213	39.657	12.289	46617.20	40888.500	12.289
1031.05	0.999	13.834	14.603	-5.563	45.213	39.657	12.288	46662.40	40928.900	12.287
1032.05	0.999	13.834	14.603	-5.563	45.213	39.657	12.288	46707.60	40969.300	12.286
1033.05	0.999	13.834	14.603	-5.563	45.213	39.658	12.288	46752.80	41007.200	12.289

Z	z/(1+z)	LTD_LC	LTD_HHC	%Error	CD_LC	CD_HHC	%Error	LD_LC	LD_HHC	%Error
(1)	(2)	(3)	(4)	(5)	(6)	(7)	(8)	(9)	(10)	(11)
1034.05	0.999	13.834	14.603	-5.563	45.213	39.658	12.288	46798.00	41047.800	12.287
1035.05	0.999	13.834	14.603	-5.563	45.213	39.658	12.288	46843.20	41088.400	12.285
1036.05	0.999	13.834	14.603	-5.563	45.213	39.658	12.288	46888.40	41126.600	12.289
1037.05	0.999	13.834	14.603	-5.563	45.213	39.658	12.287	46933.60	41167.400	12.286
1038.05	0.999	13.834	14.603	-5.564	45.213	39.658	12.287	46978.90	41205.700	12.289
1039.05	0.999	13.834	14.603	-5.564	45.213	39.658	12.287	47024.10	41246.600	12.286
1040.05	0.999	13.834	14.603	-5.564	45.213	39.658	12.287	47069.30	41285.100	12.289
1041.05	0.999	13.834	14.603	-5.564	45.213	39.658	12.287	47114.50	41326.200	12.286
1042.05	0.999	13.834	14.603	-5.564	45.213	39.658	12.287	47159.70	41364.800	12.288
1043.05	0.999	13.834	14.603	-5.564	45.213	39.658	12.286	47204.90	41406.100	12.284
1044.05	0.999	13.834	14.603	-5.564	45.213	39.658	12.286	47250.10	41444.800	12.286
1045.05	0.999	13.834	14.603	-5.564	45.213	39.658	12.286	47295.40	41483.700	12.288
1046.05	0.999	13.834	14.604	-5.564	45.213	39.658	12.286	47340.60	41525.200	12.284
1047.05	0.999	13.834	14.604	-5.564	45.213	39.659	12.286	47385.80	41564.200	12.286
1048.05	0.999	13.834	14.604	-5.565	45.213	39.659	12.286	47431.00	41603.200	12.287
1049.05	0.999	13.834	14.604	-5.565	45.213	39.659	12.285	47476.20	41642.400	12.288
1050.05	0.999	13.834	14.604	-5.565	45.213	39.659	12.285	47521.40	41684.200	12.283
1051.05	0.999	13.834	14.604	-5.565	45.213	39.659	12.285	47566.60	41723.500	12.284
1052.05	0.999	13.834	14.604	-5.564	45.287	39.659	12.427	47689.00	41762.800	12.427
1053.05	0.999	13.834	14.604	-5.564	45.287	39.659	12.427	47734.30	41802.200	12.427
1054.05	0.999	13.834	14.604	-5.565	45.287	39.659	12.427	47779.60	41841.800	12.428
1055.05	0.999	13.834	14.604	-5.565	45.287	39.659	12.426	47824.90	41881.300	12.428
1056.05	0.999	13.834	14.604	-5.565	45.287	39.659	12.426	47870.20	41921.000	12.428
1057.05	0.999	13.834	14.604	-5.565	45.287	39.659	12.426	47915.40	41960.700	12.428
1058.05	0.999	13.834	14.604	-5.565	45.287	39.659	12.426	47960.70	42000.500	12.427
1059.05	0.999	13.834	14.604	-5.565	45.287	39.659	12.426	48006.00	42040.400	12.427
1060.05	0.999	13.834	14.604	-5.565	45.287	39.659	12.426	48051.30	42080.400	12.426
1061.05	0.999	13.834	14.604	-5.565	45.287	39.660	12.426	48096.60	42120.400	12.425
1062.05	0.999	13.834	14.604	-5.565	45.287	39.660	12.425	48141.90	42160.500	12.425
1063.05	0.999	13.834	14.604	-5.565	45.287	39.660	12.425	48187.20	42200.700	12.423
1064.05	0.999	13.834	14.604	-5.566	45.287	39.660	12.425	48232.50	42238.300	12.428
1065.05	0.999	13.834	14.604	-5.566	45.287	39.660	12.425	48277.70	42278.600	12.426
1066.05	0.999	13.834	14.604	-5.566	45.287	39.660	12.425	48323.00	42319.000	12.425
1067.05	0.999	13.834	14.604	-5.566	45.287	39.660	12.425	48368.30	42359.500	12.423
1068.05	0.999	13.834	14.604	-5.566	45.287	39.660	12.424	48413.60	42397.400	12.427
1069.05	0.999	13.834	14.604	-5.566	45.287	39.660	12.424	48458.90	42438.000	12.425
1070.05	0.999	13.834	14.604	-5.566	45.287	39.660	12.424	48504.20	42478.700	12.423
1071.05	0.999	13.834	14.604	-5.566	45.287	39.660	12.424	48549.50	42516.800	12.426
1072.05	0.999	13.834	14.604	-5.566	45.287	39.660	12.424	48594.80	42557.600	12.423
1073.05	0.999	13.834	14.604	-5.566	45.287	39.660	12.424	48640.00	42595.900	12.426
1074.05	0.999	13.834	14.604	-5.566	45.287	39.660	12.424	48685.30	42636.900	12.424
1075.05	0.999	13.834	14.604	-5.567	45.287	39.661	12.423	48730.60	42678.000	12.421
1076.05	0.999	13.834	14.604	-5.567	45.287	39.661	12.423	48775.90	42716.400	12.423
1077.05	0.999	13.834	14.604	-5.567	45.287	39.661	12.423	48821.20	42754.900	12.426
1078.05	0.999	13.834	14.604	-5.567	45.287	39.661	12.423	48866.50	42796.200	12.422
1079.05	0.999	13.834	14.604	-5.567	45.287	39.661	12.423	48911.80	42834.900	12.424
1080.05	0.999	13.834	14.604	-5.567	45.287	39.661	12.423	48957.00	42876.300	12.421
1081.05	0.999	13.834	14.604	-5.567	45.287	39.661	12.422	49002.30	42915.100	12.422
1082.05	0.999	13.834	14.604	-5.567	45.287	39.661	12.422	49047.60	42954.000	12.424
1083.05	0.999	13.834	14.604	-5.567	45.287	39.661	12.422	49092.90	42995.700	12.420
1084.05	0.999	13.834	14.604	-5.567	45.287	39.661	12.422	49138.20	43034.700	12.421
1085.05	0.999	13.834	14.604	-5.567	45.287	39.661	12.422	49183.50	43073.800	12.422
1086.05	0.999	13.834	14.604	-5.568	45.287	39.661	12.422	49228.80	43112.900	12.423
1087.05	0.999	13.834	14.604	-5.568	45.287	39.661	12.422	49274.00	43152.100	12.424
1088.05	0.999	13.834	14.604	-5.568	45.287	39.661	12.421	49319.30	43194.200	12.419
1089.05	0.999	13.834	14.604	-5.568	45.287	39.661	12.421	49364.60	43233.600	12.420
1090.05	0.999	13.834	14.604	-5.568	45.287	39.662	12.421	49409.90	43273.000	12.420
1091.05	0.999	13.834	14.604	-5.568	45.287	39.662	12.421	49455.20	43312.500	12.421
1092.05	0.999	13.834	14.604	-5.568	45.287	39.662	12.421	49500.50	43352.100	12.421
1093.05	0.999	13.834	14.604	-5.568	45.287	39.662	12.421	49545.80	43391.800	12.421
1094.05	0.999	13.834	14.604	-5.568	45.287	39.662	12.421	49591.10	43431.500	12.421
1095.05	0.999	13.834	14.604	-5.568	45.287	39.662	12.420	49636.30	43471.300	12.421
1096.05	0.999	13.834	14.604	-5.568	45.287	39.662	12.420	49681.60	43511.100	12.420
1097.05	0.999	13.834	14.604	-5.568	45.287	39.662	12.420	49726.90	43551.100	12.420
1098.05	0.999	13.834	14.604	-5.569	45.287	39.662	12.420	49772.20	43591.100	12.419
1099.05	0.999	13.834	14.604	-5.569	45.287	39.662	12.420	49817.50	43631.200	12.418
1100.05	0.999	13.834	14.604	-5.569	45.287	39.662	12.420	49862.80	43671300	12.417

8. Conclusion

By modifying our recently proposed light speed expanding Hubble-Hawking universe, in this paper we are presenting a very simple model of light speed rotating universe with a possible halt. It is absolutely against to the current notion of accelerating universe and dark energy. In this context, we would like to appeal that, based on the rate of decrease in current and future cosmic temperature, our proposal can be verified. Proceeding further, so far, no single cosmological observation has shed light the direct existence of dark energy and no single observation has reported a direct measure of galactic receding speed and direct measure of galactic accelerating speed. Point to be noted is that, whether galaxy is receding or revolving about a center also is not clear. It's a general and commonly followed belief that galactic distance is a measure of galactic receding speed. It may be noted that, based on proposed red shift definition, Hubble's law can be considered as a representation of ending stage of cosmic expansion having light speed rotation.

We agree that, in this paper, we are not providing sufficient cosmological explanation for the reasons of current cosmic halt, but it may be noted that factors like initial high cosmic expansion speed, decelerating mode of cosmic expansion with increasing mass and decreasing temperature, current sub zero cosmic temperature of 2.7 K, very small value of the current Hubble parameter and observed very minor fluctuations in current cosmic temperature can be considered as favorable conditions for further analysis. Considering our proposed energy based definition of red shift, it seems compulsory to review the basics of Lambda cosmology. If one is willing to consider red shift as a measure of galactic distance, one can get a chance to study the observable universe in a new dimension accompanied by light speed rotation. As explained in section (5), equations (8) to (12) are having very strange origin and need a careful review at fundamental level. If it is an accidental coincidence, as the equations are strongly coupled with gravitational and cosmic physical constants, then one must think about the scope, applicability and validity of those equations in a different manner with reference to Dirac model of large numbers or quantum gravity or final unification. We are sure to say that, theory point of view, these equations are having good scientific background compared to dark energy like ambiguous entities. With a joint research associated with microscopic physics and cosmic physics, true nature of cosmic expansion can be understood. As there exists no strong experimental

evidence for the currently believed dark matter, until its detection, dark matter can be considered as a representation of super gravity of galactic baryon mass associated with its cut-off mass limit at (180 to 200) million solar masses.

Qualitatively and quantitatively, in a theoretical approach, compared to the historical arguments on cosmic rotation, our views seem to be more coherent, strongly connected with quantum gravity and are closer to observational findings. Hence, we sincerely appeal the science community to recommend our light speed rotating model of the Hubble-Hawking universe for further research.

Acknowledgements

In preparing this paper, author Seshavatharam is greatly inspired by Dr. Mohsen Lutephy and Dr. Dimitar Todorov Valev for their thought provoking concepts on quantum cosmology associated with no further expansion. Seshavatharam is indebted to Professors Shri M. Nagaphani Sarma, Chairman; Shri K.V. Krishna Murthy, founder Chairman, Institute of Scientific Research in Vedas (I-SERVE), Hyderabad, India; and Shri K.V.R.S. Murthy, former scientist IICT (CSIR), Govt. of India, Director, Research and Development, I-SERVE, for their valuable guidance and support in developing this subject. Authors are very much thankful to the anonymous reviewers for their valuable suggestions in improving the quality of the paper.

Appendix A: C++ program for estimating various galactic distances

```
#include <conio.h>

#include <iostream.h>

#define c 299792.458

 int main(){

float z=0.05;

  do{

    z = z +1;

 float H0 = 66.893;

// Hubble constant (km/s/Mpc) - adjust according to taste

 float  OM = 0.32;  // Omega(matter) - adjust according to taste

  float OL = 0.68;    // Omega(lambda) - adjust according to taste

  float OR = 0.42/(H0*H0);

 // Omega(radiation) - this is the usual textbook value

  long i;

  long n=10000;          // Number of steps in the integral

  float OK = 1-OM-OR-OL;        // Omega(k) defined as 1-OM-OR-OL

  float HD = 3.2616*c/H0/1000;  // Hubble distance (billions of light years).
See section 2 of Hogg
```

```
float a, adot;            // Redshift "z", Scale Factor "a", and its derivative "adot"
float DC, DCC=0, DT, DTT=0, DA, DL, DM;
float age, size;          // The age and size of the universe
for(i=n; i>=1; i--) {     // This loop is the numerical integration
 a = (i-0.5)/n;           // Steadily decrease the scale factor
 // Comoving formula
 (See section 4 of Hogg, but I've added a radiation term too):
 adot = a*sqrt(OM*pow(1/a,3)+OK*pow(1/a,2)+OL+OR*pow(1/a,4));
// Note that "a" is equivalent to 1/(1+z)
 DCC = DCC + 1/(a*adot)/n;  // Running total of the comoving distance
 DTT = DTT + 1/adot/n;
 // Running total of the light travel time (see section 10 of Hogg)
 if (a>=1/(1+z)) {      // Collect DC and DT until the correct scale is reached
  DC = DCC;             // Comoving distance DC
  DT = DTT;             // Light travel time DT
 }
}
// Transverse comoving distance DM from section 5 of Hogg:
if (OK>0.0001) DM=(1/sqrt(OK))*sinh(sqrt(OK)*DC);
```

```
 else if (OK<-0.0001) DM=(1/sqrt(fabs(OK)))*sin(sqrt(fabs(OK))*DC);
 else DM=DC;
 age = HD*DTT;              // Age of the universe (billions of years)
 size = HD*DCC;             // Comoving radius of the observable universe
 DC = HD*DC;                // Comoving distance
 A = HD*DM/(1+z);           // Angular diameter distance (section 6 of Hogg)
 DL = HD*DM*(1+z);          // Luminosity distance (section 7 of Hogg)
 DT = HD*DT;                // Light travel distance
  float dt,zn,cd,ld;
 zn=(z/(z+1));              // Modified red shift
 dt=zn*HD;                  // Estimated light travel distance
 cd=exp(zn)*dt;             // Estimated comoving distance
 ld=cd/(1-zn);              //Estimated luminosity distance
cout<<z<<","<<zn<<","<<DT<<","<<dt<<","
     <<((DT-dt)/DT)*100<<","<<DC<<","<<cd<<","
     <<((DC-cd)/DC)*100<<","<<DL<<","<<ld<<","<<((DL-
ld)/DL)*100<<endl;
 } while (z<=1100.0);
}
```

References

[1] Cosmin Andreia, Anna Ijjasb and Paul J. Steinhardt. Rapidly descending dark energy and the end of cosmic expansion. Proceedings of the National Academy of Sciences, 119(15) e2200539119, 2022.

[2] Perlmutter S et al. Measurements of Ω and Λ from 42 High-Redshift Supernovae. The Astrophysical Journal, 517(2): 565, 1999.

[3] Fulvio Melia (Arizona U. and Arizona U., Astron. Dept. - Steward Observ.). Fitting the Union2.1 SN Sample with the R_h=ct Universe. Astron.J. 144, 110, 2012.

[4] Nielsen J.T, Guffanti A, Sarkar S. Marginal Evidence for Cosmic Acceleration from Type Ia Supernovae. Nature, Scientific Reports 6(Oct): 35596, 2016.

[5] Lisa Goh Wan Khee. Thesis: Modified Statistical Analysis of Type 1a Supernovae Data. Supervisor. Supervisor: Shao Chin Cindy Ng, 2018-2019, National University of Singapore, Singapore.

[6] Saadeh Daniela et al. How Isotropic is the Universe? Phys. Rev. Lett. 117:13, 131302, 2016.

[7] Birch P. Is the Universe rotating? Nature. 298, 451-454, 1982.

[8] C. Sivaram, Kenath Arun. Primordial Rotation of the Universe, Hydrodynamics, Vortices and Angular Momenta of Celestial Objects. The Open Astronomy Journal, 5, 7-11, 2012.

[9] Vladimir A Korotky, Eduard Masár Yuri N Obukhov. In the Quest for Cosmic Rotation. Universe, 6:14, 2020.

[10] Gianluca Calcagni et al. Lectures on classical and quantum cosmology. PoS (CORFU2021) 317, 2022.

[11] Lopez-Corredoira M. Tests and Problems of the Standard Model in Cosmology. Foundations of Physics, 47, 711-768, 2017.

[12] Di Valentino, E., Melchiorri, A. & Silk, J. Planck. Planck evidence for a closed Universe and a possible crisis for cosmology. Nat Astron. 4, 196–203, 2020.

[13] George Ellis, Julien Larena. The case for a closed universe, *Astronomy & Geophysics,* 61(1), 1.38–1.40,2020.

[14] Will Handley. Curvature tension: evidence for a closed universe. Phys. Rev. D 103, 041301, 2021.

[15] Hubble E.P. A Relation between Distance and Radial Velocity among Extra-Galactic Nebulae. Proceedings of the National Academy of Sciences of the United States of America, 15, 168-173, 1929.

[16] Kurt Godel. Rotating Universes in General Relativity Theory. Proceedings of the international Congress of Mathematicians in Cambridge, 1: 175-81, 1950.

[17] Wang, P. et al. Possible observational evidence for cosmic filament spin. Nat. Astron. 5, 839–845, 2021.

[18] Seshavatharam U.V.S. Physics of Rotating and Expanding Black Hole Universe. Progress in Physics. 2 (April), 7-14, 2010.

[19] Tatum E.T, Seshavatharam U.V.S, Lakshminarayana S. The basics of flat space cosmology. International Journal of Astronomy and Astrophysics, 5,116-124, 2015.

[20] Seshavatharam U.V.S, Tatum E.T, Lakshminarayana S. The Large Scale Universe as a Quasi Quantum White Hole. International Astronomy and Astrophysics Research Journal. 3(1):22–42, 2021.

[21] Seshavatharam U.V.S, Lakshminarayana S. Light speed expanding white hole universe having a red shift of [z/(1+z)]. World Scientific News, 162, 87-101, 2021.

[22] Seshavatharam U.V.S, Lakshminarayana S. On the role of cosmic mass in understanding the relationships among galactic dark matter, visible matter and flat rotation speeds. NRIAG Journal of Astronomy and Geophysics. 10(1),1-15, 2021.

[23] Seshavatharam U.V.S, Lakshminarayana S. Concepts and results of a Practical Model of Quantum Cosmology: Light Speed Expanding Black Hole Cosmology. Mapana Journal of Sciences. 21(2), 2022.

[24] Seshavatharam U.V.S, Lakshminarayana S. Unified Quantum Gravity Pertaining to Nuclear and Cosmic Physics. Quantum Physics Letters. 11(2),23-30, 2022.

[25] Seshavatharam U. V. S, Lakshminarayana S. Weak Interaction Dependent Super Gravity of Galactic Baryon Mass. Journal of Asian Scientific Research, 12(3), 146–155, 2022.

[26] Seshavatharam U. V. S, Lakshminarayana S. Light Speed Expanding Hubble-Hawking Universe. Preprints 2022, 2022090279. https://doi.org/10.20944/preprints202209.0279.v3.

[27] Seshavatharam U. V. S, Lakshminarayana S. A rotating model of light speed expanding Hubble-Hawking universe, in Proceedings of the 2nd Electronic Conference on Universe, 16 February–2 March 2023, MDPI: Basel, Switzerland, doi:10.3390/ECU2023-14065

[28] Seshavatharam U. V. S, Lakshminarayana S. An open review on light speed expanding Hubble-Hawking universe.11(2): 322, 2023. (45 pages)

[29] Hawking S. Black hole explosions? Nature 248, 30-31, 1974.

[30] Planck Collaboration: Planck 2015 Results. XIII. Cosmological Parameters.

[31] Jos´e Luis Berna et al. Robustness of baryon acoustic oscillation constraints for early-Universe modifications to ΛCDM. Phys. Rev. D 102, 123515, 2020.

[32] David Hogg. Distance Measures in Cosmology. arXiv:astro-ph/9905116, 2000.

[33] Pacetti, S., Tomasi-Gustafsson, E. The origin of the proton radius puzzle. Eur. Phys. J. A 57, 72, 2021.

[34] Milgrom M. A Modification of the Newtonian Dynamics as a Possible Alternative to the Hidden Mass Hypothesis. The Astrophysical Journal , 270, 365-370, 1983.

[35] Banik I. and Zhao H. From Galactic Bars to the Hubble Tension: Weighing Up the Astrophysical Evidence for Milgromian Gravity. Symmetry, 14, 1331, 2022.

[36] Brownstein J. R. and Moffat J. W. Galaxy Rotation Curves Without Non-Baryonic Dark Matter. The Astrophysical Journal , 636, 721-741, 2006.

[37] Sivaram, C., Arun, K. & Rebecca, L. MOND, MONG, MORG as alternatives to dark matter and dark energy and consequences for cosmic structures. J. Astrophys. Astron. 41, 4, 2020

[38] Kyu-Hyun Chae et al. Testing the Strong Equivalence Principle: Detection of the External Field Effect in Rotationally Supported Galaxies. The Astrophysical Journal, 904(1), 2020, 20(pp).

[39] D. W. Sciama. On the Origin of Inertia. Monthly Notices of the Royal Astronomical Society, 13(1), 34-42, 1953.

[40] Shen Z et al. A Tip of the Red Giant Branch Distance of 22.1 ± 1.2 Mpc to the Dark Matter Deficient Galaxy NGC 1052–DF2 from 40 Orbits of Hubble Space Telescope Imaging. The Astrophysical Journal Letters. 914(1):L12, 2021.

[41] Ogle, P.M., et al. A Break in Spiral Galaxy Scaling Relations at the Upper Limit of Galaxy Mass. The Astrophysical Journal Letters , 884, L11, 2019.

[42] Gamow G. Rotating Universe? Nature. 158, 549, 1946.

[43] E.T. Whittaker. Spin in the universe, Yearbook of Roy. Soc. Edinburgh, (1945) 5.

[44] Hawking S. On the rotation of the Universe. Monthly Notices of the Royal Astronomical Society, 142, 129-141,1969.

[45] Godlowski, W. Global and Local Effects of Rotation: Observational Aspects. International Journal of Modern Physics D. 20, 1643, 2011.

[46] Jo˜ao Magueijo et al. Cosmology with a spin. Phys. Rev. D 87, 063504, 2013.

[47] Chechin L.M. Does the Cosmological Principle Exist in the Rotating Universe? Gravitation and Cosmology. 23(4): 305-310, 2017.

[48] Longo M.J. Are Cosmic Isotropy Limits from Analyses of the Cosmic Microwave Background Credible? Preprints 2020, 2020110520

[49] Shamir L. Asymmetry in Galaxy Spin Directions-Analysis of Data from DES and Comparison to Four Other Sky Surveys. Universe, 8, 397, 2022.

[50] Nodland Borge and Ralston John P. Indication of Anisotropy in Electromagnetic Propagation over Cosmological Distances. Phys. Rev. Lett. 78(16), 3043-3046,1997.

[51] Pavan Kumar Aluri et al. Is the Observable Universe Consistent with the Cosmological Principle? arXiv:2207.05765 [astro-ph.CO] 2022

[52] Seshavatharam U.V.S, Lakshminarayana S. Applications of Hubble Volume in Atomic Physics, Nuclear Physics, Particle Physics, Quantum Physics and Cosmic Physics. J. Nucl. Phy. Mat. Sci. Rad. A. 1(1), 45-60, 2013.

[53] Seshavatharam U.V.S, Lakshminarayana S. Black hole Cosmos and the Micro Cosmos. International Journal of Advanced Astronomy. 1(2), 37-59, 2013.

[54] Seshavatharam U.V.S, Lakshminarayana, S, Sai B.V.S.T. Is red shift an index of galactic 'atomic light emission' mechanism? International Journal of Physics, Vol. 1, No.3, 49-64, 2013.

[55] Seshavatharam U.V.S and Lakshminarayana S. Cosmologically

Strengthening Hydrogen Atom in Black Hole Universe. J. Nucl. Phy. Mat. Sci. Rad. A. Vol-3, No-2, 265–278, 2016.

[56] U. V. S. Seshavatharam and S. Lakshminarayana. Is Planck's constant a cosmological variable? International Journal of Astronomy, 2(1): 11-15, 2013.

[57] Seshavatharam, U.V.S., Lakshminarayana, S. Role of Four Gravitational Constants in Nuclear Structure. Mapana-Journal of Sciences.18,1,21, 2019.

[58] Seshavatharam, U.V.S. Lakshminarayana, S. Implications and Applications of Electroweak Quantum Gravity. International Astronomy and Astrophysics Research Journal. 2(1),13-30, 2020.

[59] Seshavatharam U.V.S and Lakshminarayana S. Is reduced Planck's constant - an outcome of electroweak gravity? Mapana Journal of Sciences. 19(1),1-13, 2020

[60] Seshavatharam, U.V.S, Lakshminarayana S. 4G model of fitting RMS radius of proton. Nucleus 2022: Fundamental problems and applications. Moscow July 11–16, 2022. Book of abstracts, 88-89,2022. https://events.sinp.msu.ru/event/8/contributions/613/attachments/594/1212/ID_25_24_uvssa_sln_14July2022.pdf

[61] P.A. Zyla et al. (Particle Data Group), Prog. Theor. Exp. Phys. 2020, 083C01 (2021) and 2021 update.

[62] Hawking, S.W., Hertog, T. A smooth exit from eternal inflation?. J. High Energ. Phys. 2018, 147, 2018.

[63] Alis J Deason et al. The edge of the Galaxy. Monthly Notices of the Royal Astronomical Society. 496(3), 3929–3942, 2020.

[64] Pijushpani Bhattacharjee et. al. (2014) Rotation Curve of the Milky Way out to ~ 200 kpc. ApJ 785, 63. (13 pages)

HADRONIC JOURNAL 46, 207 - 218 (2023)
DOI 10.29083/HJ.46.02.2023/SC207

TREATMENT OF LAUNDAU-GINZBURG THEORY WITH CONSTRAINTS

Walaa I. Eshraim
New York University Abu Dhabi
Saadiyat Island, P.O. Box 129188
Abu Dhabi, U.A.E.
weshraim@fias.uni-frankfurt.de

Received May 22, 2023

Abstract

Treatment of a singular Lagrangian with constraints using the canonical Hamiltonian approach is studied. We investigate Landau-Ginzburg theory as a constrained system using the Euler-Lagrange equation for the field system and the canonical approach. The equations of motion are obtained as total differential equations in many variables. It is shown that the simultaneous solutions of the Landau-Ginzburg theory with constraints by canonical approach lead to obtaining canonical phase space coordinates and the reduced phase space Hamiltonian without introducing Lagrange multipliers and without any additional gauge fixing condition.

keywords: Lagrangian and Hamiltonian approach, Singular Lagrangian, Landau-Ginzburg theory.

PACS: 11.10.Ef, 03.65.-w

1 Introduction

Singular Lagrangian systems represent a special case of more general dynamics called constrained systems. A general feature of constrained systems is the existence of constraints in their classical configurations.

The Lagrangian L of any physical system with N degrees of freedom is a function of N generalized coordinates q_i and N generalized velocities $\dot{q}_i$ as well as the time τ,

$$L \equiv (q_i, \dot{q}_i, \tau), \quad i = 1, ..., N.$$

If the velocities can be expressed in terms of the coordinates and the momenta, L is referred to as regular, otherwise, it is singular. Singular Lagrangian systems represent a special case of more general dynamics called constrained systems. A general feature of a constrained system is the existence of its classical configuration.

The basic ideas of the classical treatment and quantization of such systems were initiated and developed by Dirac [1]. He distinguished between two types of constraints; first- and second-classes. In the case of unconstrained systems, the Hamilton-Jacobi theory provides a bridge between classical and quantum mechanics. The first study of Hamilton-Jacobi equations for arbitrary first-order actions was carried out by Santilli [2]. Gitman and Tyutin [3] discussed the canonical quantization of singular theories as well as the Hamiltonian formalism of gauge theories in an arbitrary gauge. In the recent past, the canonical method based on the Hamilton-Jacobi formulation was developed to investigate singular systems [4, 5, 6, 7, 8]. In this formalism, there is no need to distinguish between first and second constraints as in the Dirac theory [9, 10]. Also, in the canonical method which has been developed by Güler's [11, 12], the equations of motion were written as total differential equations. In Ref. [13], the discrete singular system was treated as a continuous system. Hamiltonian and Lagrangian formulations are used together. The Hamilton-Jacobi formulation of constrained systems has been studied as seen as in Refs. [14, 15, 16]. Moreover, in Refs. [17, 18, 19, 20] Hamilton-Jacobi quantization have been used to obtain the Path integral quantization for several constraint systems. Our aim in this work is to use the Euler-Lagrange equation to treat the system

of a constrained system, the Landau-Ginzburg theory, and to compare the results to those obtained by Hamilton-Jacobi formulation.

The paper is arranged as follows: In section 2, a brief discussion of the canonical Hamiltonian method is given, together with a treatment of a singular system as a continuous system. Next, in section 3, Lanfau Ginzburg theory is treated as a singular constrained field system. Finally, in section 4, several concluding remarks follow.

2 Theoretical framework

In this section, we review the Hamilton-Jacobi formulation of constrained systems [1, 2], which the starting point of this method is to consider the Lagrangian $L \equiv L(q_i, \dot{q}_i, \tau), i = 1, 2, \ldots, n$, with the Hess matrix

$$A_{ij} = \frac{\partial^2 L(q_i, \dot{q}_i, \tau)}{\partial \dot{q}_i \, \partial \dot{q}_j}, \qquad i, j = 1, 2, \ldots, n, \tag{1}$$

of rank $(n-r), r < n$. Then the r momenta are dependent. The generalized momenta P_i corresponding to the generalized coordinates q_i are defined as

$$p_a = \frac{\partial L}{\partial \dot{q}_a}, \qquad a = 1, 2, \ldots, n-r, \tag{2}$$

$$p_\mu = \frac{\partial L}{\partial \dot{q}_\mu}, \qquad \mu = n-r+1, \ldots, n, \tag{3}$$

The singularity of the system enables us to solve Eq.(2) for $\dot{q}_a$ as

$$\dot{q}_a = \dot{q}_a(q_i, \dot{q}_\mu, p_a; \tau) \equiv \omega_b. \tag{4}$$

By substituting Eq.(4) into Eq.(3), we obtain the constraints as

$$H'_\mu = p_\mu + H_\mu(\tau, q_i, p_a) = 0, \tag{5}$$

where

$$H_\mu = -\frac{\partial L}{\partial \dot{q}_\mu}\bigg|_{\dot{q}_a \equiv \omega_a}. \tag{6}$$

In this formulation the usual Hamiltonian H_0 is defined as

$$H_0 = -L + p_a\dot{\omega}_a - \dot{q}_\mu H_\mu. \tag{7}$$

Like functions H_μ, the function H_0 is not an explicit function of the velocities $\dot{q}_\nu$. Therefore, the Hamilton-Jacobi function $S(\tau, q_i)$ should satisfy the following set of Hamilton-Jacobi partial differential equations (HJPDE) simultaneously for an extremum of the function:

$$H'_\alpha\left(t_\beta,\ q_\alpha,\ P_i = \frac{\partial S}{\partial q_i},\ P_0 = \frac{\partial S}{\partial t_0}\right) = 0, \tag{8}$$

where
$\alpha, \beta = 0, n-r+1, \ldots, n;$ $\quad a = 1, 2, \ldots, n-r,$ and

$$H'_\alpha = p_\alpha + H_\alpha. \tag{9}$$

The canonical equations of motion are given as total differential equations in variables t_β,

$$dq_p = \frac{\partial H'_\alpha}{\partial p_p}\, dt_\alpha, \quad p = 0, 1, \ldots, n; \quad \alpha = 0, n-r+1, \ldots, n, \tag{10}$$

$$dp_a = -\frac{\partial H'_\alpha}{\partial q_a}\, dt_\alpha, \qquad a = 1, \ldots, n-r, \tag{11}$$

$$dp_\mu = -\frac{\partial H'_\alpha}{\partial q_\mu}\, dt_\alpha, \qquad \alpha = 0, n-r+1, \ldots, n, \tag{12}$$

$$dZ = \left(-H_\alpha + p_a \frac{\partial H'_\alpha}{\partial p_\alpha}\, dt_\alpha\right), \tag{13}$$

where

$$Z \equiv S(t_\alpha, q_a), \tag{14}$$

being the action. Thus, the analysis of a constrained system is reduced to solve equations (10-12) with constraints

$$H'_\alpha(t_\beta,\ q_a,\ P_i) = 0, \qquad \alpha, \beta = 0, n-r+1, \ldots, n. \tag{15}$$

Since the equations above are total differential equations, integrability conditions should be checked. These equations of motion are integrable if and only if the variations of H'_α vanish identically, that is

$$dH'_\alpha = 0. \tag{16}$$

If they do not vanish identically, then we consider them as new constraints. This procedure is repeated until a complete system is obtained.

In Ref. [12] the singualr Lagrangian systems are treated as continuous systems. The Euler-Lagrange equation of a singular-Lagrangian system is given as

$$\frac{\partial}{\partial x_\alpha}\left[\frac{\partial L'}{\partial(\partial_\alpha q_\alpha)}\right] - \frac{\partial L'}{\partial q_\alpha} = 0, \qquad \partial_\alpha q_\alpha = \frac{\partial q_\alpha}{\partial x_\alpha}, \tag{17}$$

with constraints

$$dG_\alpha = -\frac{\partial L'}{\partial x_\alpha}\, dt, \tag{18}$$

where L' is the "modified Lagrangian" defined as

$$L'(x_\mu, \partial_\mu q_a, \dot{x}_\mu, q_a) \equiv L(x_\mu, q_a, \dot{q}_a = (\partial_\mu q_a)\dot{x}_\mu); \tag{19}$$

and

$$G_\alpha = H_\alpha\left(x_\mu, q_a, p_a = \frac{\partial L}{\partial q_a}\right). \tag{20}$$

the solution of Eq. (17), together with the constraints equations (18), gives us the solution of the system.

3 The Landau-Ginzburg theory

The Landau-Ginzburg theory gives an effective description of phenomenon precisely coincides with scalar quantum electrodynamics, which is described by the Lagrangian

$$\mathcal{L} = -\frac{1}{4}\, F_{\mu\nu}F^{\mu\nu} + (D_\mu\varphi)^* D^\mu\varphi - k\varphi^*\varphi - \frac{1}{4}\lambda(\varphi^*\varphi)^2, \tag{21}$$

where the covariant is given by

$$D_\mu\varphi = \partial_\mu\varphi - ieA_\mu\varphi. \tag{22}$$

and the electromagnetic tensor is defined as $F^{\mu\nu} = \partial^\mu A^\nu - \partial^\nu A^\mu$ with the gauge field A^ν. In the landau-Ginzburg theory φ describes the cooper pairs. In usual quantum electrodynamics, we would put $k = m^2$, where m is the effective mass of electron.

3.1 Hamilton-Jacobi formulation of the Landau-Ginzburg theory

The Lagrangian function (21) is singular, since the rank of the Hessian matrix

$$A_{ij} = \frac{\partial^2 L}{\partial \dot{q}_i \partial \dot{q}_j}, \tag{23}$$

is three. The canonical momenta are defined as

$$\pi^i = \frac{\partial L}{\partial \dot{A}_i} = -F^{0i}, \tag{24}$$

$$\pi^0 = \frac{\partial L}{\partial \dot{A}_0} = 0, \tag{25}$$

$$p_\varphi = \frac{\partial L}{\partial \dot{\varphi}} = (D_0\varphi)^* = \dot{\varphi}^* + ieA_0\varphi^*, \tag{26}$$

$$p_{\varphi^*} = \frac{\partial L}{\partial \dot{\varphi}^*} = (D_0\varphi) = \dot{\varphi} - i\,e\,A_0\,\varphi, \tag{27}$$

From Eqs. (24), (26) and (27), the velocities $\dot{A}_i, \dot{\varphi}^*$ and $\dot{\varphi}$ can be expressed in terms of momenta π_i, p_φ and p_{φ^*} respectively as

$$\dot{A}_i = -\pi_i - \partial_i A_0, \tag{28}$$

$$\dot{\varphi}^* = p_\varphi - ieA_0\varphi^*, \tag{29}$$

$$\dot{\varphi} = p_{\varphi^*} + ieA_0\varphi. \tag{30}$$

The canonical Hamiltonian H_0 is obtained as

$$H_0 = \frac{1}{4} F^{ij} F_{ij} - \frac{1}{2} \pi_i \pi^i + \pi^i \partial_i A_0 + p_{\varphi^*} p_\varphi + ieA_0 \varphi p_\varphi - ieA_0 \varphi^* p_{\varphi^*} - (D_i \varphi)^* (D^i \varphi) + k\varphi^* \varphi + \frac{1}{4} \lambda (\varphi^* \varphi)^2. \quad (31)$$

Making use of (7) and (8), we find for the set of HJPDE

$$H_0' = \pi_4 + H_0, \quad (32)$$

$$H' = \pi_0 + H = \pi_0 = 0, \quad (33)$$

Therefor, the total differential equations for the characteristic (9-11) obtained as

$$\begin{aligned} dA^i &= \frac{\partial H_0'}{\partial \pi_i} dt + \frac{\partial H'}{\partial \pi_i} dA^0, \\ &= -(\pi^i + \partial_i A_0)\, dt, \end{aligned} \quad (34)$$

$$dA^0 = \frac{\partial H_0'}{\partial \pi_0} dt + \frac{\partial H'}{\partial \pi_0} dA^0 = dA^0, \quad (35)$$

$$\begin{aligned} d\varphi &= \frac{\partial H_0'}{\partial p_\varphi} dt + \frac{\partial H'}{\partial p_\varphi} dA^0, \\ &= (p_{\varphi^*} + ieA_0 \varphi)\, dt, \end{aligned} \quad (36)$$

$$\begin{aligned} d\varphi^* &= \frac{\partial H_0'}{\partial p_{\varphi^*}} dt + \frac{\partial H'}{\partial p_{\varphi^*}} dA^0, \\ &= (p_\varphi - ieA_0 \varphi^*)\, dt, \end{aligned} \quad (37)$$

$$\begin{aligned} d\pi^i &= -\frac{\partial H_0'}{\partial A_i} dt - \frac{\partial H'}{\partial A_i} dA^0, \\ &= [\partial_l F^{li} + ie(\varphi^* \partial^i \varphi + \varphi\, \partial_i \varphi^*) + 2e^2 A^i \varphi \varphi^*]\, dt, \end{aligned} \quad (38)$$

$$d\pi^0 = -\frac{\partial H_0'}{\partial A_0}\,dt - \frac{\partial H'}{\partial A_0}\,dA^0,$$
$$= [\partial_i \pi^i + ie\varphi^* p_{\varphi^*} - ie\varphi\, p_\varphi]\,dt, \tag{39}$$

$$dp_\varphi = -\frac{\partial H_0'}{\partial \varphi}\,dt - \frac{\partial H'}{\partial \varphi}\,dA^0,$$
$$= [(\overrightarrow{D}\cdot\overrightarrow{D}\varphi)^* - k\varphi^* - \frac{1}{2}\lambda\varphi\varphi^{*2} - ieA_0 p_\varphi]\,dt, \tag{40}$$

and

$$dp_{\varphi^*} = -\frac{\partial H_0'}{\partial \varphi^*}\,dt - \frac{\partial H'}{\partial \varphi^*}\,dA^0,$$
$$= [(\overrightarrow{D}\cdot\overrightarrow{D}\varphi) - k\varphi - \frac{1}{2}\lambda\varphi^*\varphi^2 + ieA_0 p_{\varphi^*}]\,dt. \tag{41}$$

The integrability condition ($dH_\alpha' = 0$) implies that the variation of the constraint H' should be identically zero, that is

$$dH' = d\pi_0 = 0, \tag{42}$$

which leads to a new constraint

$$H'' = \partial_i \pi^i + ie\varphi^* p_{\varphi^*} - ie\varphi\, p_\varphi = 0. \tag{43}$$

Taking the total differential of H'', we have

$$dH'' = \partial_i d\pi^i + iep_{\varphi^*} d\varphi^* + ie\varphi^* dp_{\varphi^*} - ie\varphi\, dp_\varphi - iep_\varphi\, d\varphi = 0. \tag{44}$$

3.2 Lagrangian formulation of the Landau- Ginzburg theory

Let us write the above Lagrangian in the form

$$\mathcal{L} = -\frac{1}{4}\left(\frac{\partial A_\nu}{\partial x_\mu} - \frac{\partial A_\mu}{\partial x_\nu}\right)\left(\frac{\partial A^\nu}{\partial x^\mu} - \frac{\partial A^\mu}{\partial x^\nu}\right)$$
$$+ (\partial_\mu + ieA_\mu)\varphi^*(\partial^\mu - ieA^\mu)\varphi - k\varphi^*\varphi - \frac{1}{4}\lambda(\varphi^*\varphi)^2, \tag{45}$$

The canonical momenta are defined as

$$\pi^{\nu} = \frac{\partial \mathcal{L}}{\partial(\partial_{\mu} A^{\nu})} = -F^{\mu\nu}, \tag{46}$$

$$\pi = \frac{\partial \mathcal{L}}{\partial(\partial_{\mu}\varphi)} = (D^{\mu}\varphi)^{*} = \partial^{\mu}\varphi^{*} + ieA^{\mu}\varphi^{*} = -H_{1}, \tag{47}$$

$$\pi^{*} = \frac{\partial \mathcal{L}}{\partial(\partial_{\mu}\varphi^{*})} = (D^{\mu}\varphi) = \partial^{\mu}\varphi - ieA^{\mu}\varphi = -H_{2}, \tag{48}$$

The singular Lagrangian in Eq.(18) can be treated as a continuous system by introducing

$$A_{\nu} = A_{\nu}(x_{\mu}, \varphi, \varphi^{*}),\ \varphi = \varphi(x_{\mu}),\ \varphi^{*} = \varphi^{*}(x_{\mu}). \tag{49}$$

Let us define the four-dimensional derivative of A_{ν} as

$$\frac{\partial A_{\nu}}{\partial x_{\mu}} \equiv \frac{dA_{\nu}}{dx_{\mu}} = \partial_{\mu} A_{\nu} + \frac{\partial A_{\nu}}{\partial \varphi}\frac{\partial \varphi}{\partial x_{\mu}} + \frac{\partial A_{\nu}}{\partial \varphi^{*}}\frac{\partial \varphi^{*}}{\partial x_{\mu}} \tag{50}$$

The modified Lagrangian $\mathcal{L}'$ becomes

$$\begin{aligned}\mathcal{L}' = \frac{1}{4}\Big[\partial_{\mu}A_{\nu} + \frac{\partial A_{\nu}}{\partial\varphi}\partial_{\mu}\varphi + \frac{\partial A_{\nu}}{\partial\varphi^{*}}\partial_{\mu}\varphi^{*} - \partial_{\nu}A_{\mu} - \frac{\partial A_{\mu}}{\partial\varphi}\partial_{\nu}\varphi - \frac{\partial A_{\mu}}{\partial\varphi^{*}}\partial_{\nu}\varphi^{*}\Big] \\ \times\Big[\partial^{\mu}A^{\nu} + \frac{\partial A^{\nu}}{\partial\varphi}\partial^{\mu}\varphi + \frac{\partial A^{\nu}}{\partial\varphi^{*}}\partial^{\mu}\varphi^{*} - \partial^{\nu}A^{\mu} - \frac{\partial A^{\mu}}{\partial\varphi}\partial^{\nu}\varphi - \frac{\partial A^{\mu}}{\partial\varphi^{*}}\partial^{\nu}\varphi^{*}\Big] \\ + (\partial_{\mu} + ieA_{\mu})\varphi^{*}(\partial^{\mu} - ieA^{\mu})\varphi - k\varphi^{*}\varphi - \frac{1}{4}\lambda(\varphi^{*}\varphi)^{2}\end{aligned} \tag{51}$$

The Euler-Lagrangian equation for the continuous system (13), for $q_{\alpha} \equiv x_{\mu}, \varphi, \varphi^{*}$ and $q_{a} \equiv A_{\nu}$, becomes

$$\frac{\partial}{\partial x_{\mu}}\left[\frac{\partial \mathcal{L}'}{\partial(\partial_{\mu}A_{\nu})}\right] + \frac{\partial}{\partial\varphi}\left[\frac{\partial \mathcal{L}'}{\partial(\frac{\partial A_{\nu}}{\partial\varphi})}\right] + \frac{\partial}{\partial\varphi^{*}}\left[\frac{\partial \mathcal{L}'}{\partial(\frac{\partial A_{\nu}}{\partial\varphi^{*}})}\right] - \frac{\partial \mathcal{L}'}{\partial A_{\nu}} = 0, \tag{52}$$

With the modified Lagrangian $\mathcal{L}'$, Eq.(26) takes the form

$$\partial_{\mu}F^{\mu\nu} + ie(\varphi^{*}\partial^{\nu}\varphi - \varphi\,\partial^{\nu}\varphi) + 2e^{2}A^{\nu}\varphi^{*}\varphi = 0. \tag{53}$$

Equation (27) is the first set of Euler-Lagrange equations obtained from the standard Lagrangian formulation; it is equivalent to the equations of motion obtained from the canonical method[9]. The second set of Euler-Lagrange equations of the standard Lagrangian formulation is obtained by using the constraint equations (14), that is,

$$dG_1 = -\frac{\partial \mathcal{L}'}{\partial \varphi} dx_\mu. \tag{54}$$

G_1 is obtained from the Hamiltonian formulation, Eq.(5):

$$G_1 \equiv H_1 = -(\partial^\mu \varphi^* + ieA^\mu \varphi^*); \qquad and \qquad d\varphi^* = \frac{\partial \varphi^*}{\partial x_\mu} dx_\mu$$

Thus, Eq. (28) becomes

$$(\overrightarrow{D} \cdot \overrightarrow{D}\varphi)^* - ie(2A^\mu \partial_\mu \varphi^* + \varphi^* \partial_\mu A^\mu) - k\varphi^* - \frac{1}{2}\lambda \varphi \varphi^{*2} = 0. \tag{55}$$

Similarly, from Eq.(5), we have

$$G_2 \equiv H_2 = -(\partial^\mu \varphi - ieA^\mu \varphi) \qquad and \qquad d\varphi = \frac{\partial \varphi}{\partial x_\mu} dx_\mu$$

. Then, by using Eq.(14), we get

$$dG_2 = -\frac{\partial \mathcal{L}'}{\partial \varphi^*} dx_\mu, \tag{56}$$

above equation becomes

$$(\overrightarrow{D} \cdot \overrightarrow{D}\varphi) + ie(2A^\mu \partial_\mu \varphi + \varphi\, \partial_\mu A^\mu) - k\varphi - \frac{1}{2}\lambda \varphi^* \varphi^2 = 0. \tag{57}$$

Equations (29) and (31) are the second set of Euler-Lagrange equations of the standard formulation.

4 Conclusion

The Lagrangian of Landau-Ginzburg theory gives an effective description of phenomenon precisely coincides with scalar quantum electrodynamics.

This system is studied as a singular Lagrangian using the Euler-Lagrange equation and the canonical Hamiltonian approach (Hamilton-Jacobi approach). The system is treated as a continuous field system with constraints. It is shown that this treatment is in exact agreement with the general approach. Our formalism is a mixture of the Hamiltonian and Lagrangian formulations. In the general approach, the constraint equations can be obtained from the Euler-Lagrange equations; whereas in the treatment of singular Lagrangian as fields, the constraints can be determined from Eq. (14), which is obtained with the help of the canonical Hamiltonian formalism. The equations of motion are obtained as partial differential equations, which are equivalent to those equations obtained from the canonical Hamiltonian approach.

References

[1] P. A. M. Dirac, lectures of Quantum Mechanics,Yeshiva University Press, New york (1964).

[2] R. M. Santilli, *Foundations of Theoritical Mechanics*, Spring-Verlag, Heidelbag, Berlin (1983).

[3] D. M. Gitman and I. V. Tyutin , *Quantization of Fields with Constraints*, Spring-Verlag, Heidelbag, Berlin (1990).

[4] S. I. Muslih, Nucl. Phys. B Proc. Suppl. **106**, 879-881 (2002) [arXiv:hep-th/0201003 [hep-th]].

[5] W. I. Eshraim and N. I. Farahat, Electron. J. Theor. Phys. **5**, no.17, 65-72 (2008).

[6] S. I. Muslih (2000), Nuovo Cimento **B115**, 1 (2000).

[7] S. I. Muslih (2000), Nuovo Cimento **B115**, 7 (2000).

[8] W. I. Eshraim, Alg. Groups Geom. **35**, no.4, 365-388 (2018) [arXiv:2003.06238 [physics.gen-ph]].

[9] R. Jackiw, *In Constrained Theory and Quantization Methods*, Procc. held in Montepulciano, Italy, 163 (1993).

[10] L. Faddeev and R. Jackiw, Phys., Rev. Lett., **60** 1692 (1988).

[11] Y. Güler, Nuovo Cimento **B107**, 1389 (1992).

[12] Y. Güler, Nuovo Cimento **B107**, 1143 (1992).

[13] N. I. Farahat and Y. Güler, Nuovo Cimento **A51**, 68 (1995).

[14] E. M. Rabei, Nuovo Cimento **B112**, 1447 (1997).

[15] W. I. Eshraim and N. I. Farahat, Hadronic J. **29**, no.5, 553 (2006).

[16] W. I. Eshraim and N. I. Farahat, Rom. J. Phys. **53**, 437 (2008).

[17] W. I. Eshraim and N. I. Farahat, Electron. J. Theor. Phys. **4**, no. 14, 61 (2007).

[18] W. I. Eshraim and N. I. Farahat, Electron. J. Theor. Phys. **6**, no. 22, 189 (2009).

[19] W. I. Eshraim, Alg. Groups Geom. **38**, no.2, 235 (2022).

HADRONIC JOURNAL 46, 219 - 230 (2023)
DOI 10.29083/HJ.46.02.2023/SC219

CALCULATION OF THE WAVELENGTHS OF THE LYMAN SERIES IN THE HYDROGEN ATOM BASED ON THE QUANTIZED SPACE AND TIME THEORY OF ELEMENTARY PARTICLES

Hamid Reza Karimi
Electrical Engineering Department
Islamic Azad University
South Tehran Branch
Tehran, 13651-17776, Iran
hr.karimy@gmail.com

Received February 13, 2023

Abstract

In the current article, utilizing the theory of quantization of time and space and the internal structure of elementary particles, the radiation spectrum of the excited hydrogen atom is calculated theoretically. By doing this, the electron movement parameters in the hydrogen atom have been stated in a novel way, and via generalizing these calculations, the excited states of other atoms can be calculated. It can be shown that during the transfer of the electron from a higher level to a lower one, what is the state of the electron in terms of momentum, energy, time, and length.

Keywords: Hydrogen– space and time quanta, Elementary particles

Introduction: The electron model, the time and length of which are shown schematically in the following figures1,2,3 explains the Lorentz relations[1], and by using it, it is possible to calculate the radiated energy spectrum in the excited hydrogen atom when it comes from a higher level to a lower level. The reason for the presence of the electron in the S1 level has been explained by the wavelength. In the present article, it is stated that since the components of the electron velocity vector (Y, Z) in a hypothetical Cartesian system does not become zero; it causes the electron not to fall into the nucleus.

In the fig.1, it is shown that the time for an electron is created in the form of consecutive sequences, and the length of the electron is created in the same way. We call this moving element a moton in the quanta of the past time and the quanta of the present time [1]. The medium for the creation of this sequence is the Super Dimension Axiom [1], and the super-light spin originates from the existence of this super dimension.

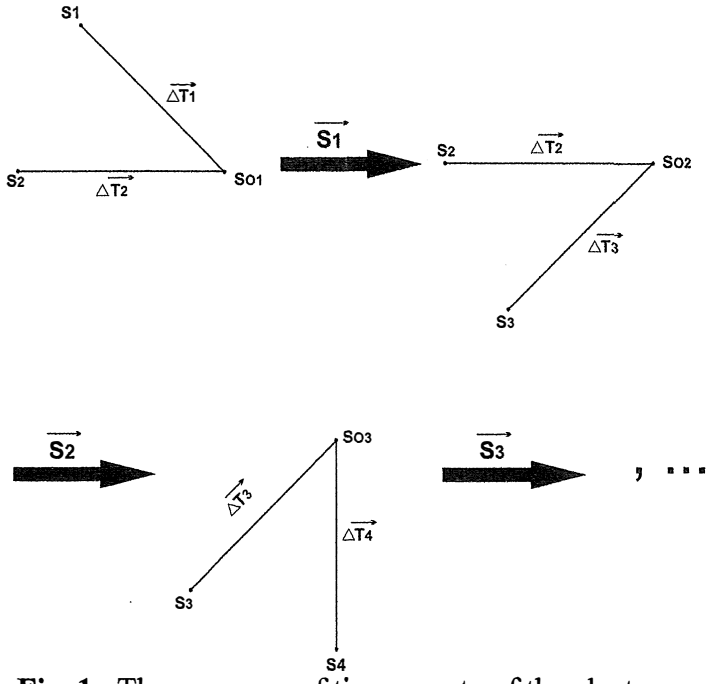

Fig. 1. The sequence of time quanta of the electron

In the Fig.1, the spatial diagram of a moton in length belonging to the quanta of the past time and the quanta of the present time is shown. The speed of an electron for an observer is determined by this sequence of quanta of space and time and it is the motons that determine the base speed in the quantum of time and space of the past independently of the external observer, and the quantum of time and space of the present depends on the environment.

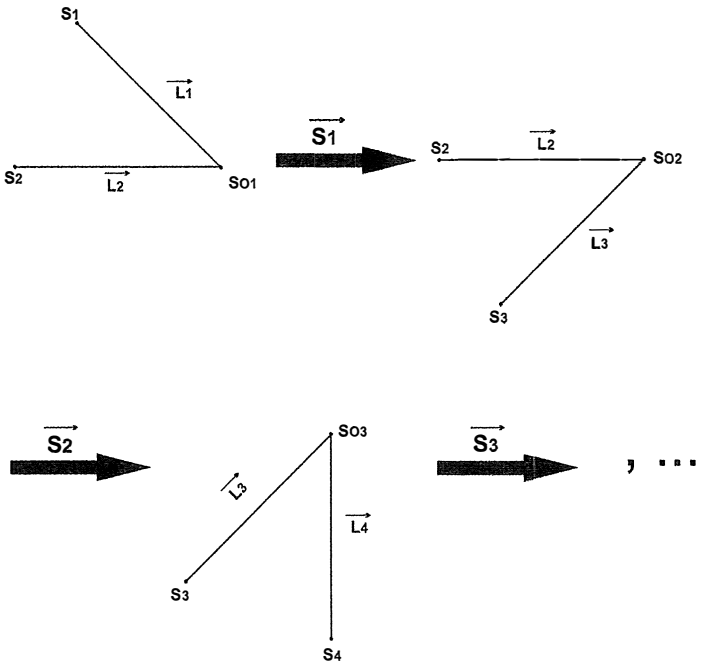

Fig. 2. The sequence of length quanta of the electron with positive spin

It is again this super dimension that performs the task of converting. For example, the time and length quanta of the present to the past time and length in the next sequence. Regarding the nature and structure of this super dimension, in my other article, some excerpts are stated about the nature of the super dimension and some information has been provided [2].

Figure 3 shows that sequences of time and space are created and passed successively by the function of moton and super-dimension. From the point of view of the experimenter, an electron is the embodiment of two sequences of both time and space.

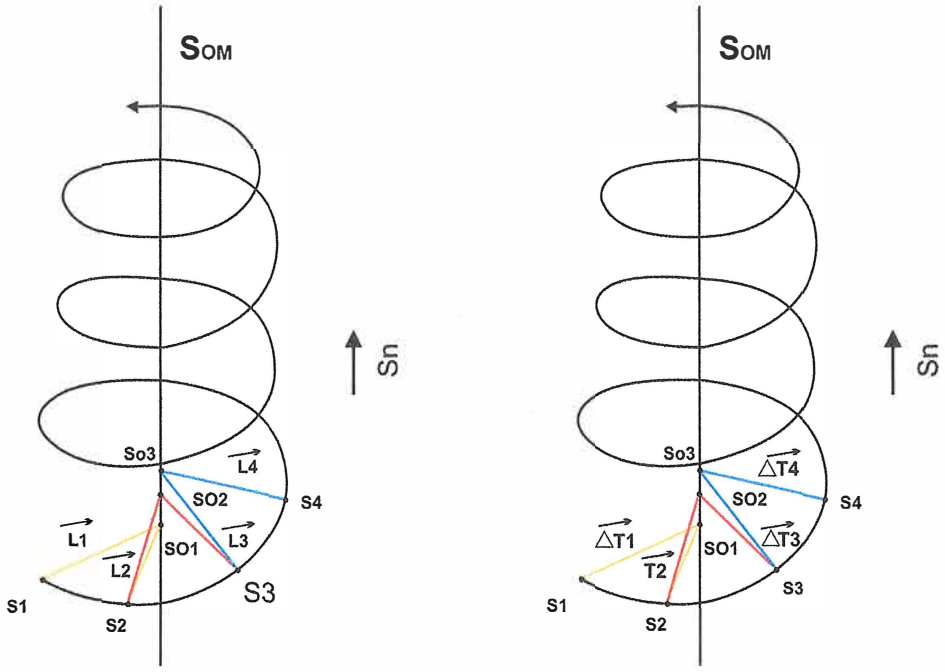

Fig. 3. The sequence of time and length quanta of an electron in super dimension $\overrightarrow{S_n}$. The electron has positive spin angular momentum with a relative velocity with respect to a local frame

At the temperature of zero Kelvin, these sequences of time and space almost coincide on a plane and can be used as inertial system. In this inertial system, the quanta of the motons have the highest value. In fig.3, the illustrated super dimension performance is obtained basis on the Planck constant. The equations of action of motons are expressed based on Einstein's equation of equivalence of energy and mass. The set of these equations determines the equations of mass, energy, momentum, and angular momentum of an electron.

1: We can find the relative velocity of a particle concerning a reference frame using Figures 1, 2, and 3: [1]

$$\vec{V}^2 = \left(\frac{\vec{l}_{1(so1)}}{\Delta\vec{T}_{1(so1)}} \times \frac{\vec{l}_{2(so1)}}{\Delta\vec{T}_{2(so1)}}\right) - \left(\frac{\vec{l}_{2(so2)}}{\Delta\vec{T}_{2(so2)}} \times \frac{\vec{l}_{3(so3)}}{\Delta\vec{T}_{3(so3)}}\right), (1)$$

$$\vec{V}^2 = (\vec{V}_Y \times V_X) - (\vec{V}_X \times \vec{V}_Z) \quad (2)$$

$$\vec{l}_0 = \vec{l}_1 = \vec{l}_{2\,(so1)} = 1.409 \times 10^{-15} m, (3)$$

$$\Delta\vec{T}_0 = \Delta\vec{T}_1 = \Delta T_{2\,(so1)} = 0.47 \times 10^{-23} s, (4)$$

$$\vec{l}_{3\,(so2)} = \frac{\vec{l}_0}{\gamma}, (5)$$

$$\Delta\vec{T}_{3\,(so2)} = \Delta\vec{T}_0 \gamma, (6)$$

$$V^2 = C^2 - \frac{C^2}{\gamma^2}, (7)$$

$$\gamma \equiv \frac{1}{\sqrt{1 - \frac{v^2}{c^2}}} : \textit{Lorentz factor} \ (8)$$

$$\vec{l} = \frac{\vec{l}_0}{\gamma}, \qquad \Delta T = \Delta \vec{T}_0 \gamma \quad (9)$$

$$|V| = \sqrt{c^2 - \frac{c^2}{\gamma^2}} : \textit{Relative velocity of the particle.(10)}$$

determination of the Lorentz factor coefficient has been explained in my other article[2]. The maximum Lorentz factor for charged particles should be 1722.9.

This is a very great achievement because the minimum wavelength for charged particles is equal to the length quanta and it is obtained by using the deBroglie formula here it is obtained based on the assumption of moton existence and this equivalence shows a great attainment between the Einstein's mass-energy formula and Planck's constant [2].

By using the desired number in Equation 10, the maximum speed of the sequence of space and time in the present time of a moton is calculated.

$$|V| = \sqrt{c^2 - \frac{c^2}{\gamma^2}} = 299792407.5 m/s \qquad (11)$$

2: The energy of the 2nd layers up to the infinite number of the excited hydrogen atom is obtained from the sum of the electric potential energy between the proton and the electron with the kinetic energy of the electron between the atom levels, and the electron kinetic energy at each level of the atom's energy level. The sign of kinetic energy is negative.
The electric potential energy between the proton and the electron is the work required for the electron to fall in the proton's electric field. If we assume that the electron and proton are fixed relative to each other in the X axis and the electron moves only in the Y, and Z plane, then:

$$\vec{V}^2 = (\vec{V}^2{}_Y \times \vec{\delta}_X) - (\vec{\delta}_X \times \vec{V}_Z)$$

(12)

Equation (12) causes the Lorentz factor to become one in the charging formula.[1]

$$q=\frac{\sqrt{(8\pi\varepsilon_0 m_0 c^2 l_0)}}{\sqrt[4]{(1-\frac{v^2}{c^2}}}=\sqrt{8\pi\varepsilon_0 mc^2 l_0}=1.602\times10^{-19}c$$

(13)

Consequently, by assuming the Bohr radius for the distance of the electron of the first layer with the proton and the electric potential energy of the first layer of the hydrogen atom, it is obtained from equation 14 [1]

$$U_1=\frac{8\pi\varepsilon_0 m_0 c^2 l_0}{4\times2\pi\times\varepsilon_0\times37556\times l_0\times1}=13.6ev$$

(14)

And if there is a movement in the X (proton-electron) axis, the relative value of this equation for potential energy is equal to Equation 15.

$$U_1=\frac{8\pi\varepsilon_0 m_0 c^2 l_0}{4\times2\pi\times\varepsilon_0\times37556\times l_0\times\sqrt{1-\frac{v^2}{c^2}}}=\frac{13.6ev}{\sqrt{1-\frac{v^2}{c^2}}}$$

(15)

We define A_0 as a basic spherical network:

$$A_0=4*2\pi*37556l_0$$

(16)

By using the fact of quantized time and length, we can prove that the angular momentum of an electron is also quantized. Therefore, electrons can only be located on surfaces that are integral multiples of A_0:

$$A=n\,A_0$$

(17)

n= (1, 2, 3, 4...)

$$U_n = \frac{13.6ev}{n\times\sqrt{1-\frac{v^2}{c^2}}}\ [1] \qquad (18)$$

n= layer number

3: The kinetic energy of the electron moving to the first layer in the excited hydrogen atom consists of two parts, one is the energy resulting from the movement along the X-axis, and the other is the energy resulting from the sum of each layer above the second layer that the electron passes through and this energy is in Y and Z graph plane. In the two states of the proton, in this calculation, these two energies are assumed to be constant.

Equation 19 is used to calculate the kinetic energy of the surface of the layers, Ka, and the energy of the path of the electron to the proton would be Kn.

$$K = p\times v = \frac{h\times v\times\sqrt{1-\frac{v^2{}_{\max}}{c^2}}}{n\times l_0\times\sqrt{1-\frac{v^2}{c^2}}} \qquad (19)$$

$n = 37556$

$$v \approx \delta \Rightarrow \sqrt{(1-\frac{v^2{}_{\max}}{c^2})} = 5.8\times10^{-5}$$
$$v = v_{\max} \Rightarrow \sqrt{(1-\frac{v^2{}_{\max}}{c^2})} \approx 1 \qquad (20)$$

This relation is a floor component relation that explains the paradoxical states in the movement of elementary particles. The fraction numerator shows that there is an uncertainty in the calculation of the elementary particle energy at zero speed. A particle can take energy or emit radiation on

the condition of observing, the quanta of time and space of the elementary particle and the surrounding space-time. If the velocity is zero in one of the X, Y, or Z axes, $\sqrt{(1-(\frac{v^2}{c^2})=1}$, and if there is a significant amount of speed in all X, Y, and Z axes, $\sqrt{(1-(\frac{v_{\max}{}^2}{c^2})=1}$. This creates a paradox, the paradox is that there is velocity, but it is not, and this paradox is solved for the ionic particle by the radiation of a photon.

By numbering the relation for the kinetic energy caused by the movement of the electron from the S1 to S2 layer, which is equal to the path length

$$L_{S2-S1} = n \times 37556 l_0 \quad (21)$$

$$K_1 = \frac{h \times 299792407.5}{37556 \times 1.409 \times 10^{-15} \times 1722.9} = 13.59 ev$$

(22)

Incredibly, the kinetic energy of the electron in the state of transition from S2 to S1 is calculated. Formula 19 is a new equation for elementary particle mechanics.

By summing the kinetic energy and the electric potential of the electron from formulas 22 and 19, the electron transfer from a level to the S1 level is obtained.

$$E_{PHOTON} = h\nu = E1 - E2 = U_1 - K_2 - U_2 - Ka_2 \quad (23)$$

$$U_N = \frac{13.6 ev}{n}$$

(24)

$$K_n = \frac{h \times 299792407.5}{(n-1) \times 37556 \times 1722.9 \times 1.409 \times 10^{-15}} \quad n \succ 1$$

(25)

$$Kan = \frac{h \times 299792407.5}{N \times 37556 \times 1722.9 \times 1.409 \times 10^{-15}}$$

(26)

Kan is the kinetic energy of each electron in the squares of the quanta of the Z and Y axes.

$$N = \frac{4\pi \times (nr)^2}{4\pi \times r^2} = n^2$$

(27)

Therefore, for the electron to fall from level S2 to S1, we will have

$$E_{photon} = h\nu = Es_1 - Es_2 = 13.6ev - 13.59ev - 6.8ev - 3.4ev = -10.2ev$$

$$\Rightarrow \lambda = 121.5nm$$

(28)

The kinetic energy of the path of electron fall from higher to lower layers destroys the electric potential energy, so the energy of 10.2 electron volts is repeated for all layers up to the sixth layer.

$$Un = -Kn + 1$$

(29)

And only the kinetic energy in the quantized squares of the Y and Z axes is added periodically.

$$E_{photon} = h\nu = Es_1 - Es_n = -10.2ev - \sum_{i=3}^{n} \frac{1}{n^2} \times \frac{h \times 299792407.5}{37556 \times 1722.9 \times 1.409 \times 10^{-15}}$$

(30)

n=2

$\lambda = 121.5nm$

n=3

$\lambda = 105nm$

n=4

$\lambda = 98nm$

n=5

$\lambda = 94.6nm$

n=6

$\lambda = 92nm$

With exact values, the linear radiation spectrum of the Lyman series for excited hydrogen is obtained by using the theory of quantization of time and space and the internal structure of elementary particles.

Conclusion: So far, for obtaining the wavelength of the radiation spectrum of the hydrogen atom, a function has been extracted from the experimental data set. But since electron is an elementary particle, this radiation should be obtained with the formulas of the elementary particles, which has been done in this article.

REFERENCES

[1] Quantized Space-Time and internal Structure of Elementary particles: A new model, Hadronic Journal 33, Number 3, 249-272.

[2] Calculation of the exact range of the mass of higgs boson in the large Hadron collider (LHC) of the basis of the quantized space and time theory, Hadronic Journal 44, Number 1, 97-108.

[3] Anomalous magnetic moment um of mouns in FNAL on the basis of quantize space and time theory. Published in Hadronic Journal 44, Number 2, 193-200.

[4] Ernest M. Henley and Alejandro Garcia. Subatomic Physics, Third edition. World Scientific Publishing Co. pte. ltd., 2007.

[5] Griffiths, David J. Introduction to elementary particles. John Wiley & Sons, Inc. 2008, Second Edition, ISBN: 978-3-527-61847-7.

[6] Robert Resnick. Introduction to Special Relativity, John Wiley & Sons, Inc., 1972.

[7] James William Rohlf. Modern Physics from α to z. John Wiley & Sons, Inc., 1994.